FRAGILITY METHODOLOGY FOR PERFORMANCE-BASED ENGINEERING OF WOOD-FRAME RESIDENTIAL CONSTRUCTION

A Thesis
Presented to
The Academic Faculty

By

Yue Li

In Partial Fulfillment
of the Requirements for the Degree
Doctor of Philosophy in the
School of Civil and Environmental Engineering

Georgia Institute of Technology

December 2005

FRAGILITY METHODOLOGY FOR PERFORMANCE-BASED ENGINEERING OF WOOD-FRAME RESIDENTIAL CONSTRUCTION

Approved by

Dr. Bruce R. Ellingwood, Advisor
School of Civil and Environmental Engineering

Dr. Donald W. White
School of Civil and Environmental Engineering

Dr. Laurence J. Jacobs
School of Civil and Environmental Engineering

Dr. Abdul-Hamid Zureick
School of Civil and Environmental Engineering

Dr. Steven P. French
College of Architecture

Date approved August, 17, 2005

In loving memory of my beloved grandma, Ai min Yu (1907-1991)

ACKNOWLEDGEMENTS

First and foremost, I would like to express my sincere gratitude to my advisor Dr. Bruce R. Ellingwood for his excellent guidance, technical expertise and continuous support through my Ph.D. studies, first at the Johns Hopkins University and subsequently at the Georgia Institute of Technology. I am indebted to him for the education, direction, encouragement and examples he has provided. His positive influence will no doubt propagate beyond the Ph.D. degree and serve me well for many years to come. I have been fortune to study under his tutelage.

My sincere appreciation goes to Dr. Barry Goodno, Dr. Laurence J. Jacobs, Dr. Donald W. White, Dr. Steve French and Dr. Abdul-Hamid Zureick, who served as my dissertation committee members or readers, and who provided me with suggestions and feedback on several aspects of my research. I would also like to express my thanks to Dr. Kenneth Will, Dr. Reginald DesRoches and Dr. David V. Rosowsky (Texas A & M University) for their assistance during my study. I am grateful to other faculty members and my fellow graduate students in School of CEE at Georgia Tech. Their support and friendship has made my school life at Tech enjoyable and memorable.

The research described in my Ph.D. dissertation was supported by the National Science Foundation (NSF) under Grant CMS-0049038. This support is gratefully acknowledged.

I want to express my heartfelt thankfulness to my family: my parents, Yingshi Li and Yuli Lin, and my brother, Qian Li. I owe them a great debt of gratitude for the love,

caring, support, and encouragement they have unconditionally provided not only my graduate studies but throughout my life. Finally, I am grateful to Yan Gu, for her love and tremendous support.

TABLE OF CONTENTS

LIST OF TABLES

LIST OF FIGURES

SUMMARY

Hurricanes and earthquakes have caused extensive property damage to wood-frame residential construction in the past two decades in the United States. In order to improve residential building performance and mitigate losses from hurricane and earthquake hazards, there is an urgent need for better understanding of building performance and improvements in design and evaluation tools.

In this study, a fragility analysis methodology is developed for assessing the response of light-frame wood construction exposed to extreme hurricane winds and earthquakes. The fragility is a conditional limit state probability, presented as a function of the 3-second gust wind speed (hurricanes) or spectral acceleration at the fundamental period of the building (earthquakes), leading to a relation between damage state probability and the hazard stipulated in ASCE Standard 7. A fully coupled probabilistic framework is proposed to assess reliability of the residential construction through convolution of the structural fragility model with hazard models. Finally, a comparative risk assessment addresses the similarities and differences in competing hurricane and earthquake hazards.

The tools above can be used to evaluate new and existing building products, model the uncertainties that are inherent to the prediction of building performance, and manage the risk that is consequent to these uncertainties economically

1 NTRODUCTION

1.1 Motivation

Housing represents an enormous social investment in the United States (for most individuals, it is their largest single asset). The majority of residential buildings in the US (approximately 90%) are light-frame wood construction. In California, 99% of all residences are of woodframe construction. (CUREE, 2000) Residential buildings with light-frame wood construction are especially susceptible to natural hazards. Hurricane Andrew (1992) alone produced insured property losses estimated at $20.2 billion (GIIS, 2004); catastrophic failures of one- and two-story light-frame residential buildings were the most frequently observed mode of building damage. The more recent Hurricanes Isabel (2003), Charley, Frances, Ivan and Jeanne (2004) are further reminders of the devastation and disruption caused by such events. According to National Oceanic and Atmospheric Administration (NOAA), the four major hurricanes in 2004 reportedly have caused more than $40 billion wind, storm and flooding damage[1]. Losses to residential construction during recent earthquakes (e.g. Loma Prieta, 1989; Northridge, 1994) have been similarly severe. The majority of fatalities in the Northridge earthquake (24 out of 25), and more than half of the estimated $16.7 billion insured loss was due to damage to wood buildings (Schierle, 2001).

[1] http://www.ncdc.noaa.gov/oa/reports/billionz.html

In a report issued subsequent to these natural disasters, the Institute for Business and Home Safety (IBHS, 2001) noted that: (a) Losses from recurring natural hazards are increasing, (b) Existing residential buildings are particularly vulnerable to natural hazards, as light-frame wood residential construction traditionally has been non-engineered, and (c) Major population growth (accompanied by construction of residential buildings) in the US is taking place in areas that are prone to natural hazards, especially along southeast coast and in California. Thus, the potential for losses to residential construction in the future may be even greater, barring changes to current design and construction practices.

The aftermath of recent natural disasters and the potential for higher losses in the future have led to intense professional and public scrutiny of real or perceived deficiencies in design and construction practices, building codes and their enforcement. (CUREE, 2000) This scrutiny has pointed to the need for an improved basis for designing new residential construction and for assessing the condition of the current residential building inventory and its vulnerability to future hazards. Such improvements to building practices require tools for evaluating new and existing building products, for modeling the uncertainties that are inherent to the prediction of building performance, and for managing the risk that is consequent to these uncertainties economically. Such advances require an integration of analytical models of structural behavior and methods of structural reliability assessment for treating the large uncertainties that are inherent to natural hazard mitigation. However, the attention paid to improving light-frame wood construction practice has been relatively small compared with other types of construction, such as concrete and steel buildings.

Performance-based engineering of wood-frame residential construction has the potential to play an important role in addressing the issues above. Protection of building occupants against injury or loss of life is of paramount importance in structural design. Thus, the main objective of current codes and standards is to prevent building failures leading to loss of life during rare events. While this objective has been essentially achieved for buildings in the United States subjected to windstorms or earthquakes, the economic losses and social disruption associated with many of these events are viewed as being unacceptable. It has become apparent that buildings designed by code, which satisfy the life safety objective, may not meet other expectations of building owners and occupants. For example, an examination of insurance claim files from Hurricanes Hugo and Andrew has revealed that most wind damage to houses is restricted to the envelope of the building. Rain entering the building leads to building contents damage and causes the loss due to damage to the building envelope to be magnified by a factor ranging from two, at lower wind speed, to nine at higher speeds (Sparks, et al. 1994). Similarly, excessive lateral drift leading to cracking of interior and exterior wall finishes during earthquakes may not be directly related to life safety, but may lead to significant nonstructural damage and loss of building function. Furthermore, current building and construction practices that are based on purely deterministic thinking may not provide a design solution that is based on targeted reliability levels for both occupant safety and desired economic protection. The uncertainties in demand on the built environment from both wind and earthquake hazards are very large. Performance-based engineering can offer more risk-consistent methods for dealing with the future impact of uncertain seismic

and wind hazards on communities, devising appropriate policies for natural hazard mitigation, and for evaluating designs of specific building structural systems.

1.2 Objective and scope

The research objective of this study is to provide a technical basis for reducing the tremendous losses caused by hurricane and earthquake hazards, through better understanding the performance of residential construction and investigation of vulnerability of the building inventory. The following are tasks that support this objective.

1.2.1 General methodology for assessing probabilistic response

A general probability-based methodology is required for condition assessment of light-frame residential construction under various levels of hurricanes and earthquakes. It provides a framework for the treatment and analysis of uncertainties in demand and capacity and is the basis for a rational quantification of performance-based engineering of light-frame residential construction. Because of the complex nature of structural system behavior (some components within the structural system may respond in the nonlinear range), the fragility analysis requires a combination of finite element based structural analysis and reliability tools to evaluate structural responses to extreme winds and earthquakes. Conditional probabilities of the structural systems for various performance

limits will be developed as functions of hurricane wind speed or earthquake ground acceleration.

1.2.2 Strategies for improving structural safety and performance

Structural safety and performance of residential construction are affected by many variables and sources of uncertainty. It is crucial to identify key parameters that influence the vulnerability of light-frame residential construction, as this identification provides a basis for improving building performance under extreme winds and earthquakes according to the relative importance of each variable. Furthermore, this process can identify the main sources of uncertainty that affect building performance, providing insight on areas to target for further modeling and data collection efforts.

1.2.3 Comparative risk assessment for hurricane and earthquake hazards

In certain areas of the United States, both hurricane or earthquake hazards may be significant. A comparative assessment of risks due to wind, earthquake and similar natural hazards is desirable for public policy and disaster planning purposes, as well as for insurance underwriting. The comparative assessment addresses differences and similarities between the two competing natural hazards. It provides insights on building design and construction strategies that would achieve an overall risk that is consistent with social objectives, represent an optimal investment in natural hazards mitigation, and

offer a methodology to evaluate effectiveness of current design codes in addressing multiple hazards.

1.3 Organization

Chapter 2 describes losses to residential construction due to hurricanes and earthquakes in more detail. Chapter 2 also reviews current design practices for wood residential building structures. Concepts of performance-based engineering, probabilistic risk assessment and structural fragility analysis are introduced. A comprehensive literature review reveals the current state-of-the-art for evaluating performance of wood-frame construction and points out areas requiring further investigation.

Chapter 3 presents a reliability-based assessment of residential building structural response to hurricane effects, introducing the notion of hurricane fragility and its role in a fully coupled reliability analysis. Three typical residential configurations are selected to represent the majority of residences in hurricane-prone regions, and a fragility analysis is performed for the selected buildings. A parametric sensitivity analysis follows to identify the relative contribution of various sources of uncertainty. Failure rates predicted from the fragility analysis are compared with post-hurricane disaster surveys. Several competing hurricane wind speed models are introduced, which are convolved with the fragility to determine annual probabilities of failures for some key hurricane-resistant components. The importance of modeling uncertainty is demonstrated by simultaneously incorporating data from different structural tests and various wind speed models.

Chapter 4 develops earthquake fragility models and illustrates their role in seismic risk assessment. Four typical shear walls found in residential construction are modeled, and their hysteretic behavior under ensembles of moderate to severe earthquakes is analyzed using nonlinear time history analysis. The relationship between ground motion intensity and structural deformation are presented. A series of sensitivity analyses are performed to characterize the relative impact of individual variables on seismic fragility. Lastly, a fully coupled reliability analysis is performed by convolving seismic fragility and seismic hazard curve.

In Chapter 5, a comparative risk assessment is presented in which the differences and similarities of hurricane and earthquake hazards for residential construction are examined. Six cities are chosen in various locations in the United State that are exposed to both natural hazards. Firstly, for each city, probabilities of hurricane and earthquake damage are illustrated as a function of wind speed and spectral acceleration, respectively. Next, both hurricane and earthquake damage probabilities are presented as functions of hazard event return period, selected as a common variable to compare risks posed by these two hazards.

Chapter 6 reviews the main points of the study, summarizes the main findings and conclusions, and suggests unresolved issues to be addressed by future work.

2 NATURAL HAZARDS AND THEIR IMPACT ON LIGHT-FRAME WOOD CONSTRUCTION

Despite the tremendous losses due to hurricanes and earthquakes, relatively little attention has been given to the behavior of wood-frame residential construction under these hazards. This Chapter will look into the losses and damage caused by these hazards, current design and construction practices for wood buildings, and existing structural performance evaluation methods and tools and their deficiencies. New concepts and improved methodology needed to effectively mitigate the devastating natural hazards will be introduced.

2.1 Losses to residential construction from hurricanes and earthquakes

Hurricanes are a major threat to life safety and property in coastal areas from Texas to Maine. Residential buildings with light-frame wood construction are especially susceptible to extreme winds. In 1989, Hurricane Hugo caused insurers to pay out $4.2 billion, most of which were residential damage claims. Hurricane Andrew in 1992 produced property losses estimated at a record of $26 billion (NAHB, 1993), including insured property losses estimated at $20.2 billion (GIIS, 2004); catastrophic failures of one- and two-story light-frame buildings in residential areas during Hurricane Andrew were observed more frequently than in other types of buildings. Later in 1992, Hurricane Iniki caused $3 billion in damage (NAHB, 1993). Hurricane Hugo (1989) caused insurers

to pay out $6.0 billion most of which were residential damage claims. All insured losses are given in 2001 US dollar, with the exception of losses due to Hurricanes Opal and Iniki, which are given in 1997 $US (GIIS, 2004). Those figures do not include the uninsured losses. Had hurricane Andrew hit a major metropolitan area such as Miami or Fort Lauderdale, the losses could have been as high as $50 to $75 billion (Sheets, 1994).

At least 39 of the 50 states are subject to major or moderate seismic risk. (FEMA, 2001) The vulnerability of current wood residential construction to earthquake ground motion was made apparent by its performance during the 1994 Northridge earthquake, where the property losses to residences ($20 billion) far outweighed the loss to any other single type of building construction. Furthermore, more fatalities (24 of 25) and injuries occurred in light-frame buildings than in all other types of buildings combined (Schierle, 2001). These failure events highlight the susceptibility of wood residential construction to strong earthquakes and the weakness of current residential building practice for seismic risk mitigation. Following the Northridge earthquake, 100,000 individuals required temporary housing because their homes had been severely damaged. Included in that number were 50,000 residents whose homes were so severely damaged that they could not move back for several months. Economic losses and social disruption associated with moderate-to-severe earthquakes can be severe, even when morbidity/mortality is limited.

According to the United States Census Bureau, the population of the 168 coastal counties directly facing the Atlantic Ocean or Gulf will surpass 55 million in 2002. Another 30 million people live within fifty miles of the Gulf or Atlantic coastline. With the

increasing population in coastal areas, hurricanes will continue to be the one of most significant and potentially devastating natural hazards. Likewise, increasing population in earthquake-prone areas, such as California and the Pacific Northeast , also indicates increasing hazard exposure and a potential for substantial economic losses to residential construction.

2.2 Current design and construction practices for wood structures

Light-frame wood residential construction traditionally has been non-engineered; and most structural design and detailing has been based on prescriptive requirements rather than formal engineering analysis. Details that enhance resistance to wind and earthquake hazards have evolved over time. Modern structural design codes and standards for other construction methods are based on concepts of limit states design (or LRFD, as it commonly is termed), with safety checks that are based on structural reliability theory (Ellingwood, 1997). Such methods are beginning to be introduced fro some wood structures. For example, in LRFD of engineered wood structures, the structural safety requirement is expressed by a set of equations (ASCE Standard 16-95),

$$\lambda \varphi R_n > \Sigma \gamma_i Q_i \qquad (2.1)$$

The design strength on the left-hand side of Equation 2.1 is the product of R_n = nominal resistance of a member, component or connection adjusted to end use conditions, φ =

resistance factor that accounts for uncertainty in short-term strength as well as mode of failure, and λ = a time-effect factor that takes into account the dependence of wood strength on rate and duration of load. The nominal loads, Q_i and load factors γ_i on the right-hand side of Equation 2.1 are defined in Section 2.3 of ASCE Standard 7-02 (2003). The resistance criteria for each limit state in Equation 2.1 are based on a reliability-based assessment of and calibration to traditional practice (e.g., Galambos, et al, 1982; Ellingwood and Rosowsky, 1991).

The LRFD criteria represented by Equation 2.1 were calibrated (in a probabilistic sense) to existing practice to facilitate acceptance by structural engineers who design wood structures. This calibration process has raised several issues that must be considered in advancing the use of engineering analysis and performance-based design for light-frame wood construction. For one, the calibration was performed only for individual members, components and connections. System effects were considered only indirectly, through effective length factors in column design, response modification factors used to determine base shear in a seismic design, repetitive member adjustment factors for flexure in joists, truss chords, etc. Accordingly, such checks provide only an approximate indication of how a system of such elements might perform during an extreme event.

Furthermore, the reliability benchmarking of structural members that had been properly designed by traditional working stress design codes was essentially a tool for risk communication between reliability specialists working to develop probability-based design, standard-writing groups, and the structural engineering profession. Because of

limitations in supporting databases, the reliability benchmarks identified in the calibration process were "notional," in the sense that no attempt was made to correlate them to structural failure rates observed in service. This failure to reconcile predicted and observed failure rates makes it difficult to use such methods for hindcasting or forecasting performance of buildings during a natural disaster, for planning and implementing effective post-disaster management strategies, or for setting insurance premium rates. To achieve reasonable agreement (within the limitations imposed by statistical sampling) between calculated and observed failure rates, properly validated system reliability analysis models are essential. This is especially important in light-frame wood construction, where the body of research during the past two decades has indicated that there is an integral relationship between member, connection and system performance.

Finally, traditional design practice has focused mainly on the life safety objective, as noted above. There has been little attention paid to serviceability or economic loss issues, which do not impact life safety but may have a significant social and economic impact. Performance-based engineering of light-frame residential construction will require a broader view of the purpose of structural design.

2.3 Performance based engineering (PBE)

2.3.1 Fundamental concepts

Public safety is the primary goal of structural design. Minimization of property damage is a secondary goal. Thus, the main objective of current building codes and standards (e.g., ASCE Standard 7) is to prevent building failures leading to loss of life during rare events. While this objective has been achieved for buildings subjected to hurricanes and earthquakes, the economic losses associated with many of these events are significant, and their mitigation is of increasing concern. It has become apparent that buildings designed by code which satisfy the need of life safety objective may not meet other performance expectations.

Performance-based engineering (PBE) represents a new approach, one that aims at ensuring that a building or other facility achieves the desired performance objectives when subjected to a spectrum of natural or man-made hazards. PBE provides a rational basis for design, with flexibility in accommodating various needs of building occupants, owners and the public, while maintaining the traditional objective of life safety.

The proposals for PBE that have been published in recent years by organizations such as Federate Emergence Management Agency (FEMA), National Earthquake Hazard Reduction Program(NEHRP) and Structural Engineers Association of California (SEAOC), among others, all have common features. All proposals for PBE require that life safety (LS) must be preserved under “severe” events. Beyond this, they stipulate that collapse (collapse prevention, or CP) shall not occur under “extreme” events and that

building function (continued function or immediate occupancy - IO) should not be unduly disrupted under “moderate” events. The definitions of what is “severe,” “extreme,” or “moderate” have yet to stabilize, but are likely to be based on the annual probability of exceeding the design hazard or its return period. As an example, one might require that the building be designed so that there is no disruption of function following an event with 50% probability of being exceeded in 50 years (abbreviated in the sequel as a 50%/50-yr event), that life safety is preserved under a 10%/50-yr event, and that collapse will not occur under a 2%/50-yr event. These general performance objectives are encapsulated in a matrix of performance objectives vs. hazard levels for various building occupancies. An illustration of such a matrix is presented in Figure 2.1 (SEAOC, 1995).

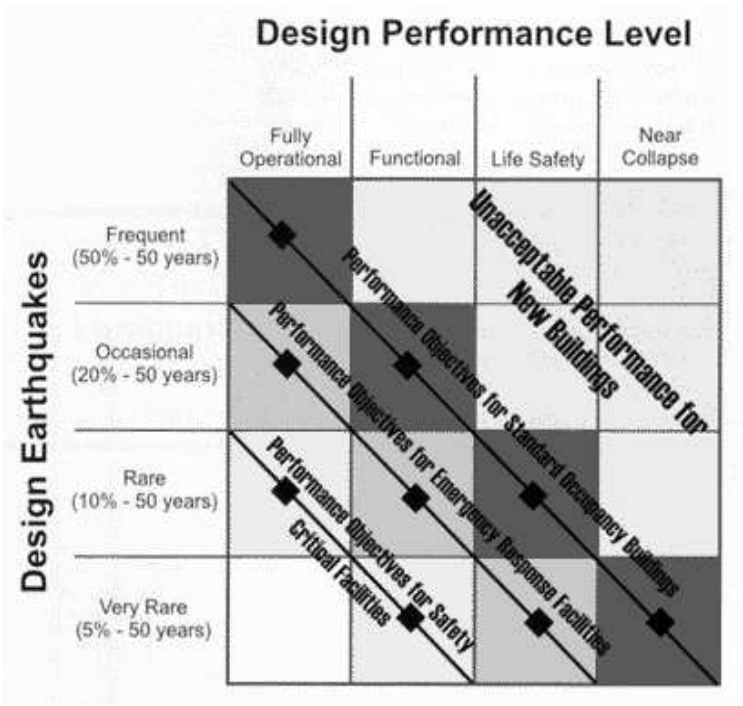

Figure 2.1 SEAOC VISION 2000 Performance Objectives (SEAOC, 1995)

A fundamental premise of PBE is that performance levels and objectives beyond life safety can be quantified, that performance can be predicted analytically with sufficient confidence, and that risk to the building from uncertain natural hazards can be managed to remain at a level acceptable to the building owner and its occupants. PBE not only can provide tools for assessing risk due to hurricanes and earthquakes but also promises reliable and predictable performance of engineered construction under wide range of loading, which can result in economic protection of property values. For example, SEAOC's Vision 2000 and FEMA 273 define performance objectives of achieving performance levels of certain seismic hazard levels. Due to uncertainties in natural hazard, structural demand and capacity, the objectives only make sense if they are probability-based.

2.3.2 Challenges for light-frame wood construction

At the present state-of-the-art, many of the tools necessary to support practical PBE for light frame wood construction either do not exist or are in early stages of development (Rosowsky and Ellingwood, 2002). Note that Figure 2.1 stipulates probability levels for the specific demands to be considered (vertical axis) but not for the probabilities of achieving specific performance objectives (shaded blocks within the matrix). Such probabilities (as one measure of acceptable risk) remain to be established. Whether a building performance requirement is met requires a mapping between the qualitatively stated objective (e.g., immediate occupancy following the 50%/50-yr event) and a response quantity and limit state (measuring force or deformation) that can be checked

using principles of structural analysis and mechanics. Such a mapping invariably requires that the behavior of the building structural system be considered as a whole. When the performance objective can be related to local damage, a limit state based on member (or connection) strength or deformation may be sufficient.

Performance-based engineering for wood construction requires more comprehensive and quantitative probabilistic and statistical procedures for managing risk and uncertainty than are found in first-generation criteria such as LRFD (Ellingwood, 1990; Ellingwood, 1997). Furthermore, the methodology must be validated as a tool for projecting losses from postulated natural hazards before being applied to building code improvements or to loss assessment and insurance underwriting. Comparisons should be made of the predicted results with failures observed in post-disaster damage surveys. Finally, while the research has been focused on PBE in earthquake engineering (PEER), its implication for hurricanes and other natural hazards has not been considered.

2.4 Probabilistic safety assessment

2.4.1 Basic method for reliability analysis

A probabilistic safety assessment (PSA) provides a structured framework for evaluating uncertainty, performance and reliability of a building system subjected to wind or earthquake hazards. As a first step in a PSA, one must identify limit states, or conditions

in which the structural system ceases to perform its intended functions in some way. The reliability problem is formulated as a vector of loads and resistances variables $\mathbf{X} = (X_1, X_2, ., X_n)$ that describe the limit condition, and may be either strength or deformation-related.

The margin of safety is defined, mathematically, as

$$Z = g(X_1, X_2 , \ldots, X_n) \qquad (2.2)$$

in which the function g( ) describes the inter-relation of load and strength variables based on principles of structural mechanics. By convention, when $Z > 0$, the structure is safe; when $Z = 0$, structure is at the limit state; when $Z < 0$, the structure fails. The probability of failure is given by the n-fold integral

$$P_f = P[\, Z < 0 \,] = \int \ldots \int_{g(x)<0} f_x(\mathbf{x}) d\mathbf{x} \qquad (2.3)$$

For most building structural systems, the region $g(\mathbf{X}) < 0$ cannot be determined in closed form, and the integration is difficult to perform analytically. The difficulty has led to the use of first- and second-order approximations and Monte Carlo simulation for reliability assessment (e.g., Melchers, 1999). First-order methods are used to calculate a reliability index β, which can be related to probability of failure approximately by

$$Pf = \Phi (- \beta) = 1 - \Phi (\beta) \qquad (2.4)$$

in which Φ(-) is the standard normal cumulative distribution. In Monte Carlo simulation, the random variables are generated according to their probability distribution to represent the structure and loading, and a series of numerical experiments are performed to determine response statistics and failure probability.

2.4.2 Sources of uncertainties

Understanding and quantification of various sources of uncertainty are essential to develop probabilistic models of wood system behavior. Uncertainties are categorized generally as inherent randomness (aleatory uncertainty) associated with the natural variability in nature and knowledge-based (epistemic uncertainty) due to imperfect modeling related to the assumptions and simplifications in engineering analysis, statistical uncertainty due to small sample size, and measurement errors. All sources of uncertainty must be considered in developing reliability-based decision tools. Some factors affecting performance of wood structures are inherently random (aleatory) in nature, and thus are irreducible at the current level of engineering analysis. Others arise from the assumptions made in the analysis of the system and from limitations in the supporting databases. In contrast to aleatory uncertainties, these knowledge-based (or epistemic) uncertainties depend on the quality of the analysis and supporting databases, and generally can be reduced, at the expense of more comprehensive (and costly) analysis.

Wood is a natural material with large variability in engineering material properties, which include modulus of elasticity and modulus of rupture (Green and Evans, 1987). In addition, wood structural systems are designed and fabricated with a large number of connection and fastener details, most of which are difficult to model mathematically, and construction quality and code enforcement can vary significantly from building to building. The behavior of connecting members and elements (e.g., nailing plates, hurricane straps, fastener arrangements) is particularly important to the performance of light-frame wood structural systems exposed to natural hazards, and has received little attention in previous reliability-based studies of wood construction. Probabilistic descriptions of material and structural properties are necessary for reliability analysis: these descriptions will be provided subsequently from a comprehensive review of recent literature (e.g., Reed et al., 1997; Rosowsky and Schiff, 1996; NAHB, 2002).

2.5 Structural fragility analysis

Rewriting Equation 2.3 by separating out one key variable that characterizes the demand, D, on the structural system, the probability of any limit state (LS) of a structure can be defined as

$$P(LS) = \Sigma P(LS \mid D = y)\, P(D=y) \qquad (2.5)$$

where P(D=y) is the probability that the demand equals a specific level y, and P(LS | D = y) is the conditional system limit state probability. The summation emphasizes the role

of the theorem of total probability in risk assessment, but in assessing risk due to natural hazards, the conditioning variable, D, can be wind speed, peak ground acceleration, spectral acceleration or other variable, depending on the way the hazard is specified and the purpose of the risk analysis. The conditional probability of failure of the system for a given loading condition is defined as the system fragility. Equation 2.5 shows that the fragility P(LS | D = y) is a key ingredient for determining the limit state probability of a structural system. Because sources in uncertainty of hurricane and earthquake demands are much greater than other variables and other scientific disciplines often are involved in their determination, it often is desirable to uncouple these dominant sources from the structural system reliability analysis.

The breakdown of risk in Equation 2.5 facilitates risk analysis and decision-making. Wind, flood and earthquake hazards often are determined by governmental agencies such as the National Weather Service or the US Geological Survey. Nowadays, such information often can be retrieved from a website for the particular building site. In contrast, the responsibility for the structural design and, by inference the structural fragility, ultimately lies with the structural engineer.

The fragility is central to the probabilistic safety analysis to assess the capability of a system to withstand a specified demand (say, a 500-yr wind or an earthquake with a 10% probability of being exceeded in 50 years; or, even more simply, a magnitude 7 earthquake centered 20 km from the building site). Such safety margins can be useful for engineering decision-making in situations where the hazard curve is technically difficult

(or costly) to define and a fully-coupled risk analysis (embodied in Equation 2.5) cannot be performed. Conversely, the fragility can be used to identify a level of demand at which there is high confidence that the system will survive. The communication of risk to stakeholders in the building process is facilitated and simplified, as the demand (or interface) variable, D = y, can be selected arbitrarily, depending on the decision at hand.

The structural system fragility often has been modeled by a lognormal cumulative distribution function (CDF) (Kennedy and Ravindra, 1984; Ellingwood, 1990; Singhal and Kiremedjian, 1996; Song and Ellingwood, 1999, Stewart and Attard, 1999; Wang and Wen, 2000). The lognormal fragility model is given by,

$$\text{Fragility} = \quad F_R(y) = \Phi[(\ln(y/m_R) / \zeta_R] \qquad (2.6)$$

where $\Phi(\cdot)$ = standard normal probability integral; m_R is median (50th percentile) capacity which is dimensionally consistent with demand y; ζ_R is standard deviation of ln(R), which describes the inherent variability in the capacity and ζ_R = logarithmic standard deviation, approximately equal to the coefficient of variation (Cov), V_R, when $V_R < 0.3$. By using the lognormal distribution, the entire fragility curve and its uncertainty can be expressed by only two parameters. The validity of the lognormal assumption must be established for wood construction.

Fragility curves for wind or earthquake hazards display the relationship between wind speed or spectral acceleration and probability of exceeding the limit states. Performance

goals must be identified and structural system limit states (LS) must be mapped from these goals before assessing structural system reliability and fragility. System limit states can be either deformation related or strength related. Deformation limit states such as excessive drift give rise to failure of windows/doors, separation of cladding from framing, or failure of roof-wall connections or stud-foundation connections. Strength limit states include structural failure of roof/wall system, sheathing removal, foundation failure, and general structural collapse.

Fragility modeling must be supported by databases to describe the medians and uncertainties in all factors known to affect the ability of the system to withstand challenges from the range of postulated hazards of interest. Sources of uncertainty in the assessment of structural response are reflected in parameter ζ_R (or V_R). In fragility analysis of light-frame wood construction, the control variables (such as the 3- second gust, spectral acceleration at the fundamental period of the building, or similar variable describing the intensity of the demand) are specified as being deterministic while all other uncertainty sources are incorporated into the analysis. For wind load, uncertainties in wind exposure factor, external and internal pressure coefficients, wind directionality, are taken into account (Ellingwood and Tekie, 1999). For earthquake load, the uncertainties in the ground motion are reflected in the suite of accelerograms selected for the analysis.

2.6 Review of literature and critical appraisal

2.6.1 Hurricane wind storms and damage to residential buildings

Post-hurricane disaster surveys have shown that the building envelope is the part of residential construction that is most vulnerable to hurricane-induced damage. Once the envelope is breached, the building and its contents are increasingly likely to suffer severe damage from water or wind effects. In recent years, experimental tests and deterministic analysis for wood frame residential construction subjected to wind load have been conducted for the following components: roof fasteners (Cunningham, 1993; Baskaran and Dutt, 1997), roof panels (Mizzell, 1994), roof-to-wall connections (Canfield, et al. 1991; Reed, et al. 1997; Rosowsky and Schiff, 1996), and glass panels (Harris, 1978; Norville and Minor, 1985). Wind load statistics for residential construction have been investigated by Ellingwood and Tekie (1999).

Post-disaster surveys (Murden, 1991; NAHB, 1993 and 1996) provide an assessment of damage to single-family homes caused by Hurricanes Hugo, Andrew, Iniki, and Opal. In addition, some studies were conducted to investigate the failures of components and related risk and economic losses due to hurricanes. Sparks et al. (1994) studied the relationship of building envelope performance to consequent insurance losses. Minor and Beason (1976) investigated window glass failures in windstorms. Design of glass panels for windborne missiles and wind pressure also was investigated (Minor, et al. 1978; Minor and Norville, 1998). Rosowsky and Cheng (1999) analyzed the probability of

failure of light-frame roof panels in high-wind regions, considering reliability of roof panels and roof-to-wall connections subject to specific wind pressures. A reliability assessment of roof component performance in Hurricane Andrew has been conducted by the National Association of Home Builders (NAHB) (1999a). Hurricane damage prediction models have been developed (Unanwa, et al. 2000; Huang, et al, 2001; Khanduri and Morrow, 2003; Cope, et al. 2003). Ellingwood et al. (2004) presented fragility assessment methodology for light-frame wood construction subjected to wind and earthquake hazards. Subsequently, Kim and Rosowsky (2005) conducted a fragility assessment for roof sheathing failure in high wind regions.

2.6.2 Earthquake-induced damage in light-frame residential construction

The primary lateral load-resisting components for seismic loading in light-frame wood construction are provided by wood frame shear walls. A typical shear wall consists of sheathing material such as plywood or oriented strand board (OSB), frame members and sheathing-to-frame connectors or fasteners. During an earthquake, horizontal seismic force is transferred through the shear walls to the foundation, and energy is dissipated through the interaction between sheathing and connectors and the anchorage of the shear wall to the foundation. Analyzing the behavior of shear walls in a wood light-frame wood building is a difficult task due to several sources of non-linearity, the complex behavior of the connections and fasteners, and the large variability (and uncertainty) in loading, structural material properties, and construction practices and techniques. A number of

experiments have been conducted recently, many as part of the CalTech-CUREe Wood Frame Project, to investigate wood shear wall behavior and to quantify their static and dynamic characteristics. The experiments involved static, dynamic, and shake table testing (Foschi, 1977; Filiatrault, 1990; Dolan and Madsen, 1992; Dinehart and Shenton, 1998; Dinehart et al. 1999; Dinehart and Shenton, 2000; Durham et. al, 2001; Folz and Filiatrault, 2000; 2001; Filiatrault et al. 2002; Paevere and Foliente, 2003; Collins et al. 2005; Bulleit et al. 2005). Most of this research focuses on construction practices that are typical in the Western United States.

At the same time, various numerical models have been developed to predict the structural behavior of wood shear walls and the entire building system. Gupta and Kuo (1987) developed a simple linear elastic building model to represent shear walls, roof diaphragms and ceiling. Richard and Russell (1989) developed a simple structural analysis model to predict the behavior of light-frame building under lateral load. Kasal et al. (1994) used the ANSYS finite element software to analyze a light-frame building. Foliente (1995) proposed an analytical model predict the performance of wood shear walls under seismic loading. A finite element model developed by Richard et al. (1998) was used to analyze shear wall under dynamic loading. In the recent CUREe-Caltech wood frame project, Filiatrault et al. (2001) investigated wood frame building performance during earthquakes. He et al. (2001) developed a nonlinear finite element model to study the performance of a 3-D light-frame timber building under static loading conditions. Kasal et al. (2004) investigated different methods of lateral force distribution

and design. Collins et al. (2005) proposed a nonlinear three-dimensional finite element model capable of static and dynamic analysis of light frame buildings.

Previous structural reliability analysis has focused mainly on reinforced concrete and steel structures (Ellingwood, et al, 1982; Galambos, et al, 1982; Frangopol, 1999; Stewart and Attard, 1999; Wang and Wen, 2000). Fragility models of such systems have been developed, and are becoming important tools for estimating their performance during extreme natural hazards (Shinozuka et al. 2000; Lee and Foutch, 2002). Fewer studies are available for light-frame wood residential construction, which traditionally has been non-engineered. With the trend toward performance-based engineering (Rosowsky and Ellingwood, 2002), reliability analyses of wood shear wall under earthquakes have been performed to predict their performance, so as to evaluate building design codes and construction practice and identify the vulnerability of wood-frame construction (Ceccotti and Foschi, 1999; Foliente, et al 1999; Rosowsky, 2002). Many analyses (Foliente, et al 2000; Van de Lindt and Walz, 2003) have incorporated the variability of earthquake loading via suites of ground motions and have treated the resistance of the shear wall as deterministic, assuming that the major uncertainty in overall shear wall response is due mainly to uncertainty in earthquake ground motion. Foliente et al. (1999) and Paevere and Foliente (2000) investigated the effects of pinching and stiffness degradation on peak response and reliability estimates. Van de Lindt (2004) summarized the evolution and state-of-the-art of wood shear wall testing, modeling, and reliability analysis.

2.6.3 Research tasks for advancing wind and earthquake hazard mitigation in light-frame construction

The above review of current methods for the analysis of performance and reliability of light-frame wood construction under wind and earthquake hazards has identified a series of tasks that appear necessary for advances to occur in natural hazard mitigation of residential construction:

- **Identification and incorporation of uncertainties in structure and natural hazards to obtain probabilities of achieving specific performance objectives**

  In comparison with other common construction materials, relatively little work has been conducted regarding performance and reliability of light-frame wood residential construction under extreme natural hazards. While some reliability analyses have been performed on wood members, connections, and local systems (Ellingwood, 1997), only a few studies have addressed reliability of light-frame wood structural systems (Rosowsky and Ellingwood 2002; Zahn, 1992; Philpot et al. 1995). Furthermore, most analyses and experimental studies conducted to understand the performance of light-frame members, connections, and structural system, have not considered the substantial uncertainties in structure and loading. There is a need for further study to systematically identify and incorporate uncertainties in structure and loading in fragility and reliability analysis for light-frame wood structural systems.

- **Bases for performance-based engineering for residential construction subjected to hurricane**

  In recent years in the United States, performance-based engineering has focused on the seismic hazard. However, the implications of the performance-based engineering paradigm are broader, and should address alternate and competing hazards (e.g. wind) in order to achieve an integrated design goal. With the move toward performance-based engineering, it should become feasible through appropriate design measures to achieve residential building performance that is consistent with social needs. To do this effectively, the relative risks associated with performance under a spectrum of natural hazards must be understood.

- **Effects of fixity or constraints of shear wall on structural fragility and reliability analysis**

  The effects of base fixity or constraints of the shear wall on structural fragility and reliability analysis have not been investigated. The nature of the anchorage of a shear wall to the foundation may determine whether or how the building system withstands earthquake effects. Most previous studies have assumed full fixity, characteristic of construction practices in the Western United States. The evaluation of the performance of wood-frame construction with various boundary conditions of shear walls will give insights on performance of wood-frame construction in regions of low to moderate seismicity in the United States, where the shear wall hold-downs are

customarily not provided or are provided at a minimum level in current building practices.

- **Simplified or rapid risk assessment**

  Tools to identify the relationship between structural response of residential construction and earthquake ground motion intensity for simplified risk analysis are lacking. For example, no attempts have been made to connect drift with spectral acceleration for wood-frame residential construction. Damage estimation procedures in several documents (e.g., FEMA 273) require that the seismic demand (drift) be related to a measure of earthquake ground motion intensity.

- **Comparative risk assessment of residential buildings for hurricane and earthquake hazards**

  Hurricane and earthquake hazards are significant in certain areas of the United States. However, there has been no systematic comparative risk assessment of residential construction exposed to hurricane and earthquake hazards. Integrated building design practices and mitigation of social and economic losses from competing natural hazards would improve overall building safety and performance by optimizing strategies to achieve an overall risk that is consistent with social objectives. To do this effectively, the relative risks associated with performance under a spectrum of natural hazards must be understood.

3 FRAGILITY AND RISK ANALYSIS FOR HURRICANE HAZARDS

3.1 Hurricane damage surveys

Following the hurricanes of the early 1990's, post-disaster surveys were conducted to document the construction characteristics of and damage to light-frame wood residential construction (NAHB, 1993, 1996 and 1999). These surveys utilized statistical sampling techniques, and provide not only a picture of construction practices and characteristics but also descriptions of structural performance in hurricanes which can be used to define performance limits and to validate fragility models.

The post disaster surveys revealed that most economic losses in hurricanes can be related to breach of the building envelope. The breach of envelope includes roof panel uplift, roof-to-wall connection failure, roof system damage, and breakage of glass in windows and doors due to excessive pressure or missile impact. The severe rains accompanying the hurricane cause severe water damage to the building contents after the envelope of the building is breached. Furthermore, the breach of envelope can lead to a significant increase of wind pressure on interior surfaces, leading to progressive failure of other portions of the buildings and even failure of the structural system as a whole in some instances. Research conducted by Sparks et al. (1994) has shown that following the first removal of a roof panel by wind uplift, the magnitude of subsequent loss can amount to 80 % of the total insurance claim. Moreover, with the roof heavily damaged or removed,

the wall may become unstable without sufficient lateral support and collapse (Manning and Nicolas, 1991). Post-disaster surveys have shown that even when some residential building systems appeared intact following the hurricane, those residences were uninhabitable for weeks or months afterward (Murden, 1991).

3.2 Structural modeling

Three basic configurations of light-frame residential buildings were identified for hurricane risk assessment, as summarized in Table 3.1. All has a simple rectangular footprint. These configurations are typical for the residential building inventory in the Southeast United States. Fragility analyses will be performed for these common building configurations and construction practices (defined, e.g., by roof type, roof sheathing, truss spacing, and nailing patterns, roof-to-wall connection and glass panel thicknesses of windows and doors). It should be noted that light-frame wood residential construction traditionally has been non-engineered. Thus, the systems discussed in the sequel represent a mix of prescriptive and experience-based practice, and have not been designed by any specific building code requiring either allowable stress or limit states design (or LRFD).

Table 3.1 Characteristics of Prototype Houses

Type	Dimensions	Number of Stories	Mean Roof Height	Gable Roof
A	28' by 40'	One	12.5'	6:12 slope, framing spaced 2', without overhang
B	28' by 40'	One	12.5'	6:12 slope, framing spaced 2', with overhang
C	28' by 40'	Two	21.5'	6:12 slope, framing spaced 2', without overhang

3.3 Probabilistic description of capacity and loading

In the fragility analysis and the subsequent full coupled reliability analysis, uncertainties in structural component and system capacities and in gravity and wind load effects are required. These uncertainties are modeled probabilistically, as presented in the following sections.

3.3.1 Wind loads on low-rise buildings

The wind pressure in ASCE Standard 7 (ASCE, 1999 and 2003) on components and cladding (C&C) and on main wind force-resisting systems (MWRS) is determined by the equation,

$$W = q_h[GC_p - GC_{pi}] \qquad (3.1)$$

in which q_h = velocity pressure evaluate at he mean roof height, G = gust factor, C_p = exterior pressure coefficient, and C_{pi} = interior pressure coefficient. The velocity pressure, q_h, is evaluated as

$$q_z = 0.00256\, K_z\, K_{zt}\, K_d\, V^2\, I \ (lb/ft^2) \qquad (3.2)$$

$$q_z = 0.613\, K_z\, K_{zt}\, K_d\, V^2\, I \ (N/m^2) \qquad (3.3)$$

in which K_z = exposure factor, K_{zt} = topography factor (taken equal to unity so as not to make the results dependent on local topography surrounding the building), K_d = wind directionality factor, V = 3-sec gust speed at elevation of 30 feet (10m) on open terrain (Exposures C in ASCE Standard 7), and I = importance factor.

The external pressure coefficients, GC_p, for low-rise buildings are area-dependent and depend on the zone of the building envelope considered, as identified in Figure 3.1. The most severe wind pressures on a roof occur in the regions of flow separation at the ridge, eave and corners (zone 2 and 3). For similar reasons, the wind pressure on walls is higher on wall corner areas (zone 5) than interior areas (zone 4).

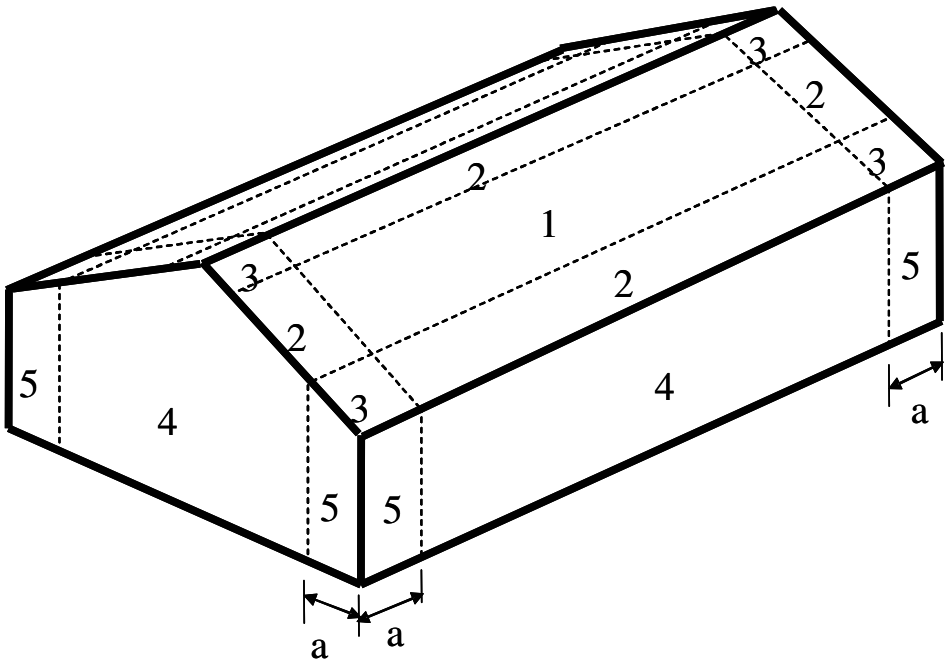

Figure 3.1 Roof and Wall Zones for Wind Pressure in ASCE Standard 7

In ASCE Standard 7, wind load is evaluated differently for components and cladding (C&C) and the main wind force-resisting system (MWRS). By definition, the MWRS is an assemblage of structural elements assigned to provide support and stability for the overall structure, and for elements of the building envelope. According to (ASCE Standard 7, 1998 and 2002; Mehta and Marshall, 1997; Mehta and Perry, 2001), roof panels, windows, and doors are modeled as C&C, while the connection of the roof truss or rafter to the wall is modeled as a MWRS.

Table 3.2 summarizes the statistics of the terms in Equation 3.1-3.3 that are required for the fragility analysis. These statistics are taken from a Delphi study, supplemented by experimental data (Ellingwood and Tekie, 1999). Statistics of exterior pressure

coefficient GC_p for different zones on the roof and wall are included. For Zone 3 on the roof, GC_p for cases C&C and MWRS, corresponding to roof panel and roof-to-wall connection, are different. Interior pressure coefficients GC_{pi} for both fully enclosed and partially enclosed buildings (following damage to the building envelop) are considered. Parameter K_d accounts in an approximate way for wind directionality effects, i.e., the non-coincidence of building orientation and unfavorable wind direction. More sophisticated models involving matches of GC_p and extreme winds determined from the wind rose at specific sites lead to the observation that for buildings where the orientation to strong wind is unknown, wind pressures typically are 75 – 95 % of the worst-case values computed from ASCE Standard 7 (Rigato et al. 2001). This observation is consistent with the statistics for K_d presented in Table 3.2.

Table 3.2 Wind Load Statistics

Variable	One story without roof overhang (Type A)		One story with roof overhang (Type B)		Two story without roof overhang (Type C)	
	Mean	Standard Deviation	Mean	Standard Deviation	Mean	Standard Deviation
K_z (Exposure B)	0.57	0.12	0.57	0.12	0.63	0.12
K_z (Exposure C)	0.8	0.12	0.8	0.12	0.84	0.12
GC_p (C & C) Zone 3	1.81	0.22	3.18	0.38	1.81	0.22
GC_p (MWRS) Zone 3	0.86	0.15	0.86	0.15	0.86	0.15
GC_p (C & C) Zone 4	0.9	0.09	0.9	0.09	0.9	0.09
G_{cpi} (Fully Enclosed)	0.15	0.05	0.15	0.05	0.15	0.05
G_{cpi} (Partially Enclosed)	0.45	0.09	0.45	0.09	0.45	0.09
K_d	0.89	0.14	0.89	0.14	0.89	0.14

C & C : Component and Cladding
MWFRS: Main Wind-Force Resisting Systems

3.3.2 Dead load statistics

The dead loads on roof panels, trusses and roof-to-wall connections are based on the weights of roof panel material and the roof system, respectively. The dead load is assumed to remain constant in time (added weight due to re-roofing is not considered herein) and can be modeled by a normal distribution with a mean value as defined in Table 3.3 and a coefficient of variation of 0.1 (Ellingwood et al., 1982). The dead load

on the roof is available to counteract the effects of wind uplift, and in that load combination it stabilizes the roof and increases its resistance.

Table 3.3 Dead Load Statistics

	Mean	COV	CDF	Source
Roof Panel	1.6 psf (0.077kPa)	0.1	Normal	NAHB (1999)
Roof-to-Wall Connection	15 psf (0.718kPa)	0.1	Normal	Rosowsky and Cheng (1999)

3.3.3 Resistance statistics

Panel uplift resistance

Probabilistic models of resistance of roof panels and roof-to-wall connections to wind uplift are obtained directly from laboratory tests of prototype components rather than by structural analysis. Table 3.4 summarizes the uplift resistance of 4 ft x 8 ft (1.2m x 2.4m) roof panels with two nailing patterns. The nominal diameters for "6d" and "8d" nails are 0.113 in and 0.131 in (2.9 mm and 3.3 mm), respectively. In the laboratory tests, rafters were spaced at 2 ft (600mm) on center (o.c.) and were parallel to the short side 4 ft (1.2 m) of the roof panel. The nail spacing notation "6"/12" means that the panel is nailed to the rafters 6 in (150mm) on center along the panel perimeter and 12 in (300mm) o.c. in the interior of the panel.

Table 3.4 Panel Uplift Resistance Statistics

Nail Type/Spacing	Mean	Cov	CDF	Source
6d nails- 6"/12"	25 psf	0.15	Normal	Rosowsky and Schiff (1996)
8d nails- 6"/12"	60 psf	0.15	Normal	

Roof-to-wall connection resistance

Table 3.5 summarizes the statistics of uplift capacity of two common types of roof-to-wall connections: a connection in which the rafter is connected to the upper sill by three "8d" toenails and a connection in which the rafter is connected to the wall using an H2.5 hurricane clip, installed as per manufacturer specifications. Two sets of data were located for the same clip connection. The first set is from laboratory tests of 15 specimens conducted at Clemson University (Reed et al, 1996). The second set was obtained from tests of 16 specimens conducted at the University of Missouri (Canfield et al. 1991).

Table 3.5 Roof-to-Wall Connection Statistics

Connection Type	Mean	Cov	CDF	Source
3*8d Toe Nail	410 psf	0.34	Normal	NAHB (1999)
Hurricane Clip (Clemson University)	1312 psf	0.1	Normal	Reed et al. (1996)
Hurricane Clip (University of Missouri)	1212 psf	0.15	Normal	Canfield et al. (1996)

Glass resistance to wind pressure and missile impact

The American Society of Testing and Materials (ASTM) Standard E-1300 (2003) specifies the strength of annealed glass as the strength under uniform wind pressure with a 60-sec load duration with a probability of failure 0.008. The 60-sec resistance value of annealed glass can be converted to a 3-sec strength that is consistent with the 3-sec gust wind used in ASCE Standard 7 by multiplying by a factor of 1.2 (Minor and Norville, 1998). A Weibull cumulative distribution is a common model for defining the probability of failure of brittle materials such as glass, and it is used to model strength of glass to uniform wind load (Norville and Minor 1985). Norville and Minor (1985) found that the coefficient of variation of glass strength is in the range of 0.22 to 0.27, and it is assumed to be 0.25 in the following analysis. The aspect ratios (height/width) of windows and glass doors are assumed to vary from 1:1 to 1:2, typical values for windows and sliding glass doors. Two different thicknesses of annealed glass panels, namely 3 mm (1/8 in)

and 5 mm (3/16 in), were selected for the glass fragility analyses, with different areas of 20 sq ft (1.1 m^2) and 40 sq ft (3.6 m^2) representing small and big windows and glass sliding doors.

Statistics of glass failure due to airborne missile impact are based on research of Minor et al. (1978), who investigated the relationship between wind speed, missile impact speed and breakage. It was found that when a 0.0122 lb (0.005 kg) projectile is picked up by wind and has been accelerated over a distance of 50 ft (15 m), the impact velocity is about 35% of the speed of the wind transporting the projectile. Harris (1978) studied the effects of thickness and area of glass on glass breaking velocity, and found that the minimum breaking glass velocity is independent of area of the glass due to the local character of missile-induced failure. Three different thicknesses of glass panels, namely 5 mm, 6 mm, and 12 mm, were considered in modeling glass panel fragility due to missile impact. A lognormal distribution was used to describe the glass breaking velocity (Unanwa et al. 2000). Table 3.6 summarizes the statistics of glass capacity due to wind pressure and missile impact.

Table 3.6 Statistics of Glass Capacity

	Glass Type	Failure Mode	Mean	COV	CDF	Source
Annealed Glass (Window and Glass Door)	1/8 in; 20 sq ft	Pressure	54.47 psf	0.25	Weibull	ASTM (2003); Norville and Minor (1985);Minor and Norville (1998)
	3/16 in; 40 sq ft		32.04 psf	0.25		
	3/16 in; 20 sq ft		96.12 psf	0.25		
	3/16 in; 40 sq ft		51.26 psf	0.25		
	3/16 in thickness	* Missile Impact	22.8 mph	0.07	Log-Normal	Minor et al(1978); Harris (1978); Unanwa et al. (2000)
	1/4 in thickness		21.4 mph	0.05		
	1/2 in thickness		26.4 mph	0.07		

** Assume 15 m of acceleration of 0.005Kg missile, impact velocity is 35% of carrying wind speed. Glass resistance is adjusted to 3 sec duration loading.*

3.4 Fragility of light-frame wood systems under hurricane winds

3.4.1 Performance limit state (LS)

In performance based engineering, "failure" is defined as occurring when the building system fails to satisfy the prescribed requirement. For the reasons discussed in section 1.1.3, the limit state (LS) is related to the breach of envelope, which is closely related to the performance objective to minimize property damage. For uplift of roof panels or damage to the roof system caused by failure of the roof-to-wall connection, the limit state in Equation 2.2 can be expressed as

$$G(X) = R - (W - D) \qquad (3.4)$$

where R = resistance of panel uplift or roof-to-wall connection, W = uplift load due to wind, and D = dead load on panel or roof-to-wall connection.

The limit state for the roof sheathing is modeled as the failure of the first panel because of the strong correlation between panel removal and subsequent contents damage noted previously. Panels at the roof corner are subjected to the highest wind uplift forces according to Figure 6 - 5 in ASCE 7-98 and Figure 6 - 3 in ASCE 7-2002, where the local pressure coefficients are the highest of any point on the roof surfaces. During wind load tests for residential roofs (Mizzell and Schiff, 1994; Rosowsky and Schiff, 1996) it was found that an "equivalent tributary area" for a fastener in a critical location of a roof panel was on the order of 1-2 ft^2 (0.093 – 0.19 m^2). Once failure of a single fastener occurred, the load was distributed to the surrounding fasteners causing failure to propagate throughout the panel. The reliability of roof sheathing is modeled as a series system, defined as the first panel failure.

For the roof-to-wall connection, the second connection from the end zone of a gable roof is most critical because the tributary area of that connection lies on the critical edge of the end zones of the roof, where the pressures are amplified by the characteristics of the wind flow over and around the roof.

For breakage of windows and glass doors due to excessive wind pressure, the limit states is defined as

$$G(X) = R - W \tag{3.5}$$

where R = resistance of the glass panel to wind pressure and W = uniform wind load on glass.

For breakage of windows and glass doors due to windborne missile impact, the limit state is defined as the point at which the missile impact velocity exceeds the minimum breaking velocity of the glass panel (Harris, 1978).

3.4.2 Hurricane fragility curves

Fragilities of structural components and systems for the various performance limit states defined above are developed as a function of hurricane wind speed using the limit states defined in Equations 3.4 – 3.5. The reference wind speed, v, is the 3-sec gust wind speed at an elevation of 33 ft (10 m) in open terrain (Exposure C defined in ASCE Standard 7), providing a direct connection between the conditional probability of failure and the manner in which wind speed is specified in ASCE Standard 7 (ASCE, 2003). Basing the fragility on the 3-sec gust wind speed also facilitates the subsequent reliability analysis involving the convolution of structural fragility and hurricane hazard defined by alternative wind speed models.

First-order (FO) reliability analysis (e.g., Melchers, 1999) is used to determine the probability of failure of key components and systems that are necessary to maintain the

integrity of the building envelope and to minimize losses. The conditional probabilities of failure that form the fragility curve are obtained by increasing the wind speed in 10 mph increments and repeating the FO analysis at each wind speed.

Fragility of roof panel

Figure 3.2 illustrates roof panel fragilities for the different roof configurations and nailing details and patterns summarized in Section 3.3. The figure indicates that the roofs with roof panels installed with 6d nails are almost certain to suffer severe damage under Hurricane Andrew-like conditions (3-sec gust speed of 165 mph (74 m/s), with almost 100% certainty of losing of at least one panel. The failure rates of roof panels installed with 8d nails on roofs lacking an overhang under the same conditions are approximately 65%.

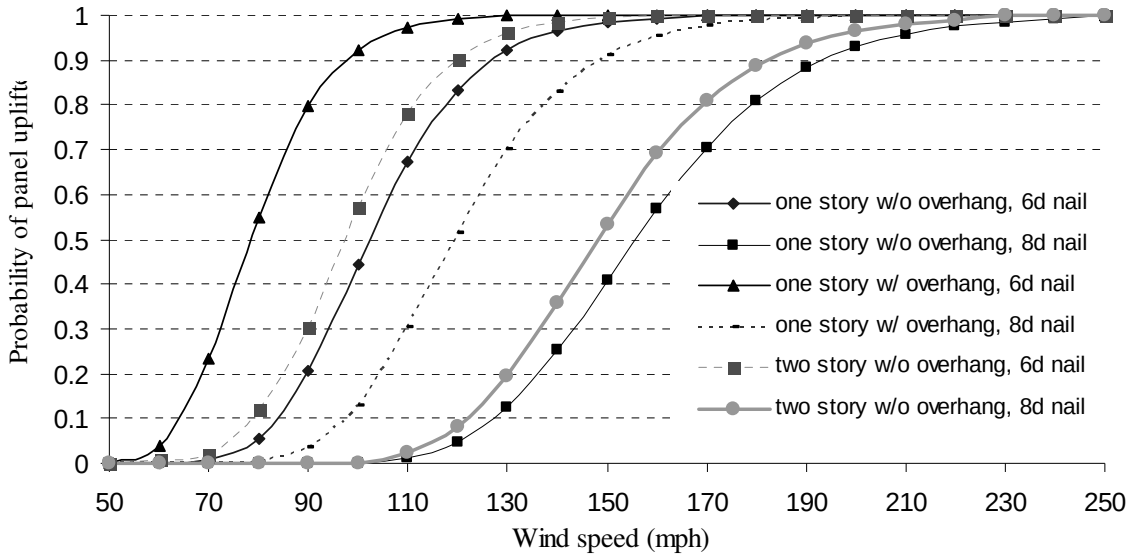

Figure 3.2 Roof Panel Fragilities for Three Typical Houses (Exposure B)

Fragility of roof-to-wall connection

Figure 3.3 compares the roof-to-wall connection fragilities for a one-story house (Type A in Table 3.1) without a roof overhang in exposures B and C. The benefit of the hurricane clip over toenailing across the range of hurricane wind speeds is readily apparent.

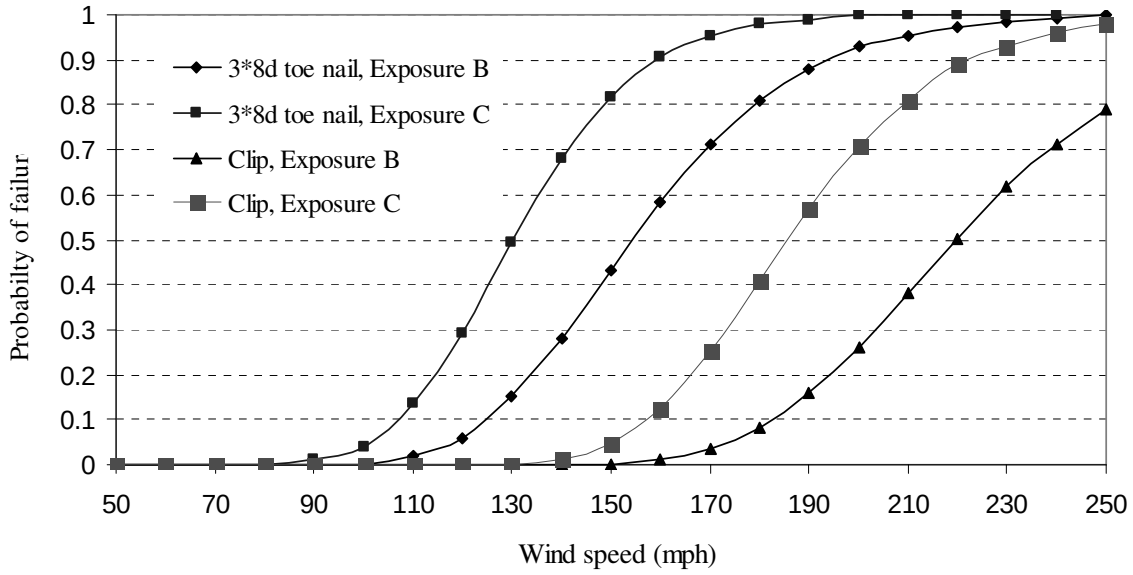

Figure 3.3 Roof-to-Wall Connection Fragilities for One-Story House without Roof Overhang

Fragility of glass due to wind pressure

Figure 3.4 illustrates fragilities of windows and doors with different glass panel thicknesses and areas for the case where glass failure is due to excessive wind pressure. Note that the glass thicknesses in this figure (and the one to follow) correspond to thicknesses for the available data summarized in Table 3.6. The vulnerability of larger windows and door is evident in this figure.

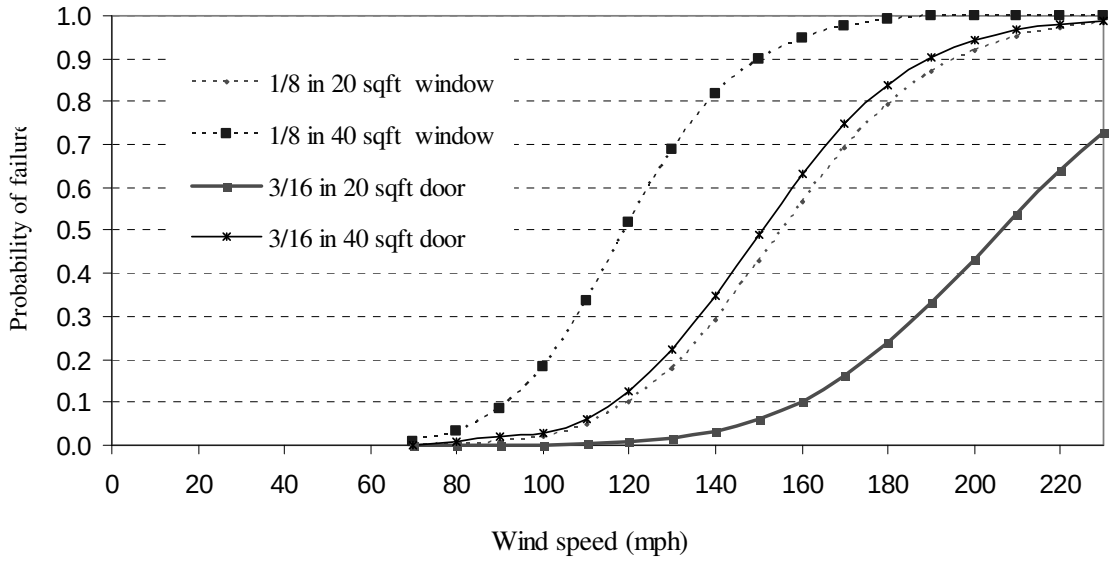

Figure 3.4 Fragility of Glass Panel due to Wind Pressure

Fragility of glass due to projectile impact

Figure 3.5 shows the fragilities of glass breakage by windborne missile impact, under the assumptions stated in section 3.3.3 regarding the projectile size and acceleration. Three types of annealed glasses, namely 3/16, 1/4, and 1/2 in (5, 6, and 12 mm), are considered, as indicated in Table 3.5. As might be expected, the glass thickness is a dominant factor in failure caused by missile impact. For example, the probability of breakage of windows or glass doors with 3/16 in (5mm) glass panels from missile impact at a wind speed 160 mph (72 m/s) is about twice as high as that for windows or doors with 1/2 in (12 mm) glass panels. However, as indicated in Section 3.3.3, the minimum breaking velocity of glass is independent of the area of the glass pane.

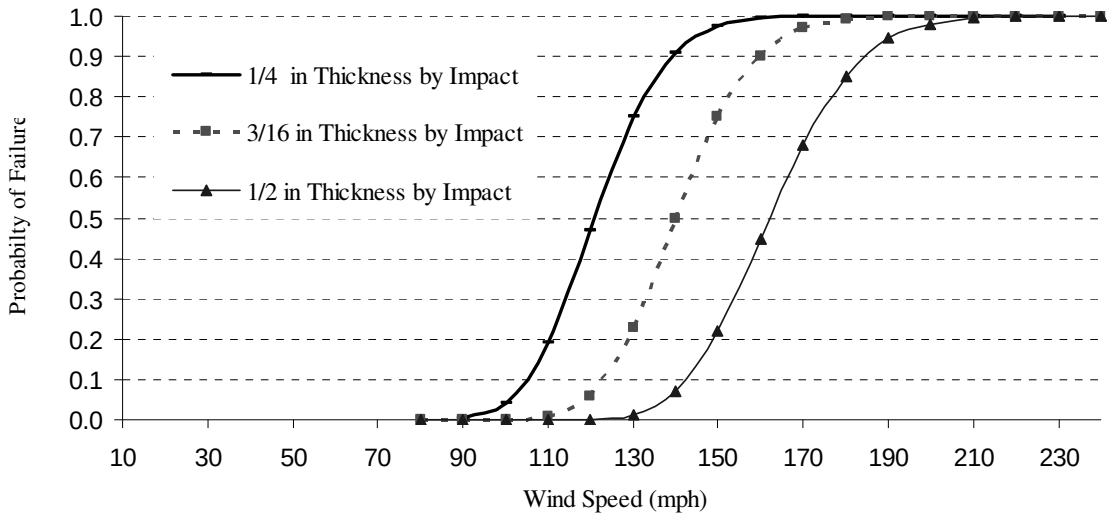

Figure 3.5 Probability of Window Failure by Missile Impact

3.4.3 Parametric sensitivity analysis

Many variables and their uncertainties affect the structural fragility. A parametric sensitivity analysis can identify the relative importance of each variable and the main sources of uncertainty that affect the structural performance, providing insight on areas where to target further modeling and data collection. The sensitivity analysis is conducted to deconstruct the fragilities of typical light-frame wood building structures into their dominant contributors. This process offers an efficient basis for improving building practice according to the relative importance of each variable.

Effects of building enclosure integrity on roof panel and connection fragilities

Figure 3.6 demonstrates the effects of full vs. partial building enclosure on the fragility of roof panels with two nailing patterns. A breach of envelope which leads to increase in the mean internal pressure coefficient from 0.15 to 0.45 plays an important role in the fragility of the panel, increasing the failure probability by approximately 15% at a given wind speed for both nailing diameters. Similarly, Figure 3.7 shows the effects of a breach of the envelope on the fragility of roof-to-wall connection. The difference in probability of connection failure before and after the envelope is breached is on the order of 20 to 30 percent. However, the failure of the clip connection is more sensitive to whether initial breach has caused the internal pressure to increase than the failure of toenail connection.

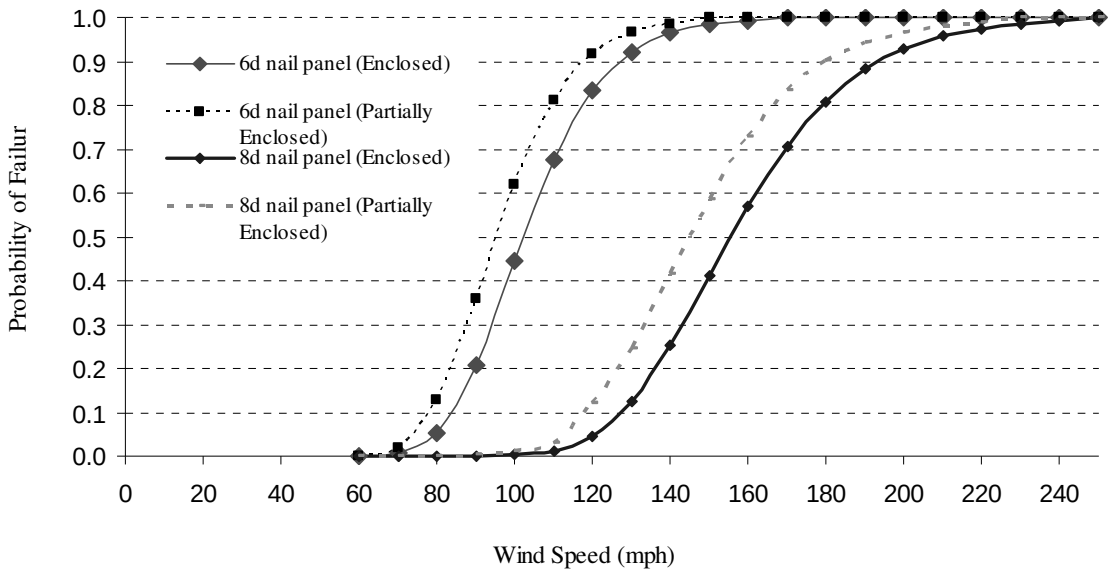

Figure 3.6 Effects of Building Enclosure on Panel Fragility of Type A House (Exposure B)

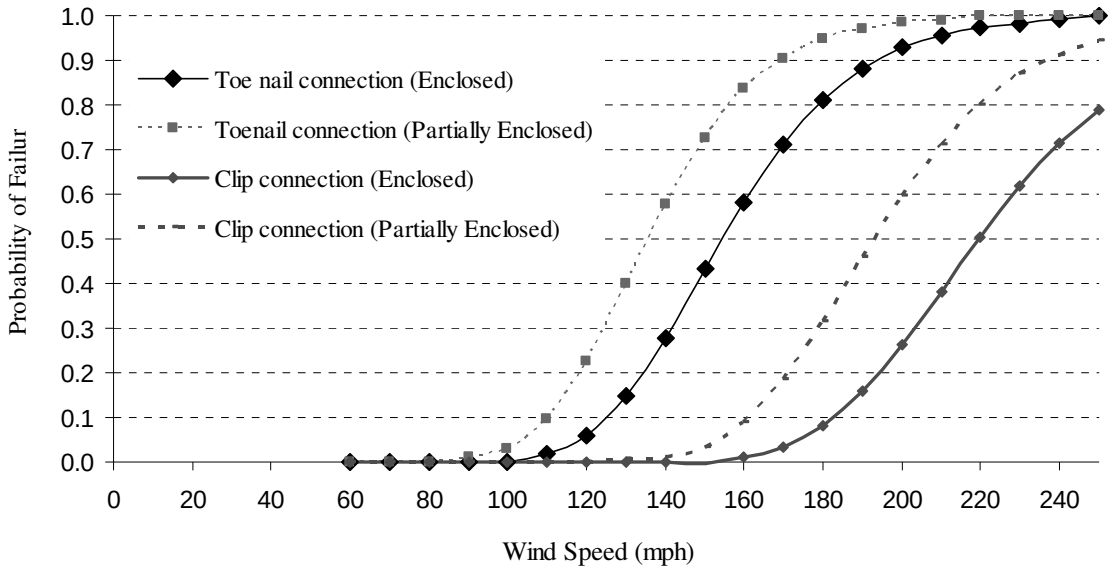

Figure 3.7 Effects of Building Enclosure on Connection Fragility of Type A House (Exposure B)

Effects of roof overhang and roof height

Figure 3.8 shows that the effects of roof overhang on panel fragility are significant because the exterior pressure coefficients (GC_p) are very different for roof zones when a roof overhang is present (from Table 3.2, mean values of 3.18 and 1.81, respectively). Conversely, the height of the roof has little impact on fragility because mean values of GC_p for one-story and two-story houses are about the same (0.57 vs. 0.63).

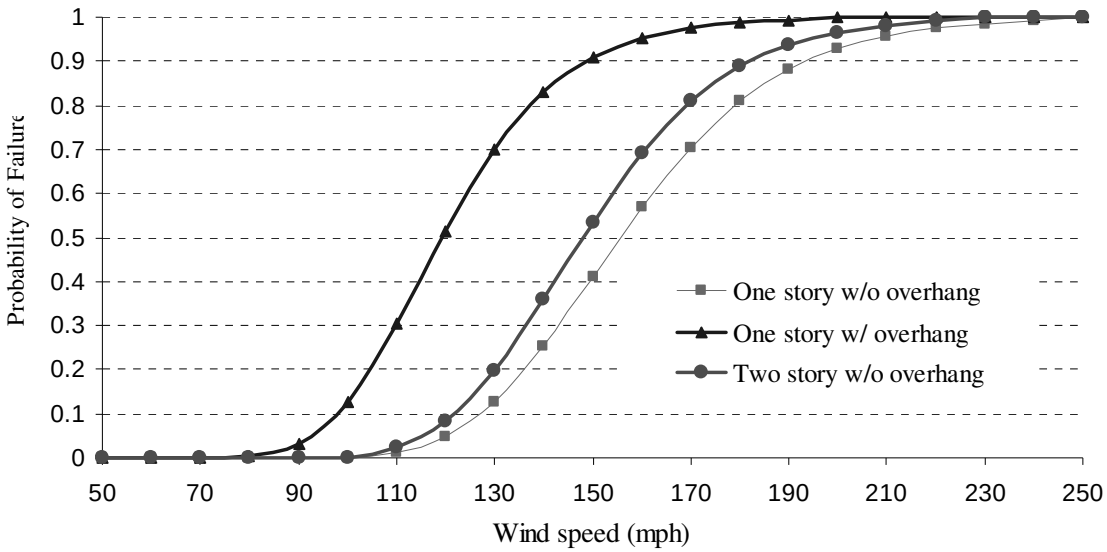

Figure 3.8 Effects of Roof Overhang and Height of House on Fragility of Roof Panel Installed with 8d Nail (Exposure B)

Effects of glass failure modes (by missile impact and wind pressure)

Figure 3.9 provides insight on the relative likelihood of glass panel failure due to missile impact and excessive wind pressure. It is assumed that the glass is 3/16 in (5mm) in thickness in all cases. It can be seem that the glass failure is dominated by wind pressure for wind speeds less than approximately 110 mph (49 m/s); conversely, the failure rate due to projectile impact becomes much higher than that due to excessive wind pressure when wind speeds exceed 110 mph (49 m/s) for larger windows or sliding glass doors (with areas of 40 sq ft or 3.6 m^2).

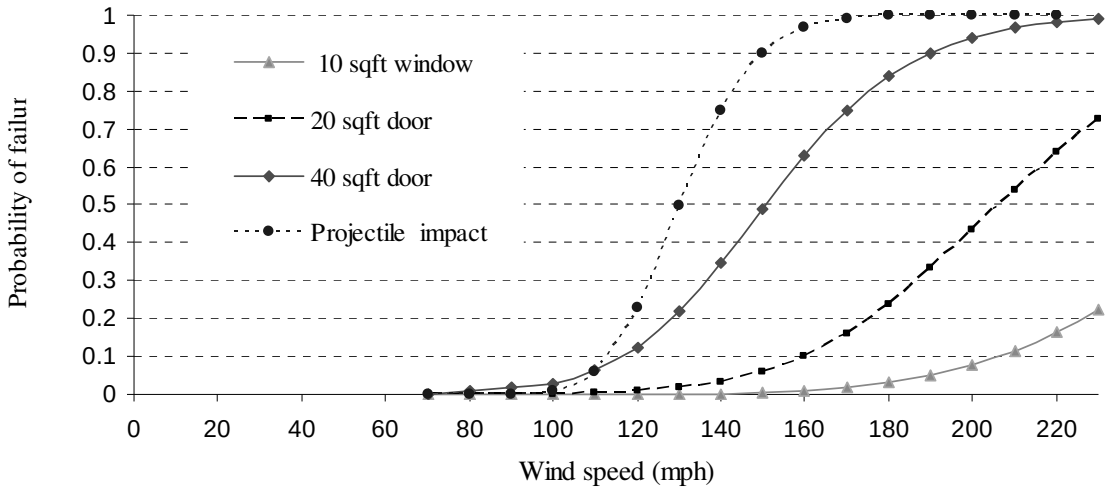

Figure 3.9 Glass Panel Fragility due to Wind Pressure and Impact

Effects of connection diameters and types

Nail size affects roof panel fragility significantly because 6d nails only offer 25 psf (1.20 Pa) mean panel resistance to uplift while 8d nails provide 60 psf (2.87 Pa) mean resistance (Table 3.3). For the roof-to-wall connection, a properly installed hurricane clip usually provides sufficient resistance while reliance on 3*8d toenails does not. If the wind speed is 170 mph in exposure B, it is 70% likely that roof-to-wall connections in a one-story residence relying on 3*8d toenails will fail, but only 5% will fail if a hurricane clip is used.

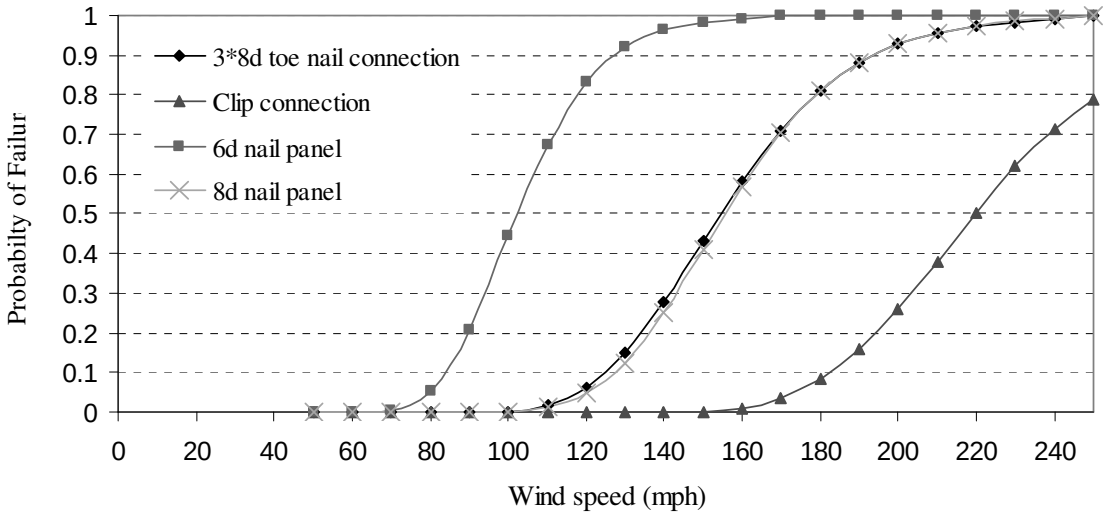

Figure 3.10 Effects of Fastener Diameters and Types on Fragility of Type A House (Exposure B)

Buildings sited in Exposure B vs. Exposure C

Building exposure (open vs. suburban) impacts the fragility because the mean value for the exposure factor (K_z) increases from 0.57 to 0.80 when the exposure changes from B to C, as can be seen in Figure 3.11. For example, the probability of failure of a roof-to-wall connection in a one-story house in exposure B utilizing 3* 8d toenailing is 58% when wind speed is 160 mph (76 m/s), compared to 88% failure rate of a similar building in exposure C.

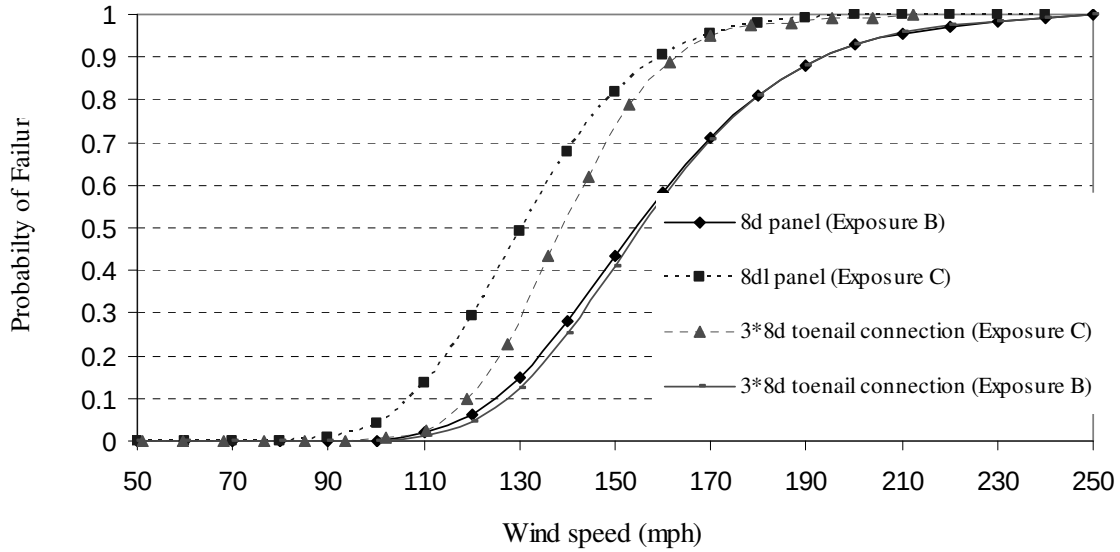

Figure 3.11 Effects of Wind Exposure on Fragility of Type A House

Among all the factors considered above, the wind speed has the most significant impact on failure probability, because the wind pressure in Equation 3.2-3.3 depends on the square of the wind speed. Hurricane wind speed modeling is described subsequently in further detail below.

3.4.4 Validation of hurricane fragility model

The hurricane fragility modeling described above must be validated before being used for risk assessment. The validation is performed by comparing fragility predictions to post-disaster surveys following hurricanes. Validation of the hurricane wind fragility analysis presents a challenge due to the complex nature of the hurricane hazard, the mix of building types in the area affected by the hurricane, and the lack of statistics suitable for

modeling system behavior of light-frame wood construction. In a specific community under study, there would be a wide variety of building configurations with various plan sizes and shapes, roof heights, roof slopes, structural systems, ages, governing building codes (if any) and design practices.

The fragility curves for different building construction characteristics in a community must be aggregated to evaluate damage levels in groups of houses in order to compare predicted and observed damage statistics. Figure 3.12 illustrates the results of the aggregation for failure of roof panels and roof-to-wall connections, and makes a comparison of the predicted damages with failures observed in post-disaster damage surveys of Hurricane Andrew (NAHB, 1993). In Hurricane Andrew, the highest 3-sec gust speed was approximately 165 mph (NAHB, 1993). Post-disaster surveys showed that 69% +/- 6% of one-story single-family houses with moderate sloped gable roofs with wood panels lost at least one roof panel. Moreover, approximately 90% of the severely damaged residences were located in exposure B (NAHB, 1993). Approximately 70% of roof sheathing panels were attached with 6d nails and 30% used 8d nails (NAHB, 1993). Approximately 50% of residences have a roof overhang; 50% either do not or have an overhang with a soffit (NAHB, 1993 and 1999a). It is assumed that the affected area surveyed was exposed to the highest wind speed. In Figure 3.12 the roof panel fragility curves for one-story houses is in exposure B. The estimated probability of at least one panel failure is approximately 90%, which is higher than the 69% observed; however it is important to note that this is based on the highest observed peak gust wind speed.

Considering that peak pressures acting on the roof occur over a very small area, this prediction can be viewed as a conservative upper bound on the failure rate.

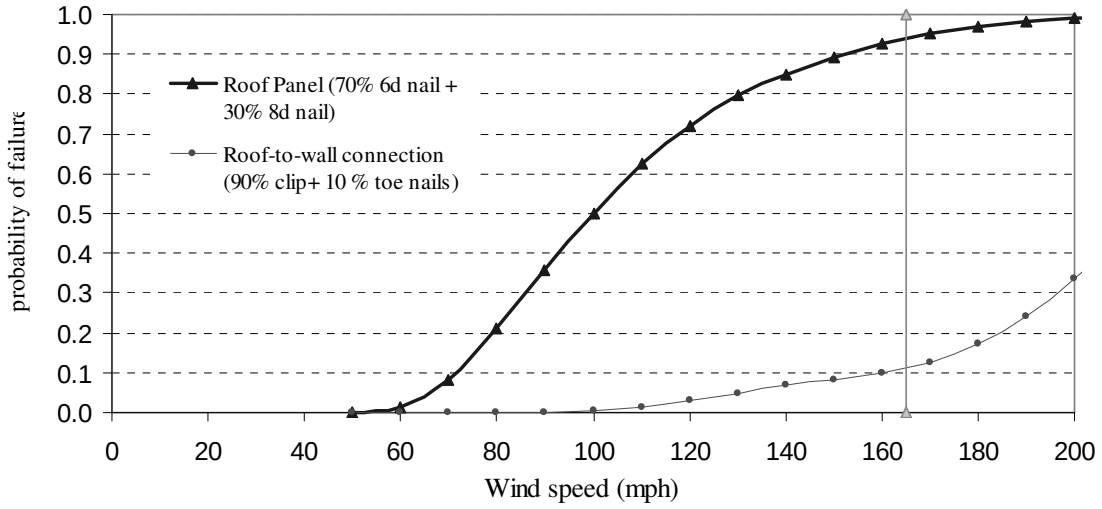

Figure 3.12 Comparison of Prediction with Post-Disaster (Hurricane Andrew) Survey

Similarly, based on data in NAHB (1993) and NAHB (1999a), it is assumed that 95 % of one-story houses in South Florida at the time used the hurricane clip for the roof-to-wall connection, while in 5% the roof truss was toe-nailed to the upper sill plate. The post-disaster survey indicated that approximately 12% of houses suffered roof-to-wall connection damage. Figure 3.12 also presents the roof-to-wall connection fragility of a one-story house in exposure population B. The estimated probability of roof-to-wall connection failure is close to 10%. Considering that the survey result of 12% included both one-story and two-story houses (in which the probability of connection failure is slightly higher due to the higher wind load for two-story house), the prediction is close to the survey result.

While these preliminary validation studies are promising, additional studies along the lines of the above are necessary to enhance the confidence in the methodology. Such studies will require more detailed information regarding the building inventory and further detailed statistical data from post-disaster surveys of building performance.

3.4.5 Validation of lognormal hurricane fragility model

The fragility curves in Figure 3.1 to 3.9 were developed directly from a series of first-order reliability analyses for increasing hurricane wind speeds. Accordingly, during the process, no assumptions were required regarding the appropriate distribution of the structural fragility model. If a particular distribution can be identified as an appropriate model for the fragility, then the development of the fragility model can be reduced to estimating the two or three parameters (e.g., median, coefficient of variation) required to define the model rather than the entire model itself. Development of fragility models (and their defining parameters) often requires simulation-based finite element reliability analysis. Since far fewer simulations are required to estimate the model parameters than to identify the model itself, knowledge that the fragility can be described by a particular cumulative distribution function (CDF) makes the fragility analysis more computationally efficient.

As noted in Chapter 2, the structural fragility often has been modeled by lognormal CDF for other structural systems. Only two parameters, median m_R and logarithmic standard

deviation ζ_R, are needed to fully describe this fragility model. Furthermore, the sampling errors associated with the estimates are much smaller than those in the estimates of lower fractiles (on the order of 5-10%) of fragility curves (e.g. Figure 3.2 to 3.11), the values that are significant in hurricane risk assessment, code development and engineering risk analysis. The question arises as to whether the lognormal CDF provides an appropriate model for hurricane fragility for light-frame wood construction. If the lognormal CDF provides a good fit from the fragility curves developed by a set of FO analyses, then the two lognormal parameters can be determined by only two first-order analyses, and the previous approach that involved a sequence of first-order analyses will be unnecessary.

A series of statistical analyses were performed to test the hypothesis that the lognormal CDF is a suitable model for fragility of light-frame wood construction subjected to hurricane winds. To begin, the CDFs ($F_R(v)$) determined from the FO analyses are plotted on lognormal paper. Such a plot for failure of a roof panel to wind uplift is illustrated in Figure 3.13; the linearity of the plot provides support for the lognormal assumption. The probability plot correlation coefficient is very close to 1 (0.997) which is presumptive evidence that a lognormal CDF is a good model for these data (Filliben, 1975).

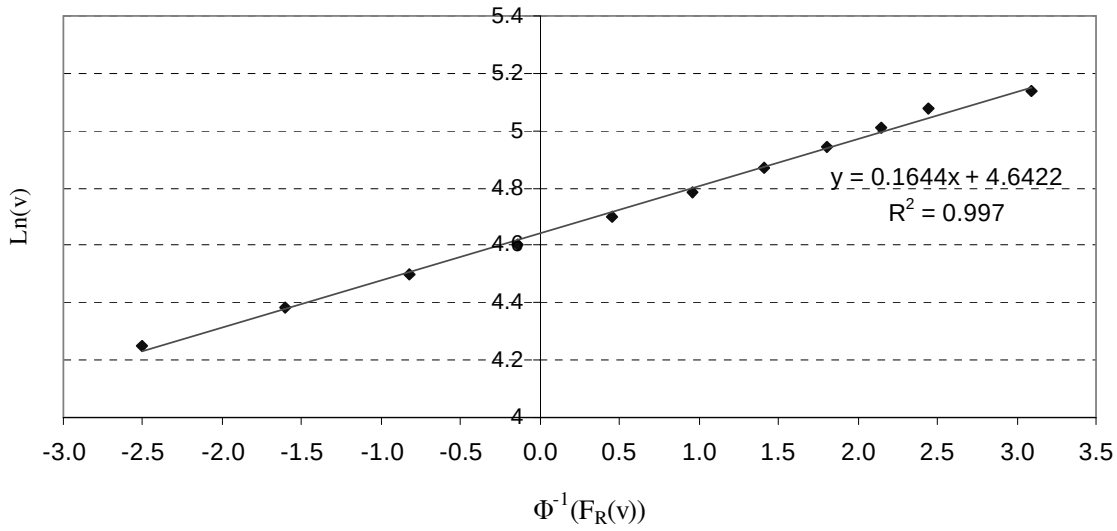

Figure 3.13 Lognormal Probability Plot (6d Nail Panel Fragility Curve, Exposure B)

Similar results were obtained for panels with other nailing patterns, roof-to-wall connection details, and glass breakage due to wind pressure and missile impact. It was noted that the lognormal model appeared superior (in terms of linearity of plot and probability plot correlation coefficient) to the Weibull distribution, despite the fact that the glass resistance to wind pressure is modeled by a Weibull distribution, as shown in Figure 3.14 and 3.15 for 1/8 in (3mm) glass panel of 40 sq ft (3.7 m^2).

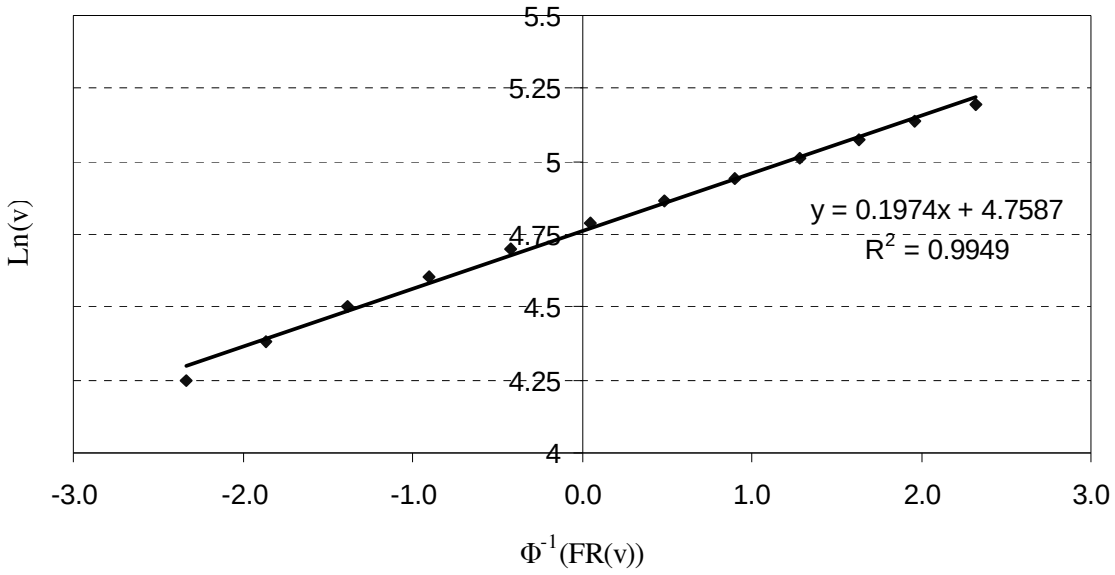

Figure 3.14 Lognormal Probability Plot (1/8 in 40 sq ft Glass Panel)

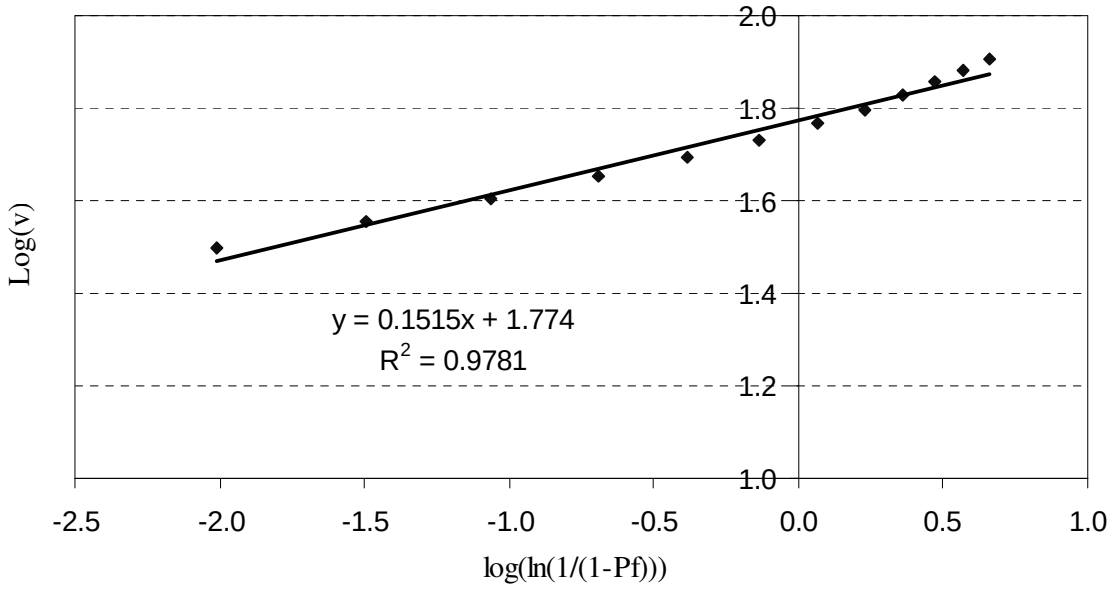

Figure 3.15 Weibull Probability Plot (1/8 in 40 sq ft Glass Panel)

Following an examination of all probability plots, a Kolmogorov-Smirnov (K-S) test was performed for all fragility curves developed from the FO analysis. The K-S test provides no evidence to reject the hypothesis (at 5% significance level) that the lognormal CDF describes the hurricane fragility of light-frame residential construction.

Table 3.7 summaries the lognormal distribution parameters for the fragilities of roof panels, roof-to-wall connections, and glass panels due to excessive pressure and missile impact. Note that the logarithmic standard deviations (coefficients of variation) for roof panels and roof-to-wall connections tend to cluster around 16 %, despite the variety of structures, exposures, and fasteners. For glass breakage due to excessive pressure, the logarithmic standard deviations are about 20%, regardless of thicknesses and area of the glass panel.

Table 3.7 Lognormal Fragility Model Parameters

	Description	Type	Lognormal Fragility Model Parameters	
			$L_n(m_R)$	ζ_R
Roof Panel	Exposure B	Type A, 6d nail	4.6422	0.1644
		Type A, 8d nail	5.0564	0.1600
		Type B, 8d nail	4.7977	0.1675
Roof-to-Wall Connection (Clemson data)	Exposure B	Type A, Toe nails	5.0491	0.1757
		Type A, Clip	5.3959	0.1428
	Exposure C	Type A, Toe nails	4.8720	0.1576
		Type A, Clip	5.2339	0.1341
Glass of Window or Sliding Door	Failure by Pressure	1/8 in 20 sq ft	5.0178	0.2086
		1/8 in 40 sq ft	4.7587	0.1974
		3/16 in 20 sq ft	5.3330	0.2248
		3/16 in 40 sq ft	4.9833	0.2096
	Failure by Impact	3/16 in	4.9400	0.1070

3.5 Reliability assessment of buildings exposed to hurricanes

3.5.1 Probabilistic safety assessment

A fully coupled reliability analysis provides a framework to incorporate uncertainties in structural system and loading and a tool to measure the performance and reliability of a structural component or system subjected to hurricane hazard on a consistent basis. The probability of failure under a spectrum of possible hurricane winds is determined by convolving the structural fragility curve and hurricane hazard:

$$P_f = \int F_R(v) * f_v(v) dv \qquad (3.6)$$

in which $F_R(v)$ is the structural fragility and $f_v(v)$ is the probability density function for hurricane wind speed. The wind speed, v, can be expressed with reference to an annual extreme wind speed, a 50-year extreme wind speed, or extreme for another reference period, depending on the purpose of the risk analysis.

3.5.2 Hurricane wind models

The hurricane hazard is expressed by a wind speed distribution function for a standard averaging time (3 sec), open terrain (Exposure C), and elevation 33 ft (10m). Because of a lack of statistics of occurrence of hurricanes at specific mileposts along the coast and the need for estimate wind speeds at long return periods for design and risk analysis purposes, hurricanes are simulated probabilistically from fundamental climatological modeling principles and data (described in more detail below), and the resulting wind speeds at specific mileposts are derived from the wind field model. These wind speed are post-processed statistically and are used to develop design wind speed maps for ASCE Standard 7 and for other purposes.

Several hurricane wind prediction models have been developed (Batts et al. 1980; Georgiou et al. 1983; Georgiou, 1985; Vickery and Twisdale, 1995 a, b; Vickery et al.

2000). The general approach used in these models is similar (Vickery et al. 2000). Statistical models of key site-specific parameters, including hurricane central pressure, radius, heading, and crossing point along the coast, are collected. Then Monte Carlo simulation is used to sample the parameters, and the wind speed is recorded when a mathematical representation of the hurricane passes the site. The physical models of the hurricane, such as filling rate and wind field, and the area over which the local climatology is assumed to be uniform, which is used to derive the statistical characterization of the hurricane, differ from model to model. In addition, some hurricane prediction models use a coast segment crossing approach, while others use a circular sub-region approach. These differences in wind field modeling affect the wind speed prediction.

Although the wind field models are different, the Weibull distribution appears to be a suitable model for hurricane wind speeds determined from all models (Peterka and Shahid, 1998; Batts et al. 1980; Vickery et al. 2000).

The two-parameter Weibull distribution CDF is given

$$F_V(v) = P(V<v) = 1 - \exp\left[-(v/u)^{\alpha}\right] \qquad (3.7)$$

The scale and dispersion parameters, u and α, are site-specific and can be determined from the published wind speed maps from the above hurricane studies that define the relationship between wind speed, V_T, and return period, T:

$$v_T = u * [-\ln(1/T)]^{1/\alpha} \quad (3.8)$$

which is derived from Equation 3.7 through

$$P(V>v_T) = 1 - (1/T) \quad (3.9)$$

Considering the area at the southern end of Florida as an example, the wind speed maps developed by Vickery et al. (2000) indicate that the 50, 100, and 1000-year return period 3-sec gust wind speed in open terrain are 132, 150 and 182 mph (59, 67 and 81 m/s), respectively. The corresponding Weibull distribution parameters are u = 61.07, α = 1.769. Similar procedures can be are applied to Batts et al. and Georgiou wind models in south Florida. The Weibull distribution parameters for the three hurricane wind speed models are summarized in Table 3.8.

Table 3.8 Weibull Distribution Parameters for Different Hurricane Wind Speed Models in South Florida (1 mph = 0.447 m/s)

Hurricane Wind Speed Model		Batts et al.	Vickery et al.	Georgiou
Wind Speed (mph)	50 year	120	132	150
	100 year	130	150	162
	1000 year	155	182	208
Weibull Distribution Parameters	u	64.86	61.07	68.33
	α	2.218	1.769	1.738

3.5.3 Limit state probabilities

Structural fragilities developed previously and the hurricane wind speed models summarized in Table 3.8 above are used to determine point and interval estimates of annual probabilities of damage to roof panels and to roof-to-wall connections. The lognormal models of structural fragility and Weibull models of wind speed are convolved by numerical integration to obtain these estimates.

The annual probabilities of failure of roof panels and roof-to-wall connections for several types of low-rise residential construction in south Florida are determined first using the Vickery et al. (2000) hurricane wind speed model, which is most recent and is the basis for the wind speed contours in ASCE Standard 7-02. The results of this analysis are shown in Table 3.9.

Table 3.9 Reliability of Roof Panel and Roof-to-Wall Connection in South Florida

	Exposure	Type	Lognormal Fragility Model Parameters		Pf
			$Ln(m_R)$	ζ_R	
Roof Panel	Exposure B	Type A, 6d nail	4.6422	0.1644	0.0540
		Type A, 8d nail	5.0564	0.1600	0.0100
		Type B, 8d nail	4.7977	0.1675	0.0320
Roof-to-Wall Connection	Exposure B	Type A, Toe nails	5.0491	0.1757	0.0110
		Type A, Clip (Clemson data)	5.3959	0.1428	0.0013
	Exposure C	Type A, Toe nails	4.8720	0.1576	0.0230
		Type A, Clip (Clemson data)	5.2339	0.1341	0.0036

A deconstruction of the limit state probability integral in Equation 3.6 reveals that a relatively small range of v accounts for the major part of P_f. One can, for example, determine (by trial and error) the range of v that comprises (90%) of P_f; that range corresponds to 85-180 mph 3-s gust wind speeds for roof panel uplift and 115-200 mph for failure of toe-nailed roof–to–wall connections. In comparison to the 50-yr return period that is the basis for the wind speed maps in ASCE Standard 7-02, the return periods associated with these wind speeds ranges from approximately 30 to 700 years. Such results suggest that further meteorological refinements and risk mitigation efforts should be focused on storms with wind speeds in this range.

3.5.4 The role of epistemic uncertainty in reliability analysis

The fragility and reliability analysis presented in previous sections include inherent (or aleatoric) uncertainties, to the extent that such uncertainties can be captured in the available databases. Epistemic uncertainties also play an important role in risk assessment, they impact the confidence with which decision makers can make judgments from the estimated limit states probabilities such as those presented in the previous section.

To illustrate this point, epistemic uncertainties arising from the use of roof-to-wall hurricane clip connection data from different sources and in hurricane wind speeds estimated from the various wind field models are considered in this section. Two sources of roof-to-wall clip connection data were obtained from different experimental programs (Reed et al. 1997; Canfield et al. 1991); the statistics are summarized in Table 3.5. Similarly, Table 3.8 summarizes the Weibull distribution parameters describing hurricane wind speed corresponding to the three wind field models in south Florida. The writer makes no judgment as to the relative validity and credibility of these different sources of data that support reliability assessment, noting only that the investigators involved all are respected in their fields and the publications from which the data have been extracted all have been peer-reviewed. The purpose here is simply to illustrate the role of epistemic uncertainty in reliability assessment through a data collection and analysis effort that is similar to challenge that might confront a typical decision-maker.

Table 3.10 summarizes the limit state probabilities associated with roof-to-wall clip connection failure due to wind uplift obtained using different connection resistance data and various wind field models. When sources of uncertainty for structural resistance and wind load are considered simultaneously, the uncertainty associated with the various wind field models is far more significant than the uncertainty from different connection testing programs. The magnitude of difference in P_f due to sources of connection resistance data is about 30-50%, while the difference in P_f resulting from the various wind speed models can reach an order of magnitude.

Table 3.10 Comparison of Effects of Hurricane Models and Sources of Roof-to-Wall Clip Connection Resistance on P_f

Hurricane Wind Speed Models		Batts et al.	Vickery et al.	Georgiou
Wind Speed (mph)	50 year	120	132	150
	100 year	130	150	162
	1000 year	155	182	208
Weibull Distribution Parameters	u	64.86	61.07	68.33
	α	2.218	1.769	1.738
Probability of Clip Connection Failure	Source (Reed et al. 1996)	0.000075	0.000438	0.00145
	Source (Canfield et al. 1991)	0.000112	0.000478	0.00185

Similarly, Table 3.11 illustrates the effects of the different hurricane wind speed models on estimated probability of failure of roof panels with 6d nailing by uplift and of roof-to-

wall connections utilizing 3* 8d toe-nails for a house without roof overhang (Type A) in exposure B. These panel and truss connection details correspond to minimum standards for residential construction practice in hurricane prone areas along the coast. Here, the choice of hurricane wind speed model also has a significant impact on the estimated probability of a panel, the highest P_f (0.137) being almost twice as high as the lowest P_f (0.077) for the roof panel with 6d nails. Similar differences are observed for the 3 – 8d toenail roof-to-wall connection.

Table 3.11 Comparison of Effect of Hurricane Model on P_f: Type A house in Exposure B

Hurricane wind speed models		Batts et al.	Vickery et al.	Georgiou
Wind Speed (mph)	50 year	120	132	150
	100 year	130	150	162
	1000 year	155	182	208
Weibull Distribution Parameters	u	64.86	61.07	68.33
	α	2.218	1.769	1.738
Pf of 6d nail roof		0.077	0.09	0.137
Pf of 3 * 8d toe nails roof-to-wall connection		0.0053	0.011	0.024

Finally, Table 3.12 illustrates the sensitivity of window failure probability due to excessive wind pressure and missile impact to the choice of hurricane wind speed models.

Table 3.12 Comparison of Effect of Hurricane Model and Thickness and Area of Glass Panel on P_f (1 in = 25.4 mm; 1 ft^2 = 0.093 m^2)

Glass Failure Mode	Glass Thickness and Area	Lognormal Fragility Model Parameters		Pf for Different Wind Speed Model		
		m_R	ζ_R	Batts et al.	Vickery et al.	Georgiou
Pressure	1/8 in 20 sq ft	5.0178	0.2086	0.0095	0.0170	0.0330
	1/8 in 40 sq ft	4.7587	0.1974	0.0470	0.0600	0.0960
	3/16 in 20 sq ft	5.3330	0.2248	0.0005	0.0022	0.0056
	3/16 in 40 sq ft	4.9833	0.2096	0.0120	0.0200	0.0390
Impact	3/16 in	4.9400	0.1070	0.0071	0.0170	0.0350

Evaluation of Equation 3.6 requires that $F_R(v)$and $f_V(v)$, and their distribution parameters, are either known or can be determined from available databases. In fact, this seldom is the case. Indeed, as noted above, while F_R and f_V are based on plausible models, they are supported by limited data. Accordingly, both F_R and f_V are, in fact, random functions (dependent on the uncertainties in their statistical parameters and, at a higher level, in the choice of probabilistic model) and the estimator of the limit state probability, P_f, is described by a probability distribution. It is this "frequency of limit state probability" that describes the epistemic uncertainty in the reliability analysis.

If the structural and climatological models are highly refined (and costly to implement), then the standard deviation (or standard error) in P_f is likely to be small; conversely, if the structural and climatological models are crude, then the standard error in P_f is relatively large. In either event, it may be useful to identify a confidence level associated with P_f to reflect the credibility of the estimate based on limitations that may exist in the underlying

models: for example, that value of P_f where the decision-maker is 95% confident that the true (unknown) P_f is less. Such statements would become relatively more conservative for less accurate structural or wind field models, and therefore allow the decision to reflect the level of uncertainty in the analysis supporting the decision.

The epistemic uncertainty (due to either hurricane and/or resistance) is displayed in a discrete form in Tables 3.10–3.12. As noted previously, the effect of epistemic uncertainty also can be displayed conveniently as a "frequency of limit state probability," either discretely by a probability mass function or continuously through a probability density function. From such frequency representations of epistemic uncertainty, one can make confidence statements on the estimated P_f, which is a performance metric that is useful in the context of decision-making. For example, consider the results presented in Table 3.10, and assume that both data sets on clip capacity and all three hurricane wind field models are equally credible. The mean and standard deviation of estimated probability, P_f, are 0.00073, and 0.0007, respectively. The 95^{th} percentile is approximately 0.0019. Thus, a decision-maker might say, "I am 95% confident that the annual failure rate of roof trusses attached to the wall with an H2.5 clip is less than 0.2%." More comprehensive test data or a better consensus on hurricane wind field models would push this value (0.002) closer to the mean, 0.000734. Similarly, for a 40 sq ft glass panel 1/8 in (3 mm) in thickness failing by excessive wind pressure, the estimated mean and standard deviation of P_f are 0.068 and 0.025, respectively, and one might state that he/she is 90% confident that the annual failure rate is less than 0.10.

3.6 Summary

A fragility analysis methodology is developed for assessing the response of light-frame wood construction exposed to hurricane winds. Performance goals and limit states (structural and nonstructural) are identified from a review of the performance of residential construction during recent hurricanes in the United States. It is assumed that contents damage and consequent structural damage result from breach of the building envelope, and the limit states are so defined: roof panels and trusses damaged by excessive wind uplift or breakage of glass panels in windows or doors by excessive wind pressure or by windborne debris. Limit state probabilities of structural systems for the performance levels identified above are developed as a function of 3-second gust hurricane wind speed. In a fully coupled reliability analysis, structural system fragilities are convolved with hurricane hazard models expressed in terms of 3-sec gust wind speed. Inherent and epistemic uncertainties are identified and displayed separately in the analysis. It was found that among all inherently random factors, wind speed is the most significant. In terms of epistemic uncertainty, the choice of wind model for risk assessment purposes is significant in terms of its impact on structural reliability and on engineering decision analysis.

4 FRAGILITY AND RISK ANALYSIS FOR SEISMIC HAZARDS

4.1 Earthquake damage surveys

As noted in Section 2.3.2, verification of whether the building performance requirements are met requires a mapping between a qualitatively stated objective (e.g., life safety for building occupancy following a 10%/50-yr event) and a structural response quantity (force or deformation) that can be checked using principles of structural analysis and mechanics or be observed in post-disaster surveys.

Post-seismic disaster surveys have shown that a large portion of structural and non-structural damage to light-frame wood residential construction can be related to excessive lateral drift of the building system (CUREE, 2000; NAHB, 1994). Acceptable behavior of light-frame wood construction during earthquakes requires that the deformations be limited. The deformation of the structural system often has been selected when system behavior must be measured through one structural response quantity (normally computed by finite element-based structural analysis), particularly when the structural response and behavior are in the nonlinear range.

Performance levels have been defined in terms of drift limits for wood framed buildings in the NEHRP Guidelines, and in other recent literature (FEMA, 1997 and 2000;

Filiatault and Folz, 2002). For example, in FEMA Report 356 (and its widely cited 1997 predecessor, FEMA Report 273) (FEMA, 2000), the immediate occupancy, life safety and collapse prevention performance levels for lateral force-resisting structural elements in light-frame wood construction subjected to seismic effects are related to transient lateral drifts of 0.01, 0.02 and 0.03, respectively. Accordingly, the structural response quantity of interest in this study will be the maximum drift (D) of the structural model of wood shear walls with various configuration and base constraints.

4.2 Model of lateral load-resisting system

4.2.1 Basic configurations of residential construction

Lateral force and deformation resistance in light-frame wood residential construction usually is provided by shear walls. Four different configurations of shear wall systems are chosen to represent typical wood frame shear walls found in residential construction in the United States. Assuming that the configuration of the house is regular and that significant torsional effects do not occur, a 2-D plane shear wall model is sufficient to represent the lateral force capacity for the building (Wang and Foliente, 2005). These shear wall models are shown in Figure 4.1 through 4.4. In all cases, the fundamental dimensional unit is a 4 x 8 ft (1.2 x 2.4m) sheathing panel modified, as appropriate to allow for door and window openings.

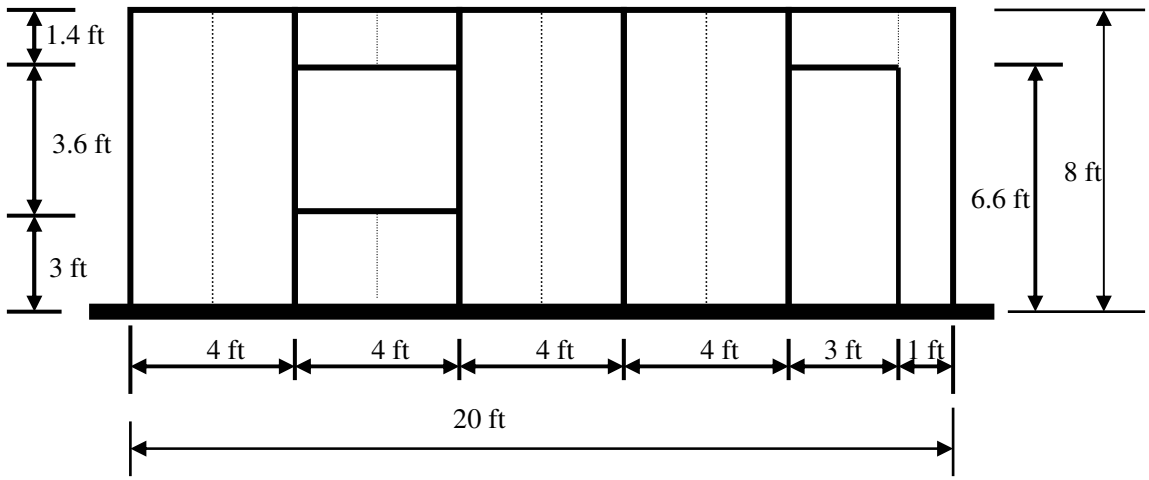

Figure 4.1 One-story Shear Wall with Door and Window Openings

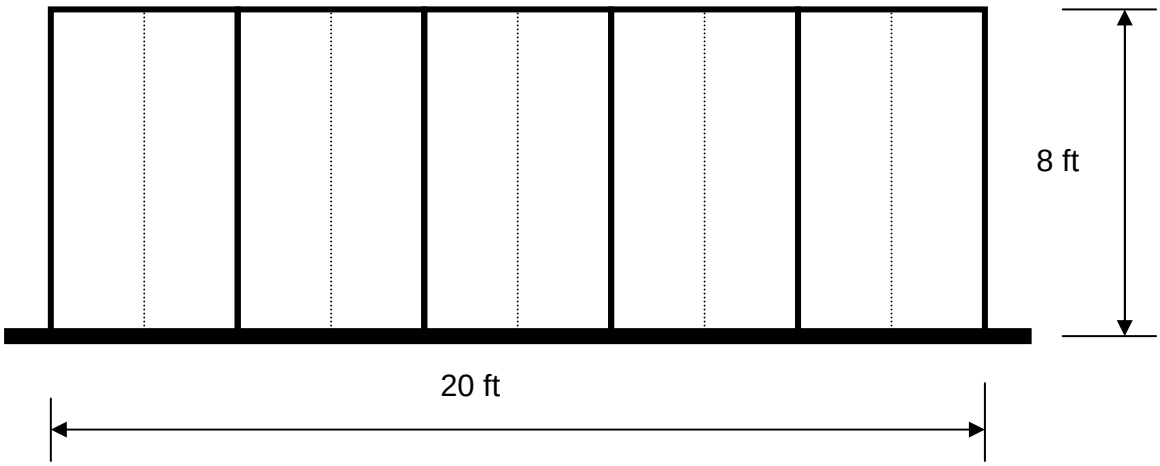

Figure 4.2 One-story Solid Shear Wall

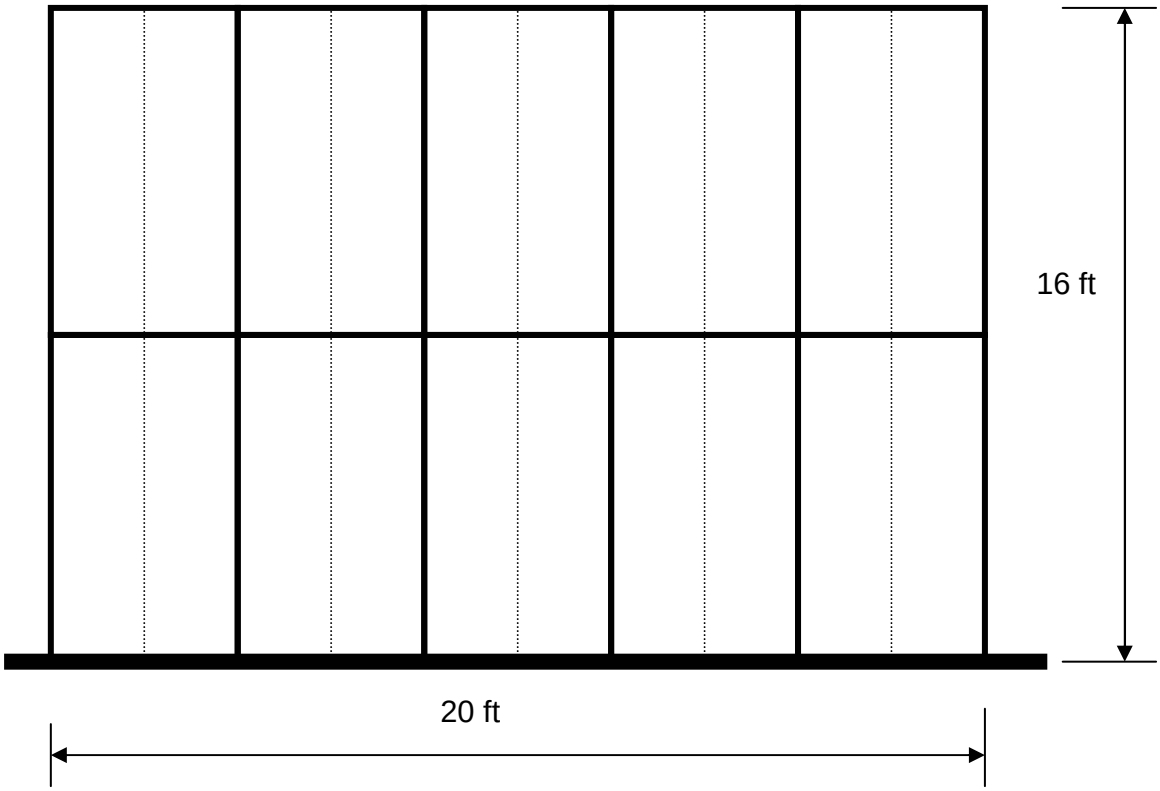

Figure 4.3 Two-story Solid Shear wall

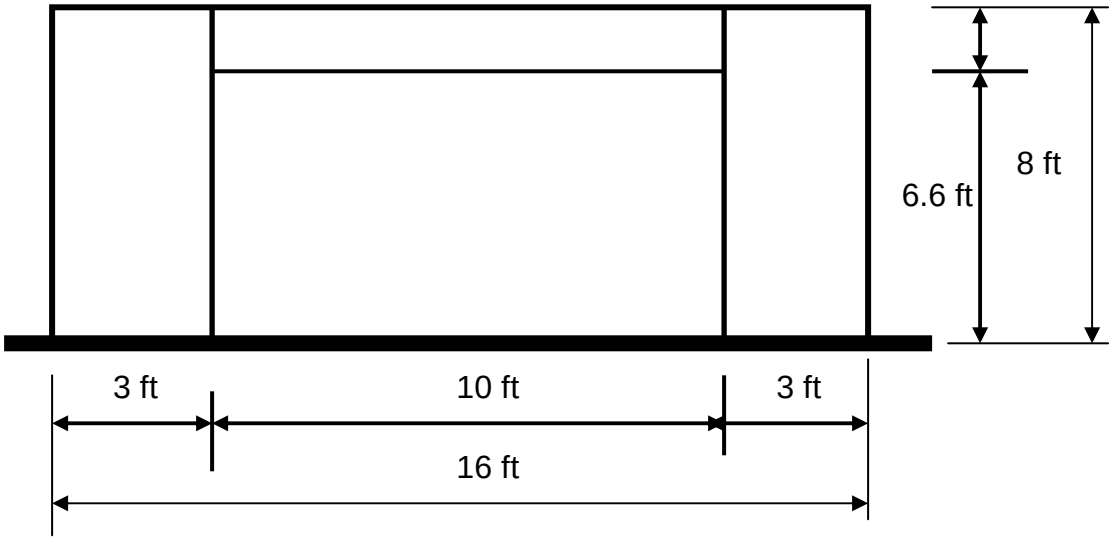

Figure 4.4 Shear Wall with Garage Door

The opening details and dimensions of the shear wall systems are illustrated in Figures 4.1 - 4.4. The exterior sheathing serves a structural function and is provided by 0.375 in (9.5 mm) oriented strand board (OSB) panels. The interior was unsheathed. Studs are spaced at 24 in (610mm) on centers. The sheathing is connected to the studs with 8d nails, which are 0.131 in (38mm) in diameter. The nails are spaced 6 in (152 mm) along the sheathing panel perimeter and 12 in (305 mm) in the panel interior. The abbreviation of this nailing pattern is 6/12. Similar abbreviation of 4/6 represents 4-in (102 mm) nailing spacing on exterior edge of panel and 6 in (152 mm) on interior panel. The shear wall is fully anchored to the foundation, as is customary building practice in the Western United States. Later in this Chapter and in Chapter 5, residential buildings with partially anchored shear walls that are typical for buildings in the Eastern United States are considered.

4.2.2 CASHEW (Cyclic Analysis of wood SHEar Walls) program

The behavior of a shear wall subjected to dynamic loading reflects several sources of non-linearity. The sources are nonlinear characteristic behavior of individual fasteners, discontinuity of shear wall (due of openings), and non-isotropic behavior of wood and wood-based materials.

The hysteretic behavior of the shear walls considered in this study was modeled by the program CASHEW (Cyclic Analysis of SHEar Walls) (Folz and Filiatrault, 2000), which

is a numerical model developed as part of the CUREE-Caltech Woodframe Project (CUREE, 2000) that is capable of predicting the force-displacement response of wood shear walls under quasi-static cyclic loading. Construction details described above, such as openings for doors and windows, fastener patterns and properties, and thickness and arrangement of sheathing panels can be included in the model. Hold-down anchorage between the shear wall and foundation is assumed to be present and properly installed, implying that the wall is fully anchored to the foundation.

Krawinkler et al. (2000) developed a testing protocol for wood frame structures, which is aimed at establishing their hysteretic behavior under cyclic load. This protocol is applied to the CASHEW model to determine the hysteretic behavior of the shear walls considered herein. The protocol loading is illustrated in Figure 4.5. Details of implementation of the protocol loading on the CASHEW models can be found in the report by Folz and Filiatrault (2000).

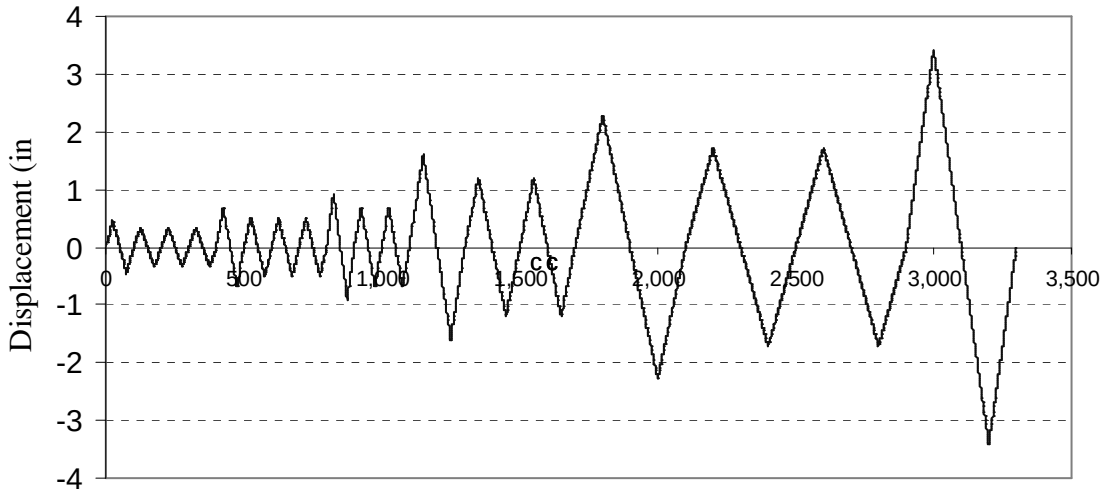

Figure 4.5 Protocol Loading for Wood Frame Structures (CUREE)

4.2.3 Hysteretic behavior of shear walls

The response of wood frame shear walls during minor earthquakes is essentially linear-elastic. However, under severe earthquake ground motion, such systems exhibit highly nonlinear hysteretic behavior, with significant stiffness degradation, pinching of the hysteretic loops and energy dissipation. The hysteretic behavior of shear wall structures and assemblies are primarily due to the behavior of the sheathing-to-frame fasteners. A common observation from experiments is that the hysteretic trace of wood shear wall assemblies is governed by the primary fasteners, here, the nails (Filiatrault, 1990). The load-deformation response of a connector in a wood shear wall is highly non-linear under monotonic loading and exhibits pinched hysteretic behavior with strength and stiffness degradation under general cyclic loading (Dolan and Madsen, 1992). Figure 4.1 shows the typical hysteretic behavior of a sheathing-to-framing fastener (Folz and Filiatrault, 2000).

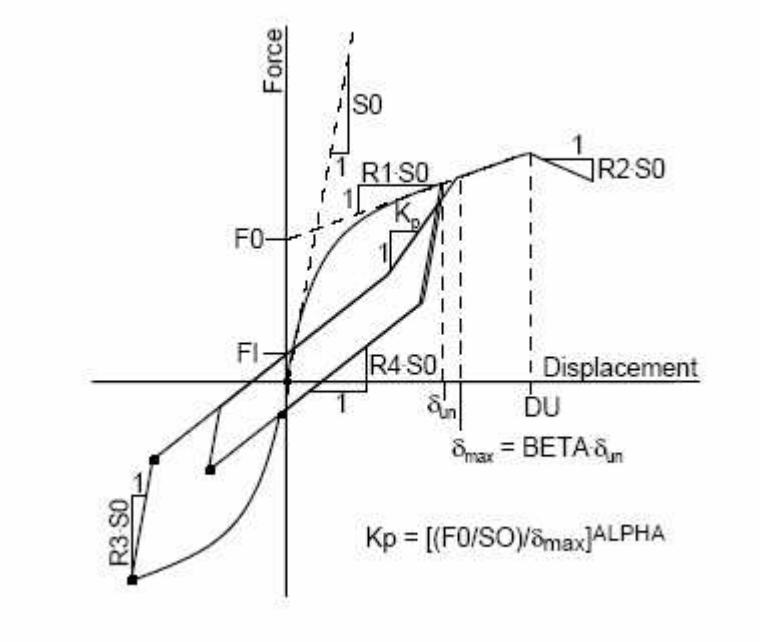

Figure 4.6 Hysteretic Response of a Sheathing-to-Framing Fastener

(Folz and Filiatrault, 2000)

Table 4.1 shows the sheathing-to-framing parameters investigated by Durham (1998) and Dolan (1989) as identified in Figure 4.6. The sheathing-to-framing parameters from Durham are used for the following fragility analyses of the shear wall models. Dolan's parameters are used in validating the CASHEW shear wall model because his study represented the only experimental data on shear walls that could be located.

Table 4.1 Fastener Parameters from Durham (1998) and Dolan (1989)

	Unit	S0	R1	R2	R3	R4	F0	F1	DU	ALPHA	BETA
Durham (1998)	US	3.203 Kips/in	0.061	-0.078	1.4	0.05	0.17 kips	0.032 kips	0.492 in.	0.8	1.1
	SI	0.561 KN/mm	0.061	-0.078	1.4	0.05	0.75 1KN	0.141 KN	12.5 mm	0.8	1.1
Dolan (1989)	US	5.179 Kips/in.	0.05	-0.06	1.4	0.027	0.27 kips	0.041 kips	0.315 in.	0.8	1.1
	SI	0.907 KN/mm	0.05	-0.06	1.4	0.027	1.01 KN	0.182 KN	8.0 mm	0.8	1.1

Hysteresis curves for the four shear walls above are depicted in Figures 4.7 to 4.10. Figure 4.7 is the relationship of lateral load and displacement for a one-story shear wall with openings subjected to the protocol test displacements in Figure 4.6. The hysteresis curves in Figure 4.7 to 4.10 all show degradation of strength (this is more apparent in Figures 4.9 and 4.10) and stiffness as the number of cycles increases and development of pinching in hysteretic loops at large deformations.

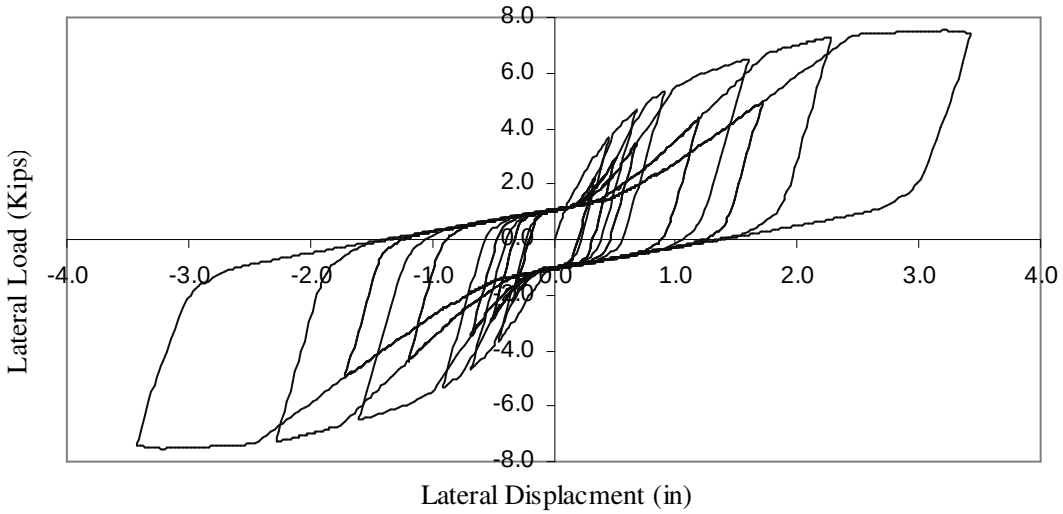

Figure 4.7 Hysteretic Shear Wall Model (One-Story Shear Wall with Opening)

Comparing Figure 4.8 and Figure 4.9, the maximum lateral force for the one and two-story shear walls are close, at 10.8 kips (48.03 kN) and 11.2 kips (49.82 kN), respectively. However, the maximum lateral displacement of the two-story shear wall is more than twice as much as that of one-story shear wall. Note that the height of two-story shear wall is twice as high as its counterpart.

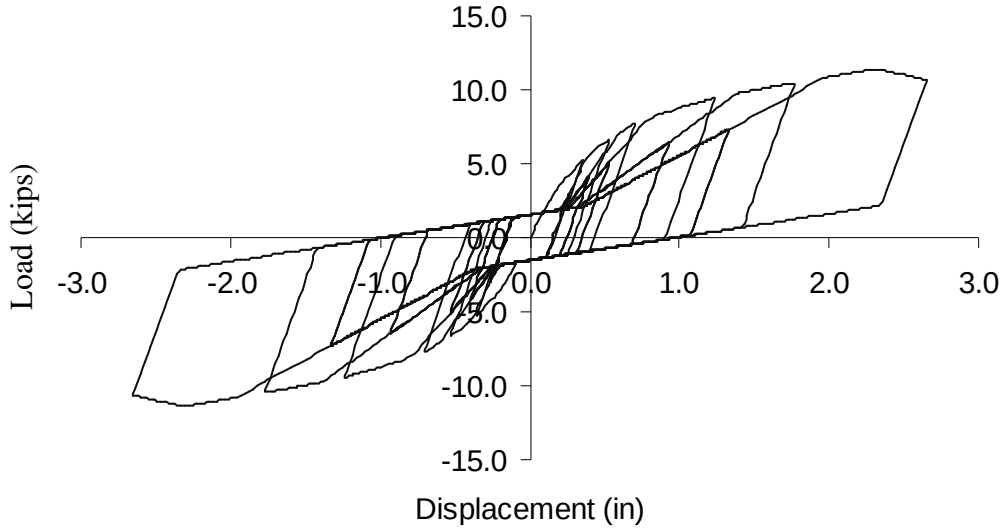

Figure 4.8 Hysteretic Shear Wall Model (One-Story Solid Shear Wall)

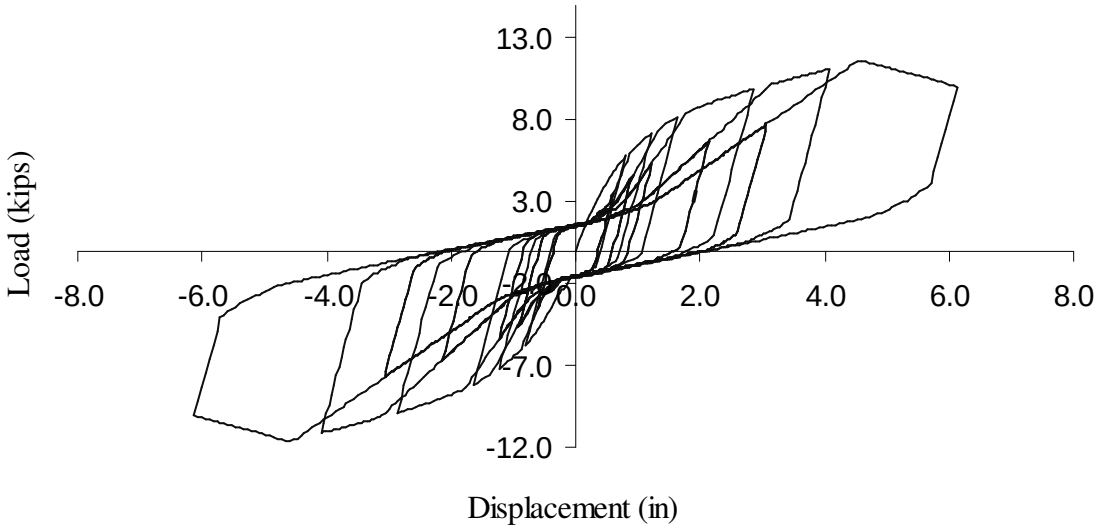

Figure 4.9 Hysteretic Shear Wall Model (Two-Story Solid Shear Wall)

Figure 4.10 illustrates the hysteretic behavior of the shear wall with the garage door. The unfavorable effect of the large opening on cyclic stiffness and strength of the shear wall is clearly evident from a comparison with the hysteresis curves in Figures 4.8 to 4.10.

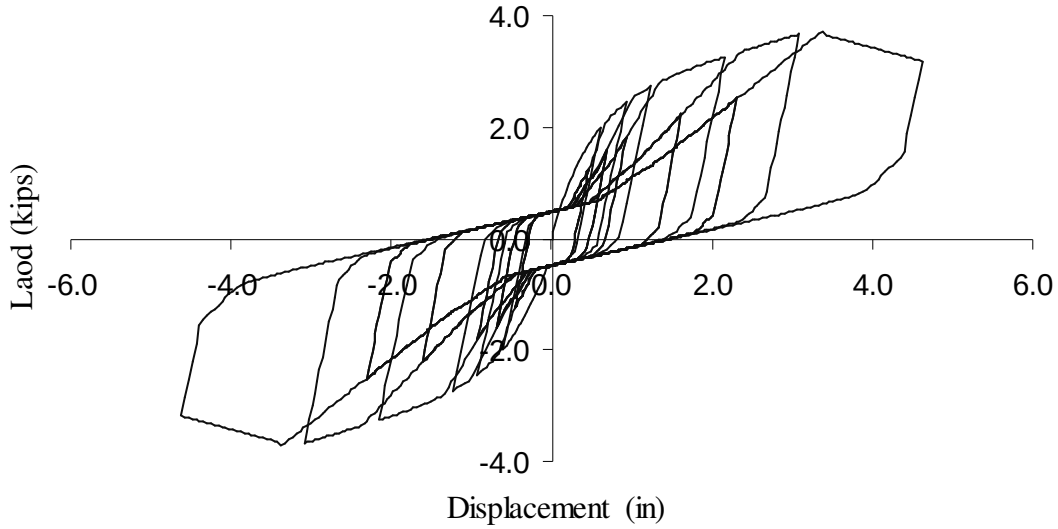

Figure 4.10 Hysteretic Shear Wall Model (Shear Wall with Garage Door)

4.2.4 Validation of shear wall model

Shear wall behavior predicted by the CASHEW model is validated by comparing predictions such as those in Figures 4.7 – 4.10 with available experimental tests. Dolan and Heine (1997) conducted sequential phased displacement cyclic tests of wood-frame shear walls with various openings and base restraint configurations. A solid one-story shear wall of 40 x 8 ft (12.2 x 2.4 m) with of tie-down anchors at both ends was tested and the monotonic load and drift are presented in dash line in Figure 4.11. In this figure, the solid line represents a nonlinear load and displacement relationship for the tested

shear wall was modeled using CASHEW. It was found that there was a reasonable match between the nonlinear load-displacement behavior observed during the test and the pushover curve predicted by CASHEW. The close agreement suggests that the CASHEW program is sufficient to model the shear wall under cyclic deformations. It also provides a basis for utilizing other results from Dolan and Heine's experiment (e.g. ratio of stiffness for shear walls with different support conditions) to apply to other shear wall models considered in the current study, which will be presented later.

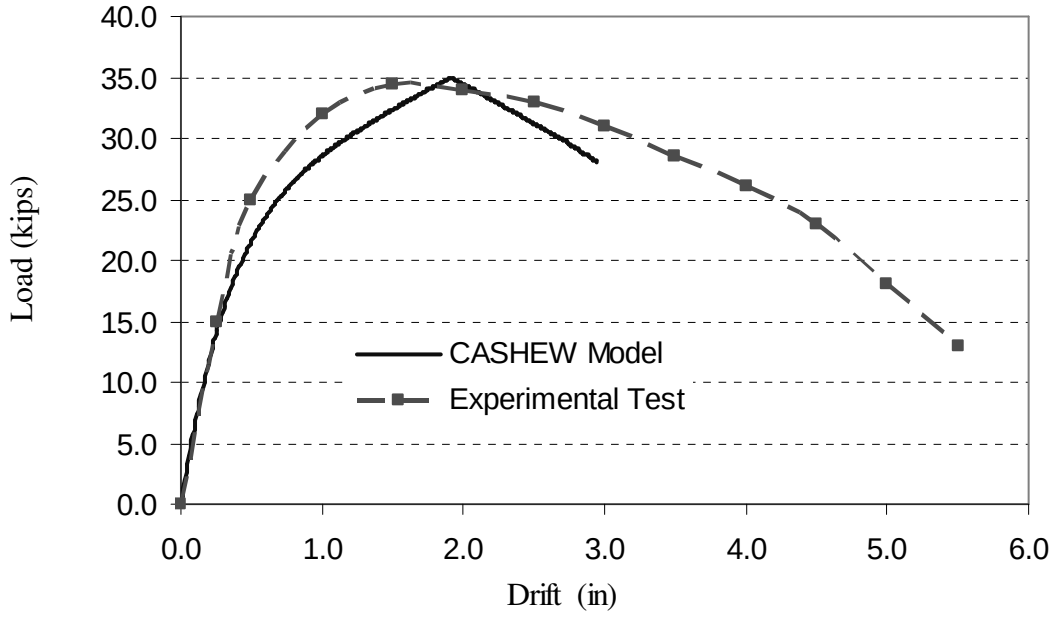

Figure 4.11 Comparison of Pushover Curve for Shear Walls
(CASHEW Model vs. Experimental Test)

4.2.5 Effects of shear wall foundation restraints

Shear wall hold-down anchors resist shear wall uplift induced by lateral loading in regions of high seismicity. In the CASHEW program, it is assumed that the shear wall is fully anchored to the foundation. The installed anchors are used to prevent uplift or sliding of the wall and to ensure a racking mode of deformation. The fully fixed anchor is referred to as a "Seismic anchor" in this study. However, partially anchored shear walls are more common in residential construction in regions of low to moderate seismicity. A partially anchored shear wall is effective for preventing residential building from sliding, but it does not prevent uplift.

Dolan and Heine (1997) quantified the effects of overturning restraint on full-scale shear walls, with and without openings, that were tested cyclically. The test results show that, as one might expect, the stiffness and strength of the shear walls increased with increasing number of tie-down anchors. In another study, Gupta and Kuo (1987) conducted tests of shear walls in which uplift occurred. It was found that a flexible foundation has a significant effect on the performance (drift) of shear wall.

The difference in the cyclic stiffness and strength capacity of single-story solid shear walls with fully anchored and partial hold-downs is about 30% (Dolan and Heine, 1997). Furthermore, it was pointed out in NAHB (1990) that shear walls with flexible foundations can only provide 70% of the lateral load support provided by rigid foundations (or fully anchored walls). Accordingly, in the present study, the cyclic

stiffness and strength of partiallly anchored shear wall are assumed to be 70 % of those values for shear walls with fully anchored hold-downs. Accordingly, the hysteretic force-deformation curve obtained from CASHEW has been scaled to account for the partially restraint at the foundation. The hysteretic curves in Figure 4.12 show the difference of one-story shear wall with and without foundation anchors. In the following sections, the shear wall models are assumed to be fully anchored to the foundation unless otherwise specified partially hold-down anchors.

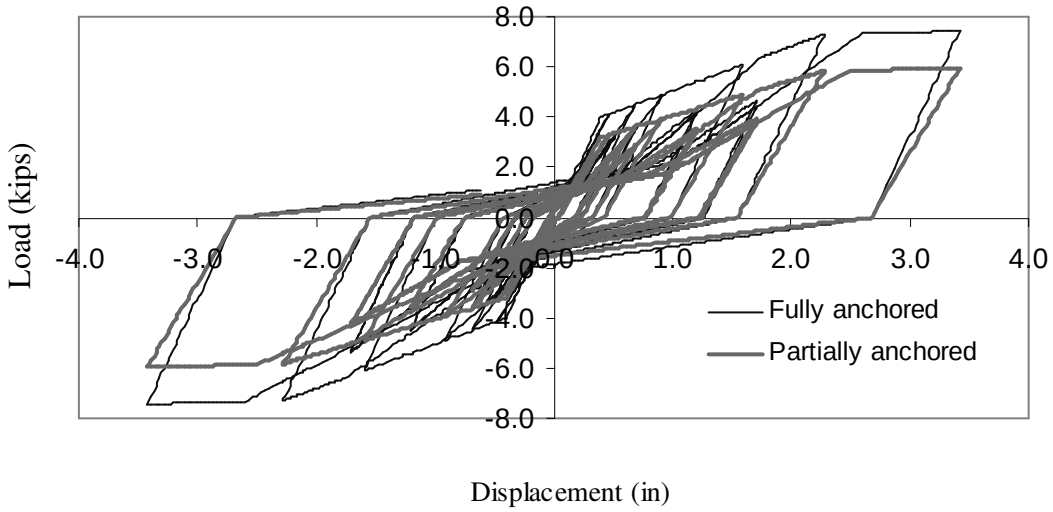

Figure 4.12 Hysteresis Curves for Fully and Partially Anchored Shear Walls (One-story with Openings)

4.3 Shear wall response to earthquake ground motions

4.3.1 Earthquake ground motion ensembles

Structural performance during earthquakes is impacted by uncertainties in both seismic loading and structural resistance. The uncertainty in seismic demand is known to be very large in comparison to the inherent variability in the structural system and its capacity (Foliente, 1997). The uncertainty in seismic demand in this study is reflected in the suite of ground motions chosen for structural performance assessment.

The ground motions developed in the SAC Project Phase II (SAC, 2000) for Los Angeles are used in the shear wall analysis. These ground motions, which are for soft rock conditions (the boundary between site categories SB and SC) were mapped for Los Angeles, CA, Seattle, WA, and Boston, MA, for a set of response spectral periods from 0.1 to 2.0 seconds at 5% damping.

The three ground motion ensembles have probabilities of 50% of being exceeded in 50 years (la41-60), 10% of being exceeded in 50 years (la01-20) and 2% of being exceeded in 50 years (la21-40). The annual exceedance probabilities for these ensembles are:

* 2% in 50 years (4.04 x 10-4 annual frequency of exceedance; return period 2,475 yr)
* 10% in 50 years (2.10 x 10-3 annual frequency of exceedance; return period 475 yr)
* 50% in 50 years (1.39 x 10-2 annual frequency of exceedance; return period 72 yr)

As an illustration, Table 4.2 shows 20 ground motion records for Los Angeles area with 2% in 50 years (la21-40). These so-called "uniform hazard" ground motions, appropriately scaled, represent the aggregation of several earthquake events of different magnitudes and epicentral distances.

Table 4.2 Ground Motion Records for Los Angeles Area (2%/50)

EQ code	Description	Earthquake Magnitude	Distance (km)	Scale Factor	Number of Points	Time Step (sec)	PGA (cm/sec^2)	PGA (g's)
la21	fn 1995 Kobe	6.9	3.4	1.15	3000	0.020	1258.00	1.28
la22	fp 1995 Kobe	6.9	3.4	1.15	3000	0.020	902.75	0.92
la23	fn 1989 Loma Prieta	7.0	3.5	0.82	2500	0.010	409.95	0.42
la24	fp 1989 Loma Prieta	7.0	3.5	0.82	2500	0.010	463.76	0.47
la25	fn 1994 Northridge	6.7	7.5	1.29	2990	0.005	851.62	0.87
la26	fp 1994 Northridge	6.7	7.5	1.29	2990	0.005	925.29	0.94
la27	fn 1994 Northridge	6.7	6.4	1.61	3000	0.020	908.70	0.93
la28	fp 1994 Northridge	6.7	6.4	1.61	3000	0.020	1304.10	1.33
la29	fn 1974 Tabas	7.4	1.2	1.08	2500	0.020	793.45	0.81
la30	fp 1974 Tabas	7.4	1.2	1.08	2500	0.020	972.58	0.99
la31	fn Elysian Park (simulated)	7.1	17.5	1.43	3000	0.010	1271.20	1.30
la32	fp Elysian Park (simulated)	7.1	17.5	1.43	3000	0.010	1163.50	1.19
la33	fn Elysian Park (simulated)	7.1	10.7	0.97	3000	0.010	767.26	0.78
la34	fp Elysian Park (simulated)	7.1	10.7	0.97	3000	0.010	667.59	0.68
la35	fn Elysian Park (simulated)	7.1	11.2	1.10	3000	0.010	973.16	0.99
la36	fp Elysian Park (simulated)	7.1	11.2	1.10	3000	0.010	1079.30	1.10
la37	fn Palos Verdes (simulated)	7.1	1.5	0.90	3000	0.020	697.84	0.71
la38	fp Palos Verdes (simulated)	7.1	1.5	0.90	3000	0.020	761.31	0.78
la39	fn Palos Verdes (simulated)	7.1	1.5	0.88	3000	0.020	490.58	0.50
la40	fp Palos Verdes (simulated)	7.1	1.5	0.88	3000	0.020	613.28	0.63

Figure 4.13 illustrates a time history of ground motion of la21 (one of the 2%/50 yr ensemble), which has a maximum PGA of 1.283 g.

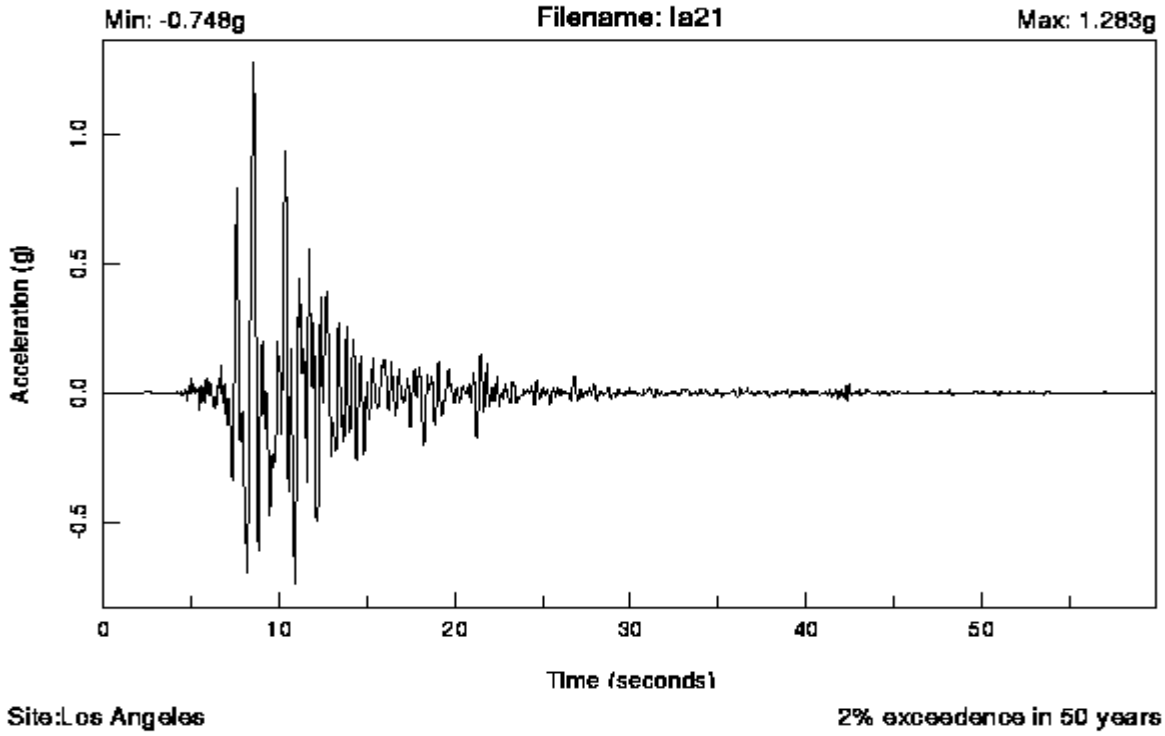

Figure 4.13 Ground Motion Record (la21)

The ground motion intensity is described by the spectral acceleration (S_a), defined as the response acceleration that is experienced by a building modeled as SDOF oscillator with 5% damping at the fundamental period of the building when it is subjected to ground motion. The 5% damping has been stipulated by the USGS as the basis for representing spectral intensities. Figure 4.14 shows the cluster of response spectra that arise from ground motions la01 through la20. The median S_a is highlighted in the red solid curve. Dispersion of S_a of is apparent in the plot.

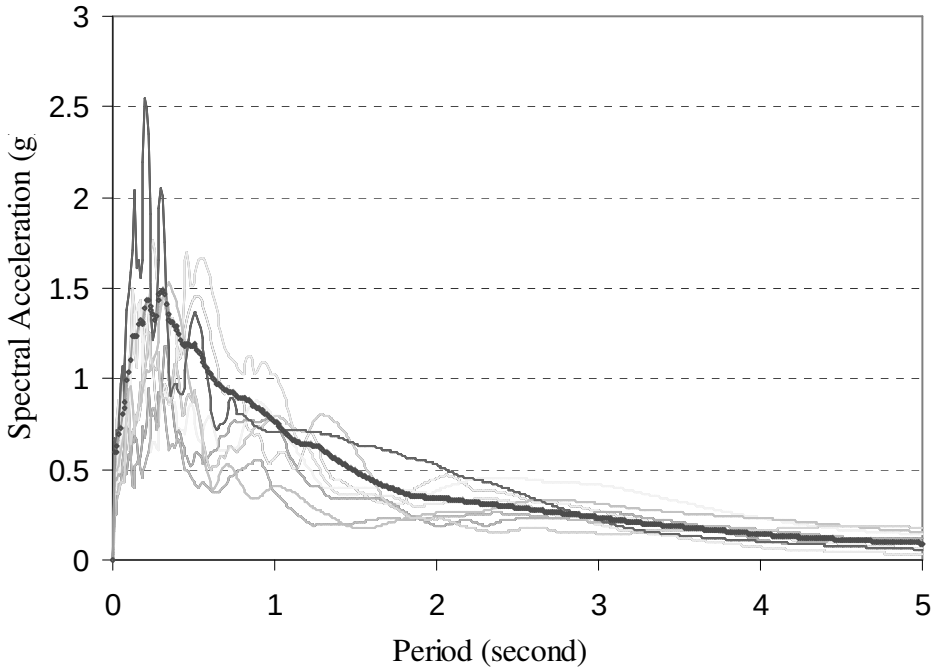

Figure 4.14 Response Spectrum for Records of la21-40

The total energy dissipation in the shear wall system is due to both viscous and hysteretic damping. The hysteretic damping is taken into account by the nonlinear force-displacement model in Figures 4.6 - 4.9. Viscous damping also must be included in nonlinear time history analysis. For example, the viscous damping was found to be about 3% of critical for full-scale woodframe structures in shake-table tests (Filiatrault et al. 2001). For light-frame wood construction in the current study, the viscous damping ratio is assumed to be 2% (Foliente, 1995).

Most low-rise wood-frame buildings have natural periods in the range of 0.06 to 0.8 seconds (Foliente, 1997). The fundamental natural periods of the buildings with the shear

walls shown in Figures 4.1 to 4.4 range from 0.17 to 0.32 sec, a range that is typical of low-rise wood residential construction. In particular, the fundamental natural period of the two-story shear wall is 0.28 sec. which is consistent with the natural period of 0.25 sec of the two-story woodframe house (Filiatrault et al. 2002), tested in the CUREE-Caltech wood-Frame project.

4.3.2 OpenSees and nonlinear time history analysis

The nonlinear dynamic response analysis of the shear walls above was conducted using the program OpenSees (Open System for Earthquake Engineering Simulation, http:\\opensees.berkeley.edu), a finite element platform developed at the Pacific Earthquake Engineering Research (PEER) to perform nonlinear dynamic time history analysis of structural systems subjected to earthquake ground motion.

The response of the shear wall with the opening in Figure 4.6 predicted by CASHEW was incorporated in a planar structural model of a typical one-story residential building developed in OpenSees. The rate of change in the degree of pinching of the hysteresis and the energy dissipation in OpenSees were adjusted by trial and error to be consistent with the prediction provided by the CASHEW model under the same loading protocol (Figure 4.5). The hysteretic behavior of the one-story shear wall model in OpenSees, illustrated in Figure 4.15, is consistent with that predicted by CASHEW model (Figure 4.6).

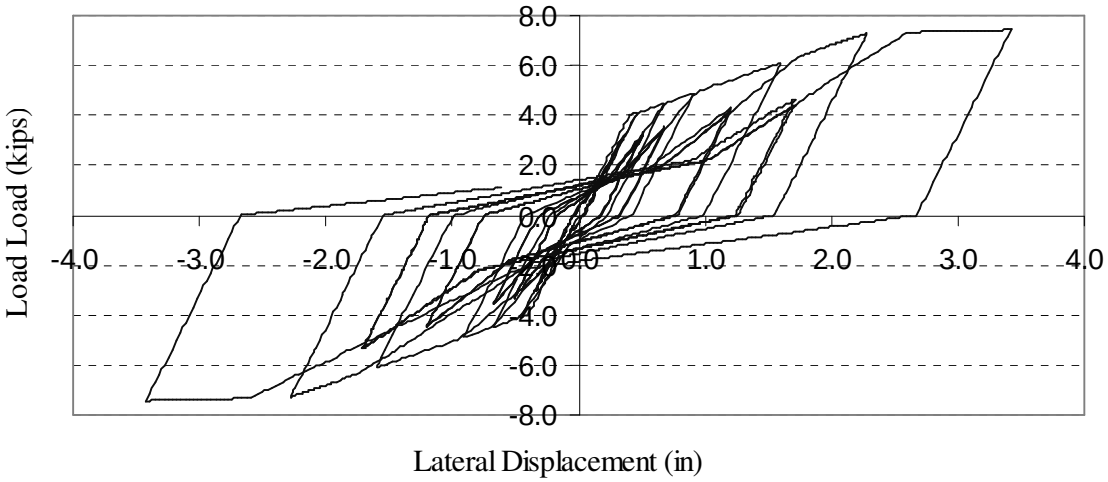

Figure 4.15 Hysterestic Shear Wall Model in OpenSees

As noted previously, shear walls behave in a highly nonlinear fashion under moderate to severe earthquakes. Nonlinear time history analysis provides the most complete picture of the behavior of the structural system subjected to earthquake ground motions. In the present study, consistent with common practice in performance based engineering, the response quantity of interest is the maximum drift at the top of the shear wall during seismic ground motion [see Figure 4.1 – 4.4], expressed as the ratio of the top of shear wall displacement to the height of the shear wall. Due to the uncertainty in ground motions, the drift is a random variable.

Figure 4.16 shows a time history analysis carried out by OpenSees for a one-story shear wall with opening subjected to the la21 ground motion record. The displacement of the shear wall virtually is zero at the first 8 sec. The shear wall then experiences nonlinear

displacements for approximate 20 cycles, with a maximum drift of 3.3 in (84 mm). The final displacement of the shear wall is close to zero, indicating little permanent deformation following the earthquake.

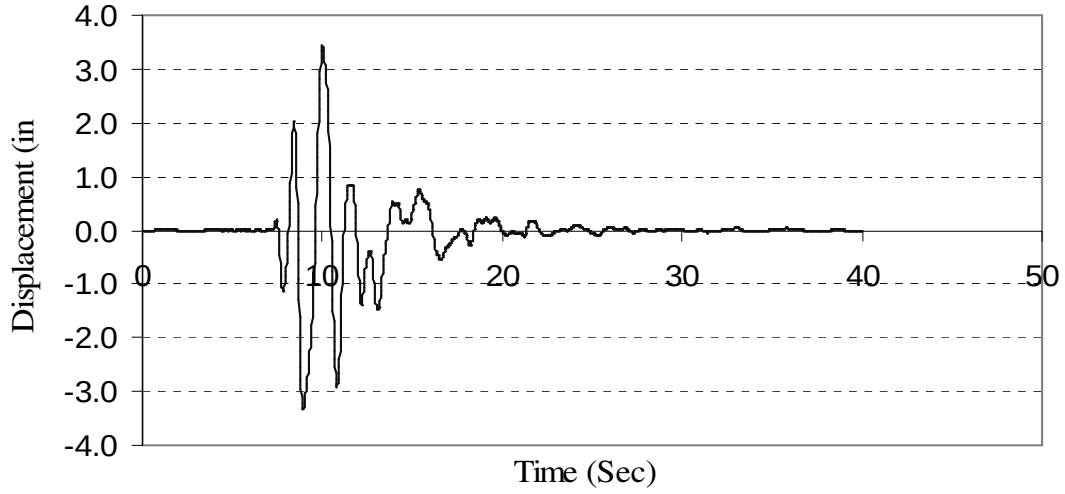

Figure 4.16 Nonlinear Time History Analysis (la21)

The maximum drifts of the shear wall models for the three sets of ground motions corresponding to various hazard levels (e.g. 2%/50) above were determined by nonlinear dynamic analysis from OpenSees. For each shear wall model, a total of 60 nonlinear time history analyses were performed, with 20 ground motions in each level of seismic hazard. The resulting drifts of the one-story shear wall with openings are rank-ordered in terms of the probability that the drift is exceeded and plotted (non-parametrically) for each of the three earthquake ensembles in Figure 4.17. The FEMA 273/356 deformation limit for life safety is 2% drift, or 1.92 in (49 mm) displacement in a wall 8 ft (2.4 m) in height. The (conditional) probability of exceeding this limit is virtually 0 for the 50/50 ground motions, while it is about 20% and 55% for the 10/50 and 2/50 ground motions,

respectively. For comparison, the probability that drifts from the 10/50 ground motions exceed the functional limit of 1% or 0.96 in (24 mm) is approximately 50%, indicating that such shear walls are likely to suffer nonstructural damage under such ground motions. Figure 4.18 to 4.20 display the probabilities of exceeding specified drifts for the other shear wall models considered (Figure 4.2 - 4.4). Figure 4.21 demonstrates the exceedance probabilities for the shear wall model with opening (Figure 4.1), when the base is not fully anchored.

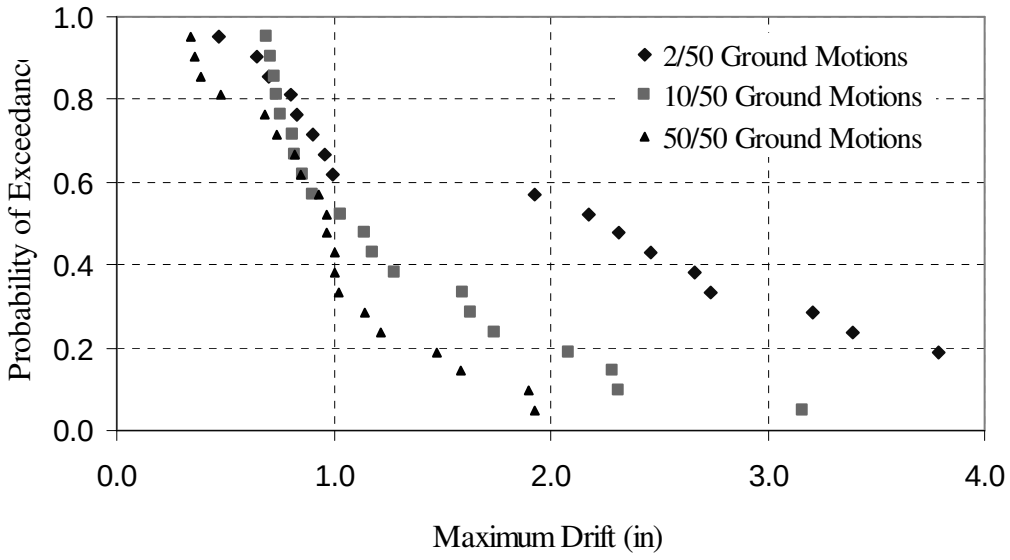

Figure 4.17 Probability of Exceedance vs. Maximum Drift (One-story Shear Wall with Openings)

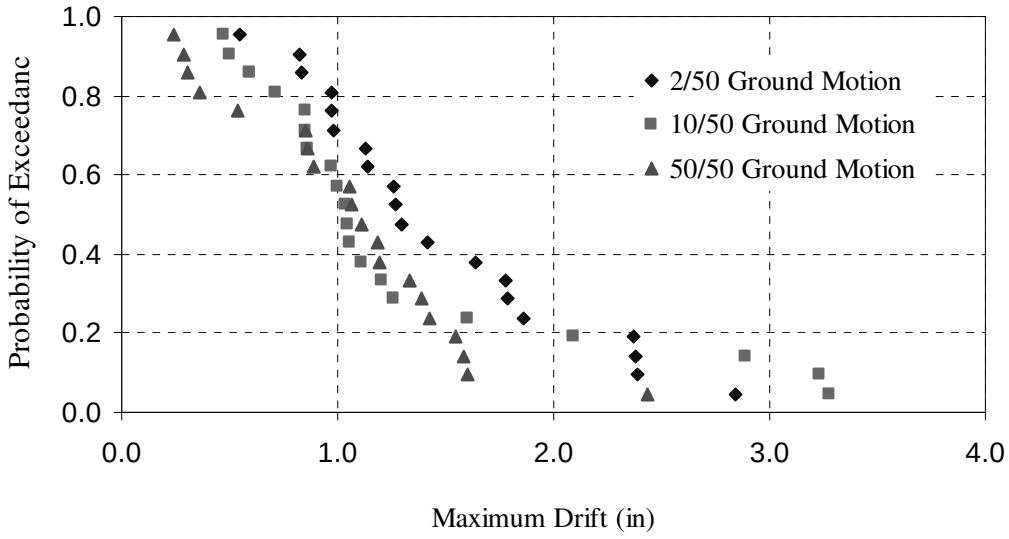

Figure 4.18 Probability of Exceedance vs. Maximum Drift (One-story Solid Shear Wall)

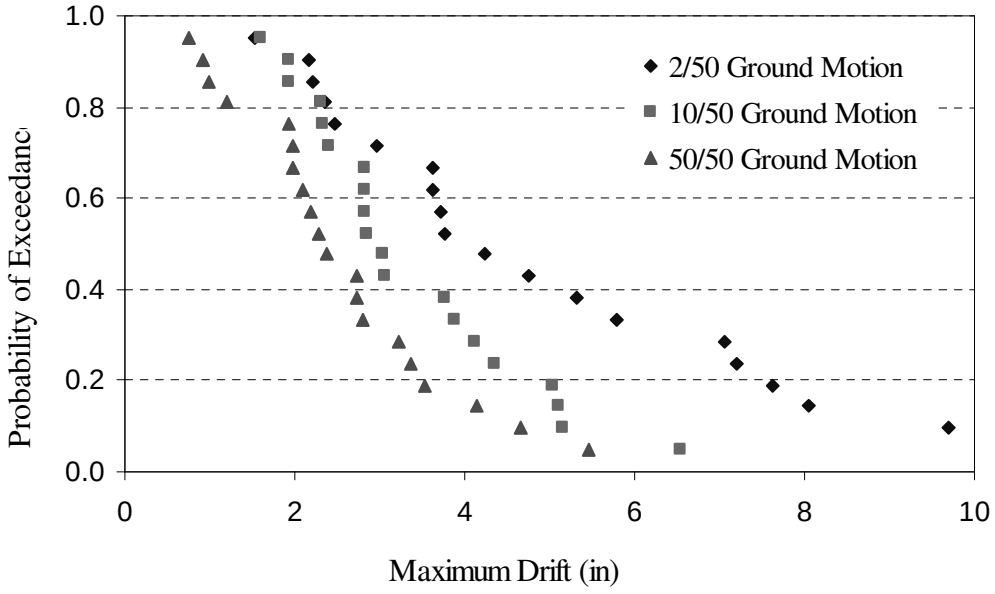

Figure 4.19 Probability of Exceedance vs. Maximum Drift (Two-story Solid Shear Wall)

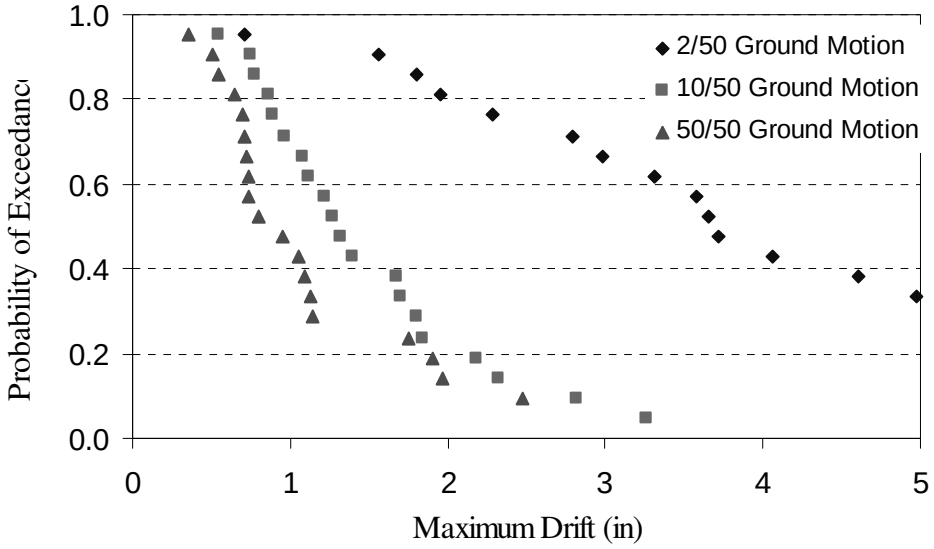

Figure 4.20 Probability of Exceedance vs. Maximum Drift (Shear Wall with Garage Door)

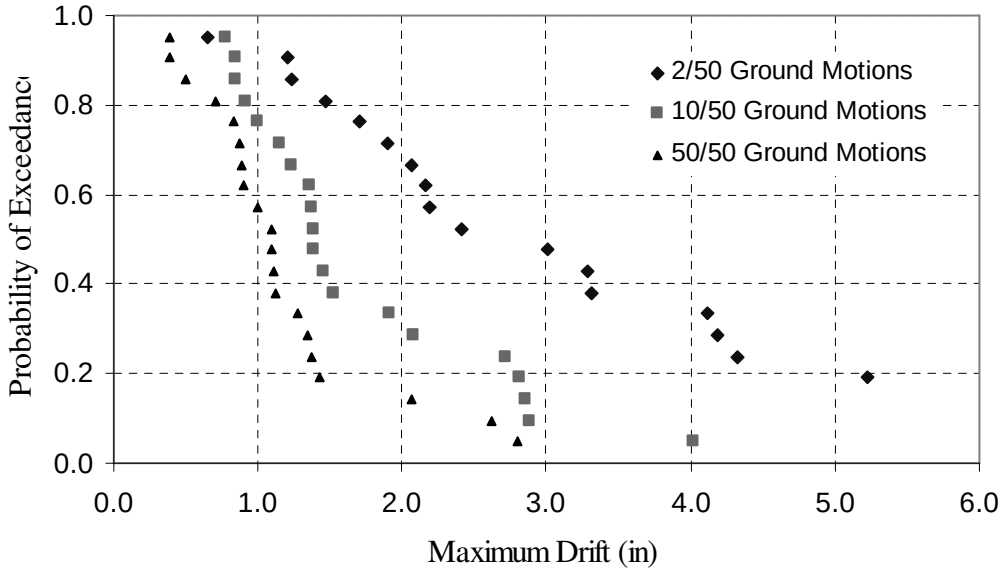

Figure 4.21 Probability of Exceedance vs. Maximum Drift (One-Story Shear Wall with Opening, Partially Anchored)

4.4 Seismic fragility curves

4.4.1 Relationship between spectral acceleration and shear wall deformation

For purposes of damage estimation and code development, it is necessary to postulate a relatively simple relationship between the seismic demand (drift) and a measure of earthquake ground motion intensity. For example, the median seismic demand on a structure can be modeled, in first approximation, by (Cornell, et al, 2002),

$$D = a(S_a)b \qquad (4.1)$$

in which S_a = spectral acceleration at the fundamental period of the structure with 5% damping ratio (this damping is selected to make the seismic intensity consistent with the specification of seismic hazard by site by the U.S. Geological Survey. The same damping ratio allows one to calculate of the annual probability of drift exceedance in Section 4.5.1), D = deformation, and a and b are constants. The scatter around this median (logarithmic standard deviation) represents the aleatory uncertainty in structural demand due random amplitude and phasing of the accelerograms in the ground motion ensemble. The constants in Equation 4.1 can be determined by a regression analysis of demands determined from OpenSees upon spectral acceleration of an elastic single-degree-of-freedom oscillator with a period equal to the fundamental period of the structure and 5% damping. Equation 4.1 was first proposed in the SAC Project for modeling seismic demand on steel moment frames and as a basis for determining simple

but risk-consistent design criteria (Cornell et al, 2002; Luco and Cornell, 2000). Its suitability for modeling seismic demand on a wood frame structure has yet to be investigated. Such an investigation is performed for the first time in this study.

Figure 4.22 presents the relationship between maximum drift and spectral acceleration for the one-story shear wall with openings (Figure 4.1). Spectral accelerations at the fundamental period of the structure (0.2 s) are obtained from response spectra of the ground motions la01-la60, as partly shown in Figure 4.14. The maximum drifts are obtained from nonlinear time history analysis. The median spectral accelerations and median maximum drifts for the 2%/50 yr, 5%/50 yr, and 10%/50 yr hazard levels are shown by the heavy solid dots in Figure 4.22. Figure 4.22 shows that, as might be expected from Figures 4.17 – 4.21, the deformations increase as the return period of the ensemble increases, although there is some overlap in the patterns. With the exception of two points (la21 and la22) in the 2/50 set, it appears that the functional relationship between deformation and S_a is not strongly dependent on the ensembles of ground motion selected to develop the relationship. This finding is consistent with that of other investigators for steel structures (Luco and Cornell, 2000). Figure 4.23 to 4.26 illustrate the relationship between maximum drift and S_a for the other shear walls.

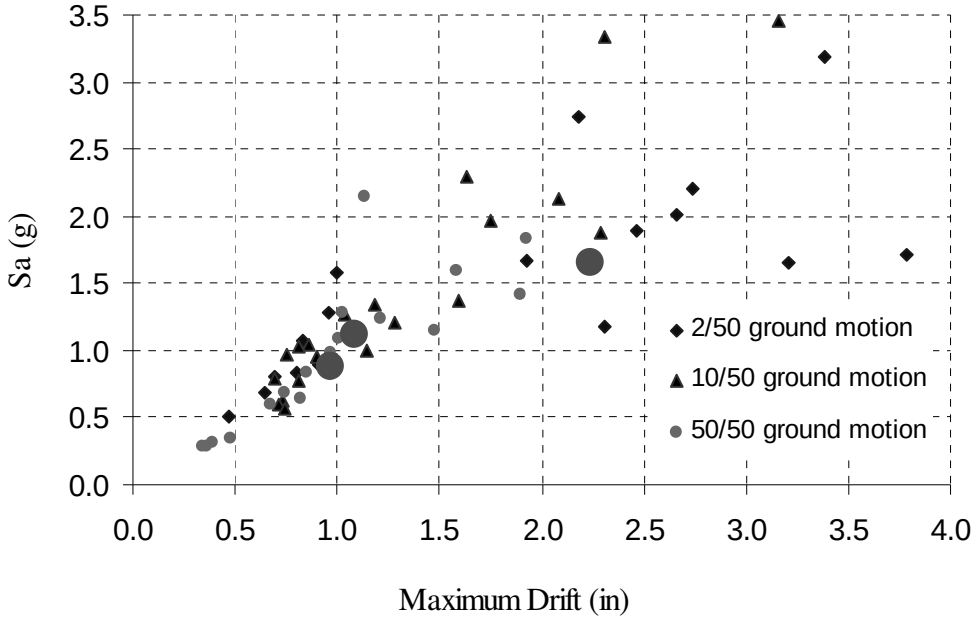

Figure 4.22 Maximum Drift vs. S_a (One-story Shear Wall with Openings)

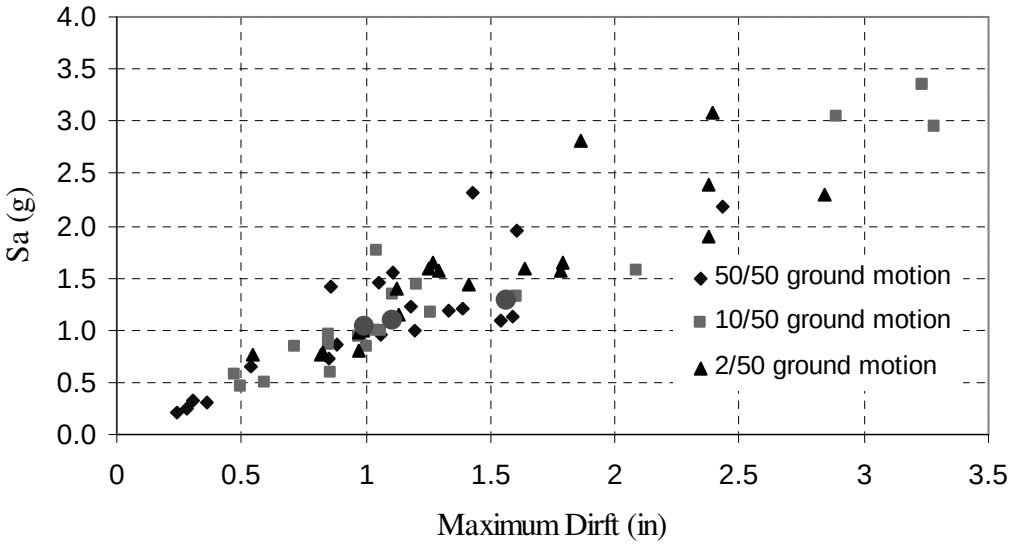

Figure 4.23 Maximum Drift vs. S_a (One-story Solid Shear Wall)

The medians of drift and spectral acceleration with 50%/50 and 10%/50 ground motion ensembles are relatively close to each other for all shear walls considered, while those for the 10%/50 and 2%/50 ensembles are separated. That is consistent with the fact that the return periods of 50%, 10% , and 2% exceedance in 50 years are 75, 475 and 2,475 years, respectively.

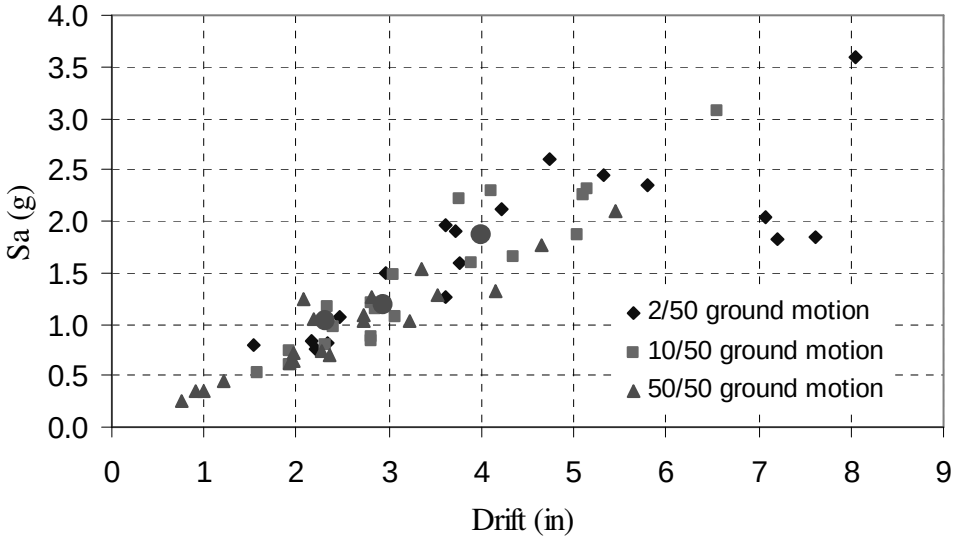

Figure 4.24 Maximum Drift vs. S_a (Two-story Solid Shear Wall)

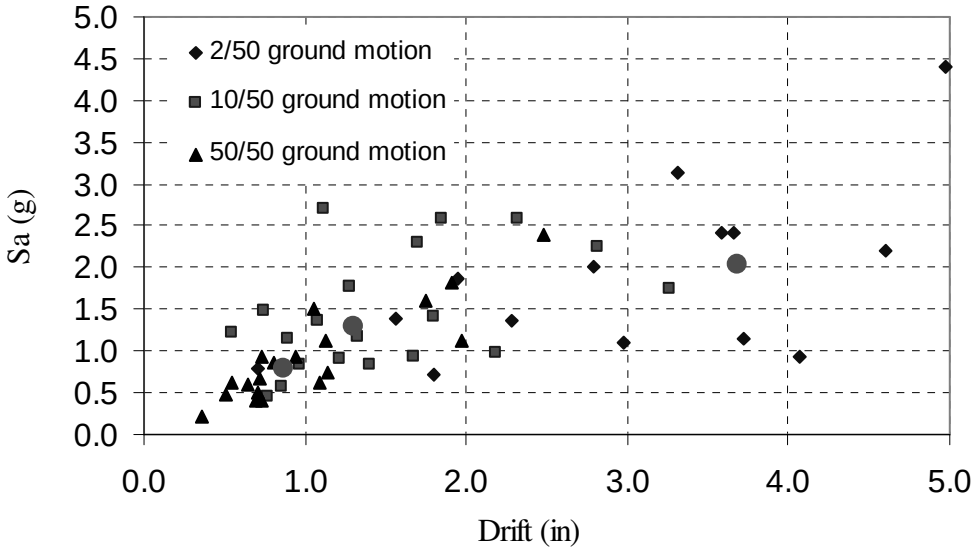

Figure 4.25 Maximum Drift vs. S_a (Shear Wall with Garage Door)

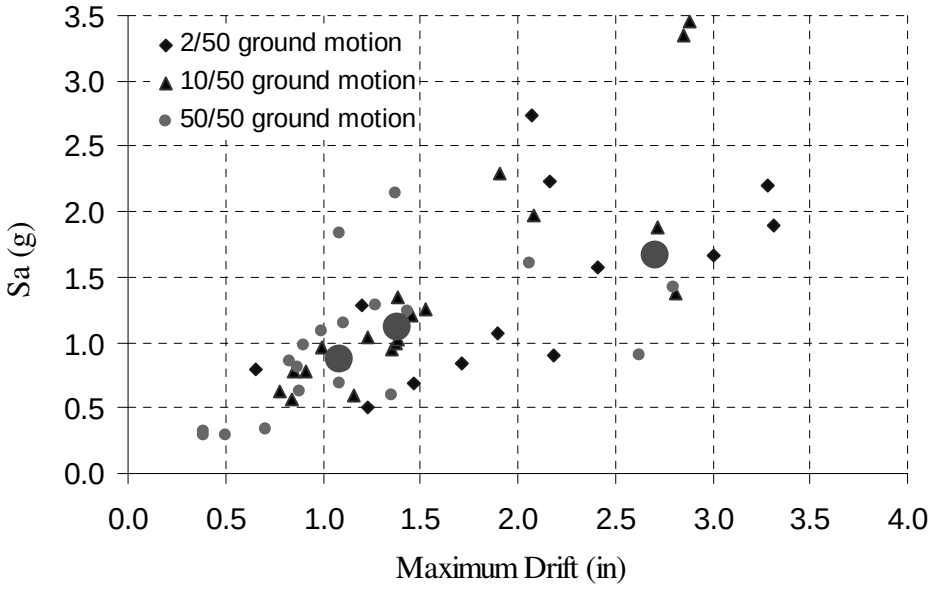

Figure 4.26 Maximum Drift vs. S_a (One-story Shear Wall with Opening, Partially Anchored)

Regression analyses are conducted to determine the constants in Equation 4.1, expressing the relationship between seismic demand (expressed in terms of maximum drift) and seismic intensity (in terms of spectral acceleration). A regression analysis of all 60 D-S_a pairs results in parameters a = 1.075 and b = 0.9832 in Equation 4.1 for the one-story shear wall with opening, with logarithmic standard deviation $\beta_{D|Sa} = 0.315$. Thus, the median seismic demand for this particular shear wall model is $D = 1.075(S_a)^{0.9832}$. Figures 4.28 to 4.31 show the results of similar regression analyses for the other shear wall models.

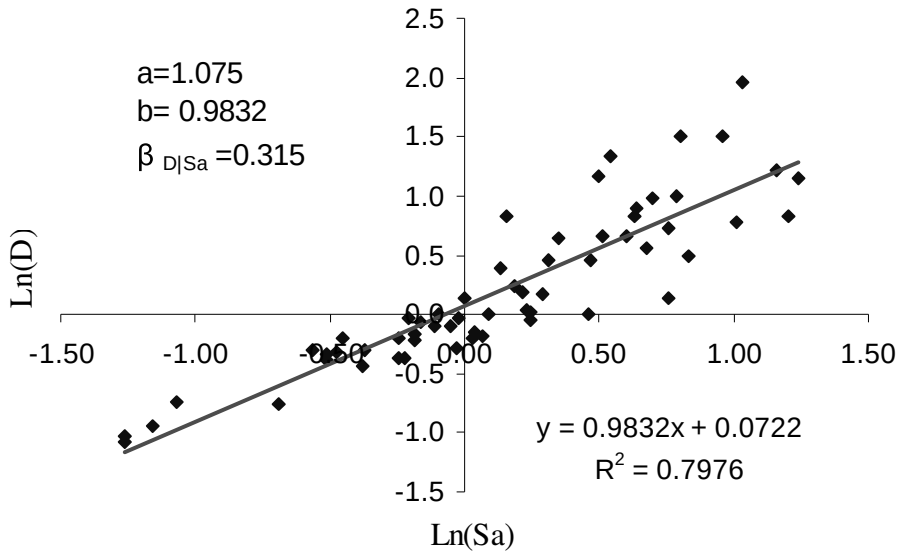

Figure 4.27 Regression Analysis of S_a on Drift (One-story Shear Wall with Opening)

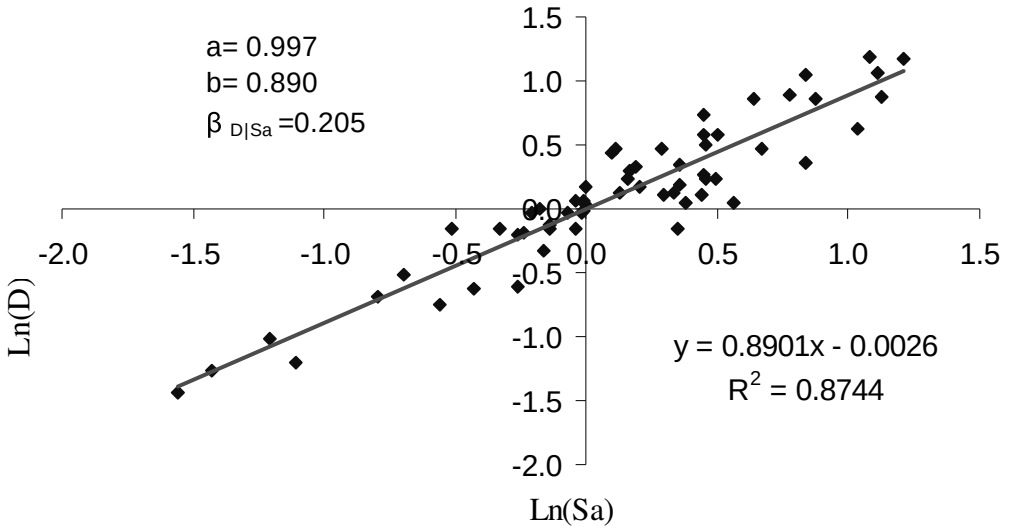

Figure 4.28 Regression Analysis of Sa on Drift (One-Story Solid Shear Wall)

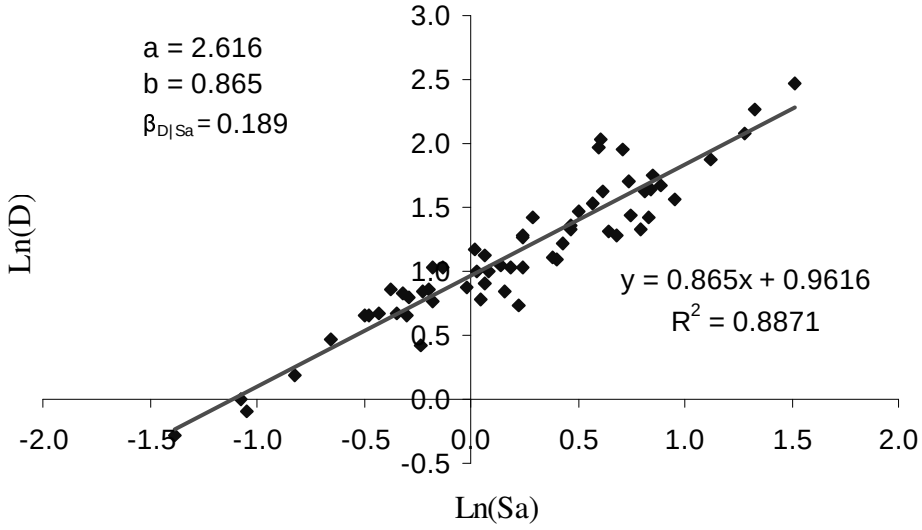

Figure 4.29 Regression Analysis of S_a on Drift (Two-story Solid Shear Wall)

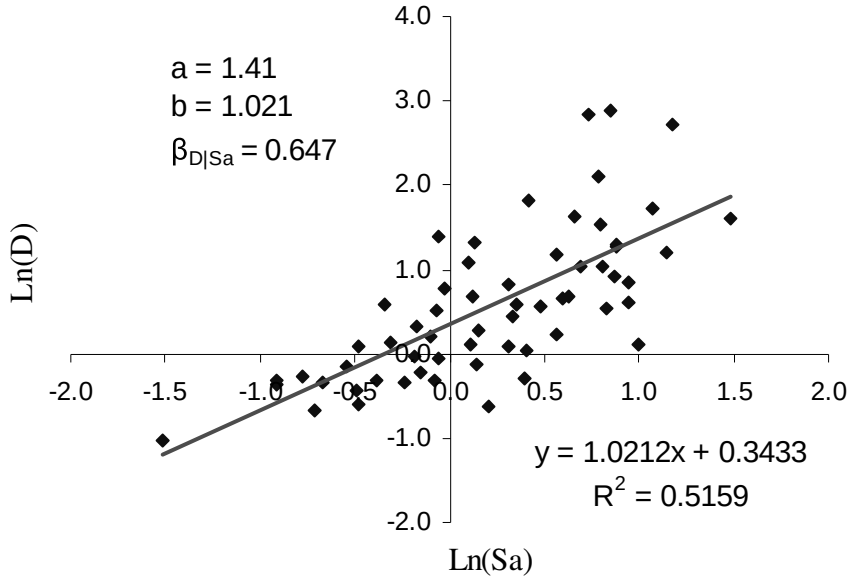

Figure 4.30 Regression Analysis of Sa on Drift (Shear Wall with Garage Door)

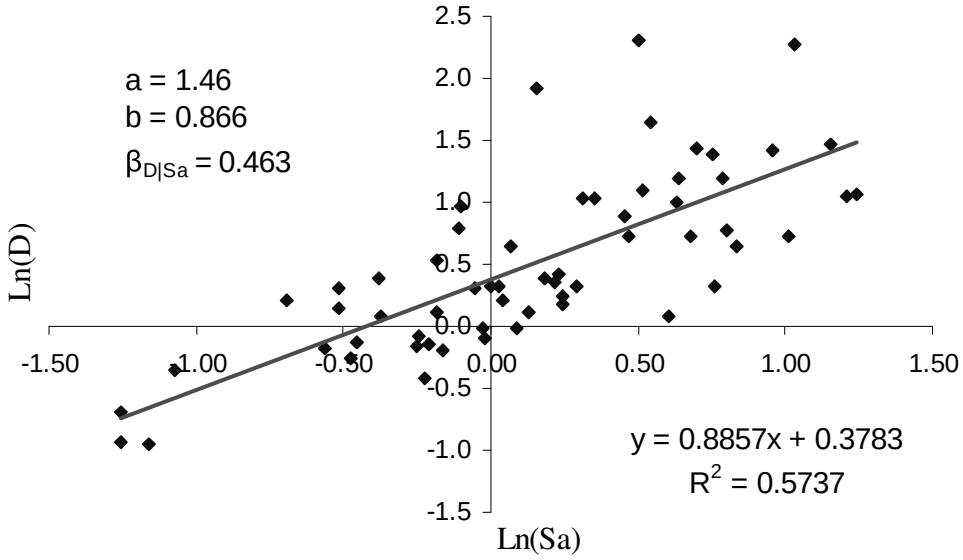

Figure 4.31 Regression Analysis of Sa on Drift (One-Story Shear Wall with Opening, Partially Anchored)

Table 4.3 summarizes the results of the regression analyses for all shear wall models considered. The exponent b in Equation 4.1 in the results displayed in Figure 4.27 to 4.31 is close to 1.0 in all cases, suggesting a (nearly) linear relationship between shear wall deformation and S_a. This result also has been observed for steel moment frames (e.g., Luco and Cornell, 2000) and for some reinforced concrete moment frames, where the fundamental periods were larger than 1.0 sec.

Table 4.3 Summary of Regression Analysis

	Period (Sec)	a	b	$\beta_{D \mid Sa}$
One-story shear wall with openings	0.22	1.075	0.983	0.315
One-story solid shear wall	0.16	0.997	0.890	0.205
Two-story solid shear wall	0.28	2.616	0.865	0.189
Shear wall with garage door	0.32	1.410	1.021	0.647
One-story shear wall with openings (partially anchored)	0.26	1.460	0.866	0.463

While the standard deviation in the deformation increases with spectral acceleration, the logarithmic standard deviation (approximately the coefficient of variation) is assumed to be constant; its value lies between 0.189 to 0.647, with an average of 0.365. This aleatory uncertainty in seismic demand is not inconsistent with what has been observed by other investigators of other structural systems (Luco and Cornell, 2000). Note that the dispersion in seismic demand given Sa, $\beta_{D \mid Sa}$, are substantial higher for the shear wall with garage door opening and the partially anchored wall than for the other remaining walls.

The structural behavior of the wood shear walls represented in Figure 4.22 to 4.26 ranges from the elastic at small S_a to the highly nonlinear at large S_a (the total deformation range is approximately h/600 to h/20, in which h is the height of the shear wall). Over this range, the relationship between D and S_a is essentially linear ($b \approx 1.0$). The implication is that one cannot clearly distinguish linear and nonlinear system behavior in terms of the total deformations in Figure 4.22 to 4.26. In other words, the total displacements of these shear walls are essentially the same, regardless of whether their responses are in the linear or nonlinear range, an example of the "equal displacement rule" first noted by Veletsos and Newmark (1960) over 40 years ago for systems in which the fundamental period exceeded approximately 1.0 sec. It is somewhat surprising to observe a similar result for low-rise wood structures, where the fundamental periods tend to be much less (the range of periods of the shear wall models considered is from 0.16 to 0.32 s).

4.4.2 Lognormal fragility model

Using procedures similar to those in Section 3.4.5 for validation of lognormal hurricane fragility model, seismic fragility could be described by lognormal cumulative distribution. With seismic median demand defined in Equation 4.1, the conditional probability that drift demand (D) exceeds a defined drift limit (d), given a specific S_a, is

$$P(D>d \mid S_a = x) = 1 - \Phi(\ln[d/ ax^b)/ \beta_{D|Sa}) \qquad (4.2)$$

in which $\Phi(\ )$ = standard normal distribution and a, b and $\beta_{D|Sa}$ are determined from the regression analysis described above. Equation 4.2 offers a convenient way to predict the conditional probability of exceeding stipulated drift limits and associated performance goals.

Figure 4.32 presents these conditional probabilities (fragilities) for immediate occupancy IO), life safety (LS) and collapse prevention (CP) performance levels (drift limits of 1%, 2% and 3%, respectively, as noted previously). Figure 4.32 illustrates the conditional failure probability (fragility) of a one-story shear wall with openings. The foundation of this shear wall is assumed to be fully anchored. Such fragilities can be used to evaluate the effectiveness of current building practices and to suggest cost-effective improvements to building codes. For example, if the median spectral acceleration (at a period of 0.2 sec) associated with the design earthquake is 1.4 g, as might be typical in areas of southern California, the probabilities of impaired function, life-threatening damage and incipient collapse are, respectively, 93.1%, 20.3% and 1.5%.

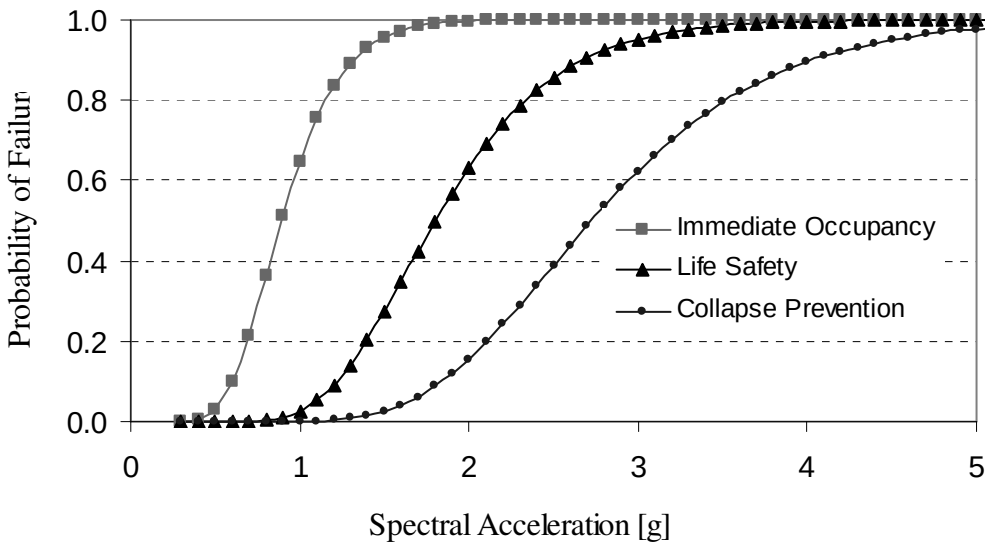

Figure 4.32 Fragility of One-story Shear Wall with Opening

Figure 4.33 shows the fragility of a one-story solid wall for the same three performance levels. This solid shear wall can be regarded as a conservative model for wood construction resisting lateral loading. While it is likely to suffer minor damage with design seismic load in LA area, which is about 1.4 g, it is expected to perform well to protect life safety and prevent collapse. The probability of collapse is virtually zero should an earthquake causing a S_a of 1.4g occur.

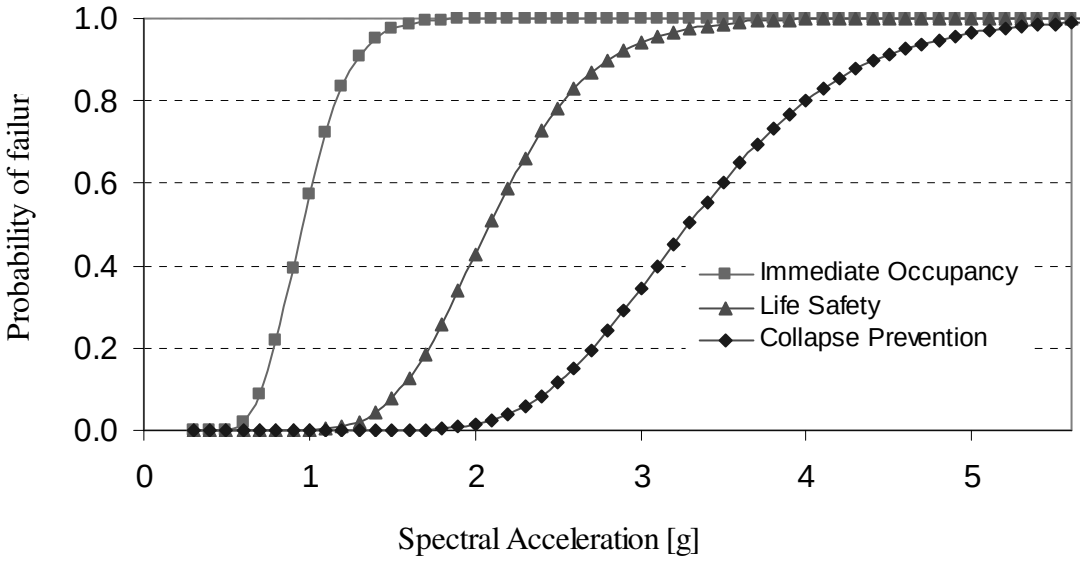

Figure 4.33 Fragility of One-story Solid Shear Wall

The lateral displacement at the eave of the two-story house subjected to ground motions is more than twice that for the one-story house; the height of the former is twice that of the latter and the interaction between shear wall panels in both floors contributes further to the drift. The fragility curves shown in Figure 4.34 are developed based on drift rather than displacement to be consistent with the deformation measure for other shear wall arrangements. When S_a exceeds 1.0 g, it is almost certain that the house will experience minor damage. Furthermore, when S_a is about 1.4 g, the probability of life-threatening damage is approximately 30%.

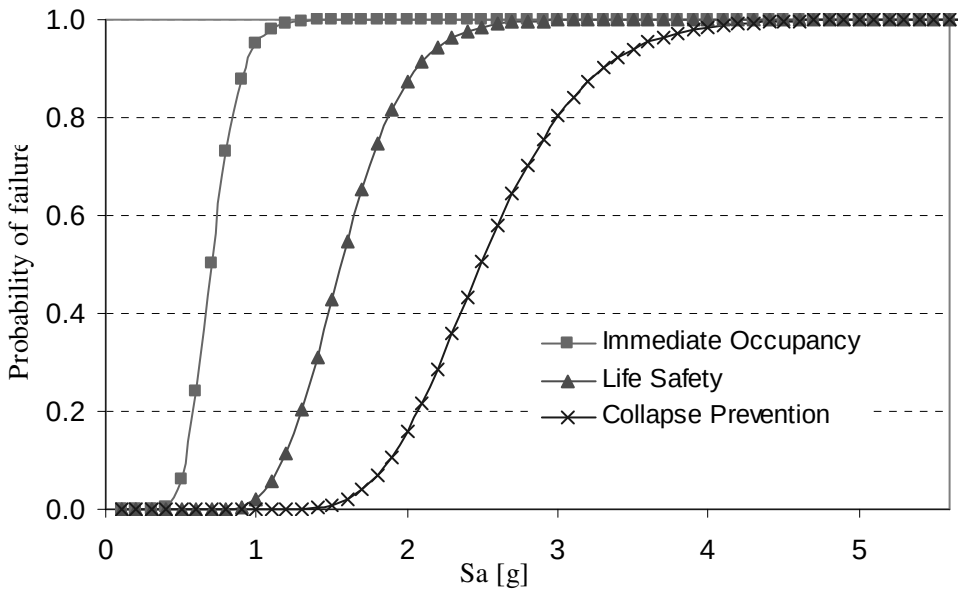

Figure 4.34 Fragility of Two-story Solid Shear Wall

The fragility curves of the shear wall with the garage door opening (Figure 4.35) can be considered as a lower limit on wall capacity to resist horizontal loading because of the weakening effect of the large opening. Should an earthquake with 1.5 g S_a impact a residence that only has this type of shear wall as a lateral load resisting system, it is expected that life threatening damage and collapse will occur with 37.5% and 57.6% probability, respectively. Surprisingly, the likelihood of impaired function (i.e. exceedance of 1% drift) for the shear wall with openings (Figure 4.4) is not significantly higher than that of the other shear walls (e.g. Figure 4.2 and 4.3). Actually, the probability of minor damage of a one-story or two-story solid wall is even higher than that for the shear wall with garage door opening subjected to the same ground motion. That means shear wall with large openings is more likely to suffer moderate and severe damage than just minor damage.

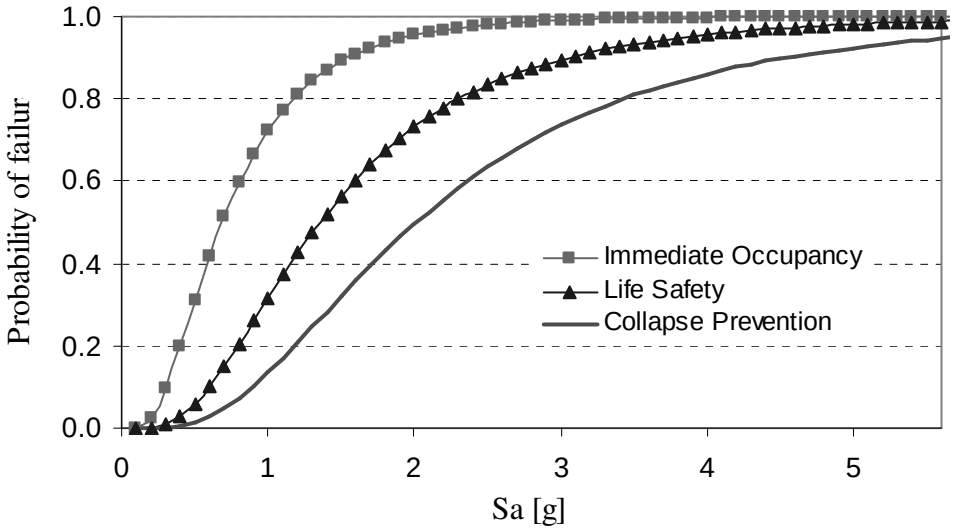

Figure 4.35 Fragility of Shear Wall with Garage Door

Figure 4.36 depicts the fragility of a one-story shear wall with hold-down partially anchored. As noted previously, this shear wall has only 70% of the cyclic stiffness and strength capacity of the same wall with its base fully anchored, and would be typical of construction in regions of low to moderate seismicity. Compared with fragility curves in Figure 4.32, which represents the same shear wall configuration except with full restraint at the foundation, the probability of failing to meet the life safety performance level is 100% higher when S_a is 1.5g. Further comparisons are presented in the ensuing sensitivity analysis.

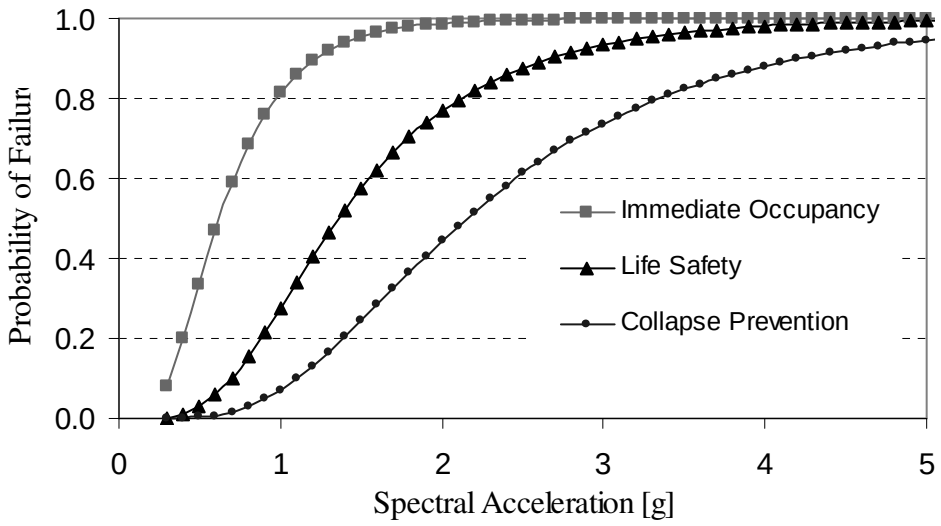

Figure 4.36 Fragility of Shear Wall with Openings (Partially Anchored)

4.4.3 Parametric sensitivity analysis

Ground motion intensity

Like the hurricane fragility presented in Chapter 3, seismic fragility is affected by individual parameters in seismic loading and structural characteristics. A sensitivity analysis is conducted to determine the relative contribution of these parameters. Among the contributors, ground motion is expected to be one of the most significant factors. As shown in Figure 4.22 to 4.26, the drift of the shear wall increases as the intensity of the ground motion increases. This is further illustrated in Table 4.4. However, the effects of the intensity on median drift of shear wall vary from configuration to configuration. For instance, the median drift demand on the one-story shear wall with openings is about

10% higher using the 10%/50 records than from using the 50%/50 records. In comparison, the median drift demand on the shear wall with garage door subjected to 10%/50 ground motions is 50% than that using the 50%/50 records.

Table 4.4 Median Drift (%) Vs. Level of Ground Motion

Level of ground motion	50%/50	10%/50	2%/50
One-story shear wall with openings	0.966	1.090	2.240
One-story solid shear wall	1.110	0.995	1.565
Two-story solid shear wall	1.160	1.470	2.000
Shear wall with garage door	0.874	1.300	3.690
One-story shear wall with openings (partially anchored)	1.089	1.380	2.710

Shear modulus of sheathing

The shear modulus of the sheathing has little effect on the performance of the shear wall, assuming that the hysteretic behavior of individual fasteners is independent of the thickness of the shear wall sheathing. Figure 4.37 shows the hysteretic behavior of two shear walls with openings, one with sheathing shear modulus of 180 psi (1,241 kPa) and the other with modulus 240 psi (1,655 kPa). The load-displacement relationships basically are identical. The fragility curves for these two walls also are virtually the same.

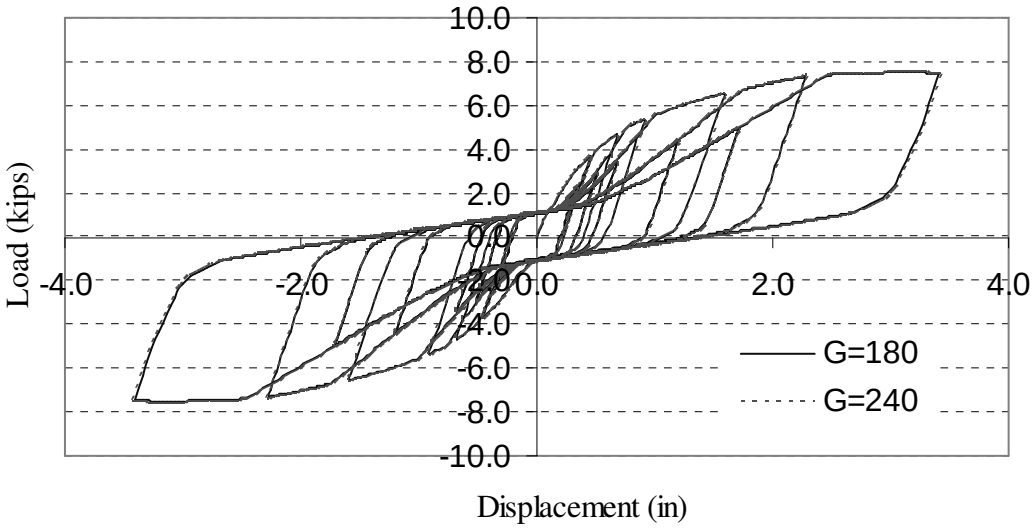

Figure 4.37 Effect of Shear Modulus of Sheathing on Shear Wall Hysteresis Curve (One-Story Shear Wall with Opening)

Fastener spacing

The overall structural deformation of the shear walls is dominated by the individual behavior of sheathing-to-framing fasteners. Subsequently, the spacing of the fasteners plays an important role in the performance of shear wall against seismic loading. Figure 4.38 illustrates two hysteretic curves for the one-story shear wall with openings, but with different fastener spacing. The hysteretic curve with exterior/interior fastener spacing of 4/6 in (102 mm / 152 mm) has a higher cyclic stiffness and strength capacity than those of its counterpart with fasteners spaced at 6/12 in.

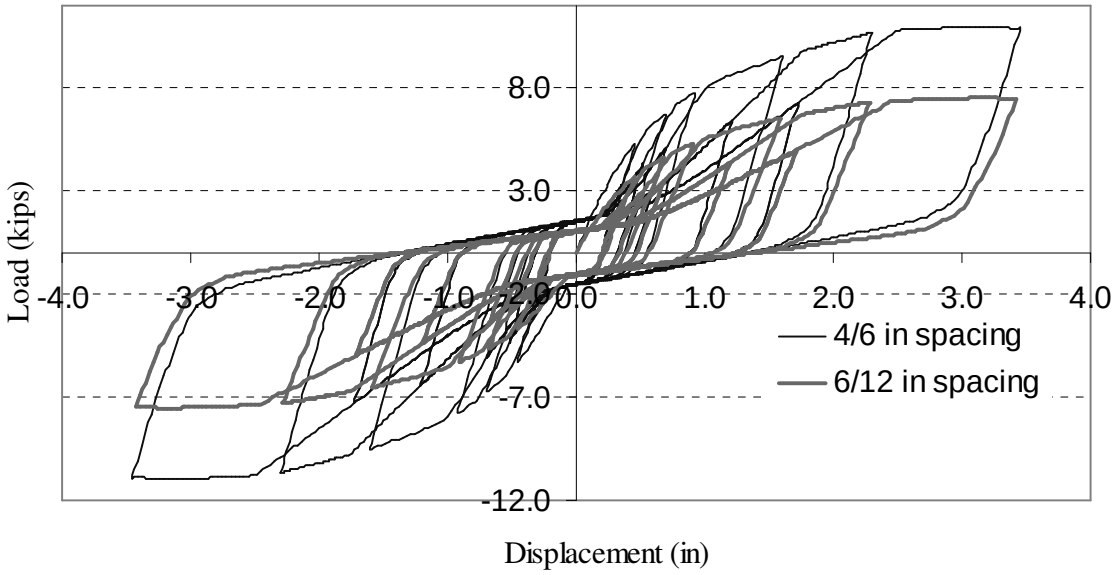

Figure 4.38 Effect of Fastener Spacing on Shear Wall Hysteresis Curve (One-Story Shear Wall with Openings)

By reducing the shear wall exterior/interior panel fastener spacing from 6/12 in to 4/6 in, the probability of exceeding the FEMA 273/356 drift limits associated with IO, LS and CP decreases moderately. The dashed lines in Figure 4.39 represent the probability of failure of the shear wall with 6/12 in fastener spacing, while the solid lines characterize the wall with 4/6 in fastener spacing. If the S_a is 1.5 g, the probability of failing to achieve the immediate occupancy and life safety performance levels using reduced fastener spacings of 4/6 in rather than 6/12 in is reduced by 8.2% and 12.3%, respectively.

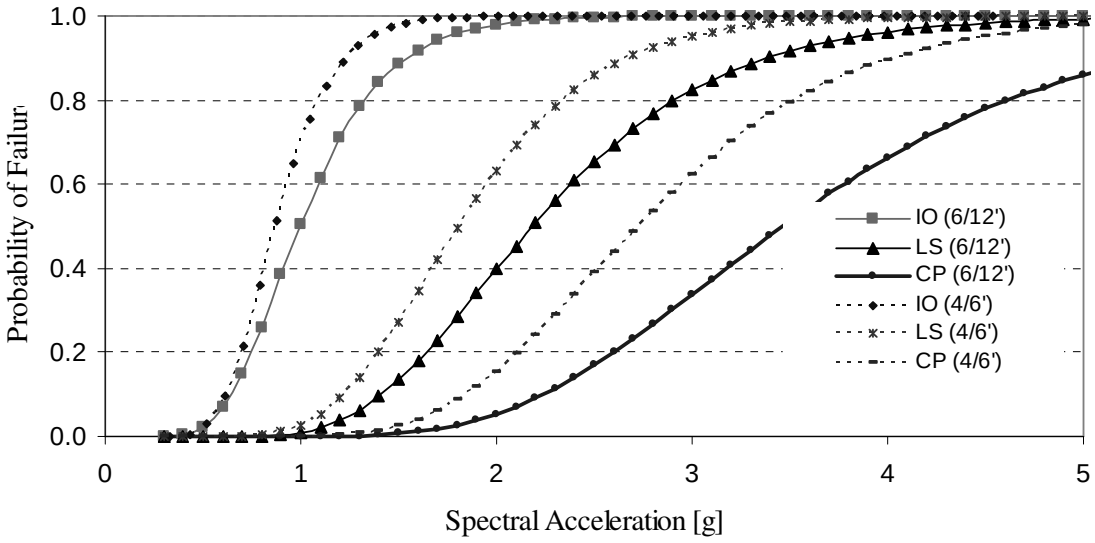

Figure 4.39 Fragilities with Different Fastener Spacing (One-story Shear Wall with Opening)

Table 4.5 lists the median drift demands on shear walls with 6/12 in and 4/6 in exterior/interior spacing of fastener when they are under ground motions with a variety of intensities. The increase in median drift caused by the 2%/50 ground motion is apparent. On the other hand, the difference is negligible for the two shear walls subjected to 10%/50 ground motions.

Table 4.5 Median Drift (%) of Shear Wall with Different Fastener Spacing

Level of ground motion	50%/50	10%/50	2%/50
Fastener spaced at 6/12 in	0.966	1.090	2.240
Fastener spaced at 4/6 in	0.902	1.085	1.640
Difference in drift	7.1%	0.5%	36.6%

Shear wall openings

The effects of openings on lateral force-resisting shear walls were investigated by Dolan and Heine (1997). They found that sheathing above and below openings typically do not contribute to overall performance of the shear wall. Figure 4.32 and 4.33 illustrate the different load-displacement curves for a one-story shear wall with and without openings. Figure 4.40 shows the fragility of the two shear wall models. In the figure, the decrease in the probability of reaching the collapse prevention (CP) drift limit for the shear wall without openings is most noticeable, following by drift limit for life safety (LS). The least difference in probability is seem for the immediate occupancy (IO) limit state.

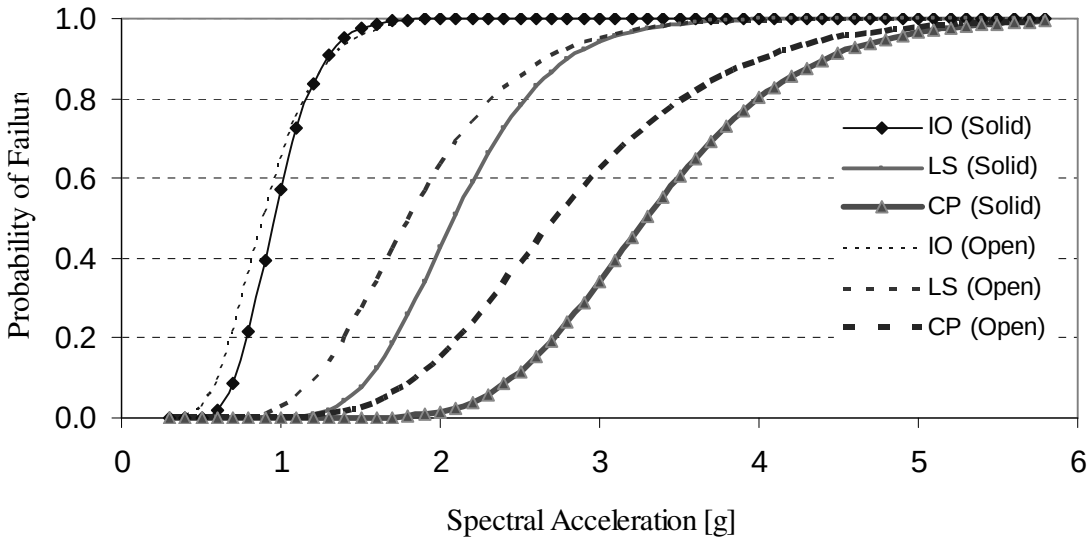

Figure 4.40 Fragility of Shear Wall with/without Openings (One-story Shear Wall)

Shear wall foundation constraints

The cyclic stiffness and strength of a shear wall without adequate hold-downs decreases significantly compared to the same shear wall with its base constrained. The partially anchored shear wall sustains larger displacements when it is subjected to an earthquake. That is obvious in Figure 4.41, where the dashed curves represent the probability of exceeding performance limits for a shear wall with fixed foundation and solid lines stand for that with partial anchor. An apparent increase in the probability of failure is seen for the limit state of collapse prevention. The increase is about 30% at the neighborhood of 2 g S_a. But the probabilities of failure tend to be the same when the S_a exceeds a particular level. This particular S_a is 1.3 g, 2.5 g, and 3.5g for limit states of immediate occupancy, life safety and collapse prevention, respectively.

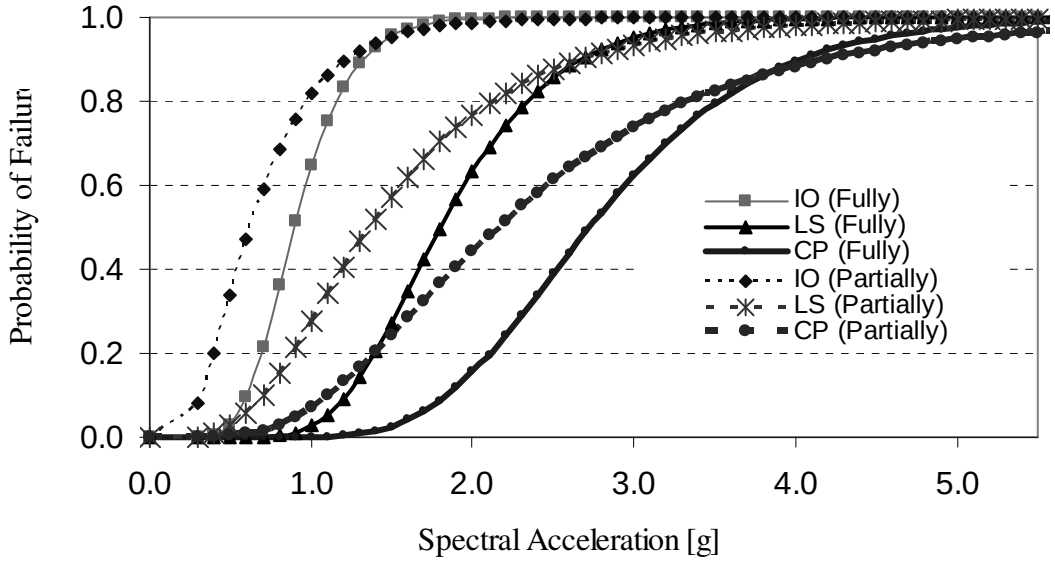

Figure 4.41 Fragility of One-story Shear Wall with Opening (Fully or Partially Anchored)

Table 4.6 summarizes the median drifts of one-story shear walls with opening subjected to three levels of ground motions. One shear wall has fully anchored hold-downs and the other has partially anchored hold-downs. The increase in drift for the poorly anchored wall ranges from 13-26% for different level of ground motions.

Table 4.6 Median Drift (%) of Shear Wall with Fully/Partially Anchored Base Constraints

Level of ground motion	50%/50	10%/50	2%/50
Fully anchored	0.966	1.090	2.240
Partially anchored	1.089	1.380	2.710
Difference in Drift	13.0%	26.6%	20.0%

4.5 Seismic reliability analysis of light-frame wood construction

4.5.1 Seismic hazard curve

Seismic hazard curves determined by the U.S. Geological Survey [http://eqhazmaps.usgs.gov] define the probability that spectral accelerations of a 5% damped oscillator at periods of 0.2, 0.3 and 1.0 sec are exceeded at specific sites. The

seismic hazard H(x), the probability that spectral acceleration S_a exceeds x can be approximately described by (Cornell et al. 2002)

$$H(x) = P[S_a > x] = k_o * S_a^{-k} \qquad (4.3)$$

which represents a linear relationship on a log-log plot. Terms k_o and k are constants. Typical values of constant k are 1-4, the higher values being typical in the western United States, while the lower values are found in the central and eastern US.

From the USGS website identified above, mean spectral accelerations in Los Angeles area are 1.26 g, 1.67 g, and 2.10 g, for an oscillator with a fundamental period of 0.2 sec and 5% damping ratio, for 10%, 5%, and 2% probabilities of exceedance in 50 years, respectively. The corresponding constants in equations 4.3 for Los Angeles area are k = 3.2 and k_o = 0.0046. Figure 4.42 shows the seismic hazard curve in Los Angeles area on log-log paper.

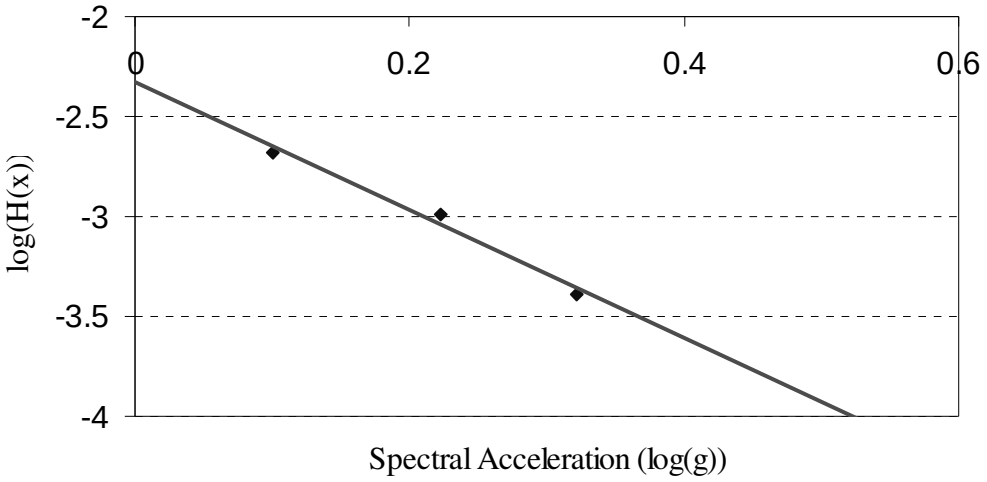

Figure 4.42 Seismic Hazard Curve (Los Angeles Area)

4.5.2 Fully coupled seismic reliability analysis

A fully coupled reliability analysis provides a framework to incorporate uncertainties in seismic demand and structural system response, and a tool to measure the performance and reliability of a structural system exposed to seismic hazard on a consistent basis. The probability of failure under a spectrum of possible earthquakes is determined by convolving the structural fragility curve and seismic hazard curve,

$$P(D > d) = \int P[D > d \mid S_a = x] \mid dH(x) \mid \qquad (4.4)$$

in which D = deformation, S_a = spectral acceleration at the fundamental period of the structure, P [D >d | S_a = x] is the structural fragility, defined as the conditional probability

of failure of certain limit states given a certain level of spectral ground motion, x, and H(x) is the seismic hazard function.

Convolving the lognormal fragility function defined in Equation 4.2 and the derivative of the seismic hazard function presented in Equation 4.3, leads to an expression for the probability that the drift exceeds a specific level, d (Cornell, et al. 2002),

$$P(D > d) = H(S_a^d) \exp\left[\frac{1}{2} \frac{k^2}{b^2} \beta_{D|S_a}^2 \right] \qquad (4.5)$$

in which (S_a^d) represents the spectral acceleration corresponding to a specific drift limit d. Using Equation 4.1, this relation is expressed by,

$$S_a^d = (d/a)^{1/b} \qquad (4.6)$$

Then, $H(S_a^d)$ is the seismic hazard with spectral acceleration of S_a^d, representing the probability that ground motion intensity S_a causes drift d to be exceeded.

Table 4.7 summarizes the annual probabilities of exceedance of various drift limits associated with three levels of performance for different shear wall configurations and base constraints. The table also includes the annual probability of occurrence of spectral accelerations that cause drifts of shear wall to exceed the FEMA 273-specified drift limits in Los Angeles. For instance, the annual likelihoods that residential construction with the one-story shear wall with openings and no hold-down anchors suffers minor damage, life

threatening damage, and incipient collapse are 8.05%, 0.62%, and 0.14%, respectively. The corresponding (mean) probabilities of an earthquake that causes the associated drifts (i.e. 1%, 2%, and 3%) are 0.18, 0.006, and 0.0014, respectively.

Table 4.7 Annual Probability of Exceedance of Drift Limits and Corresponding Seismic Hazard

Performance Limit State		Immediate Occupancy	Life Safety	Collapse Prevention
Drift Limit		1%	2%	3%
One-story shear wall with openings	$H(S_a^d)$	5.8E-03	6.1E-04	1.6E-04
	P(D>d)	1.005%	0.105%	0.028%
One-story solid shear wall	$H(S_a^d)$	4.55E-03	3.76E-04	8.76E-05
	P(D>d)	0.597%	0.049%	0.011%
Two-story solid shear wall	$H(S_a^d)$	1.24E-02	9.56E-04	2.13E-04
	P(D>d)	1.586%	0.122%	0.027%
Shear wall with garage door	$H(S_a^d)$	1.32E-02	1.50E-03	4.22E-04
	P(D>d)	8.724%	0.994%	0.279%
One-story shear wall with openings (Partically anchored)	$H(S_a^d)$	1.86E-02	1.44E-03	3.21E-04
	P(D>d)	8.048%	0.621%	0.139%

The annual probability of failing to meet the immediate occupancy objective is approximately 10 times the probability of not meeting the life safety objective for all shear wall models, except for shear wall with garage opening, for which the difference is 9 times. In comparison, the difference in annual likelihood of exceeding the drift limit associated with life safety and collapse prevention is approximately a factor of 5.

The annual probabilities that drift demands on shear walls with different configurations exceed any particular maximum drift are also calculated using Equation 4.5. The curves shown in Figure 4.43 demonstrate the annual probability of drift exceedance of different shear walls. The presence of seismic hold-down anchors is critical to the performance of wood-frame shear walls; the annual probability of exceeding various drift limits increases 6-8 times, should the shear wall not be fully anchored to the foundation. The difference decreases as the drift limit increases. The probability of exceeding specific drift limits appears to be less sensitive to whether or not the shear wall has base constraints once the drift limit has exceeded a certain level.

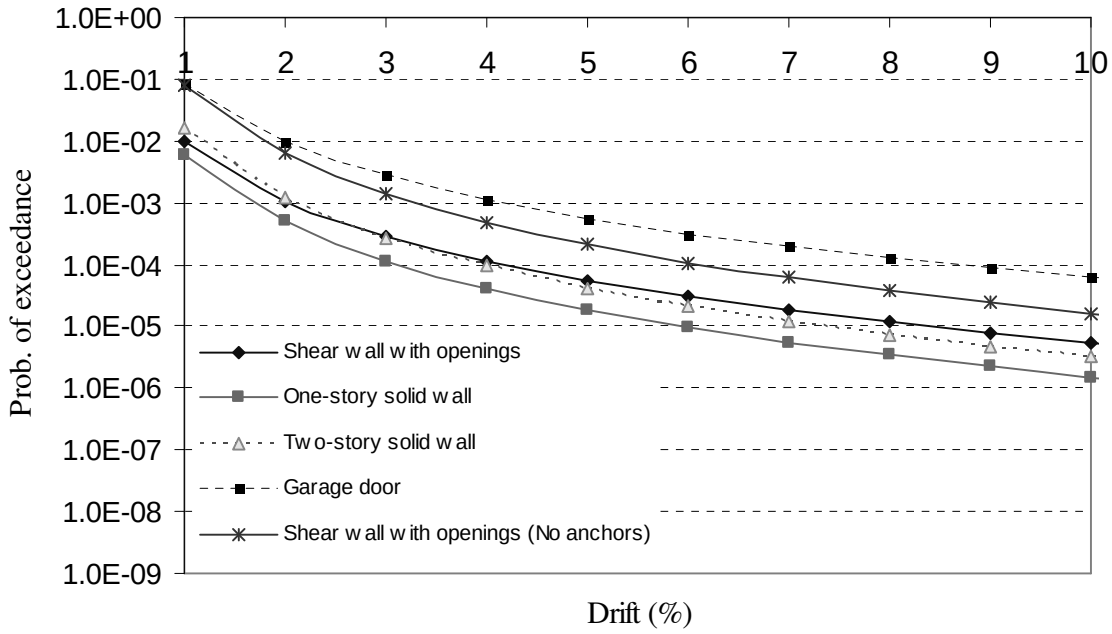

Figure 4.43 Annual Probability of Drift Exceedance of Various Shear Walls

The probability of drift exceedance for the two-story solid shear wall is higher than for the one-story shear wall with openings for drift limit less than 2%. However, when the drift limit is between 2% and 3%, the probabilities of drift exceedance of both walls are basically the same. The failure rate of the shear wall with openings is higher than that of its counterpart when drift limit is more than 3%. When the drift limit is 1%, the probabilities of drift exceedance for both the shear wall with the garage door opening and the one-story shear wall with openings are about 8%. However, as the drift limit increases, higher failure rate for garage shear wall is observed.

4.6 Summary

The vulnerability of wood residential construction to earthquake effects was evident from its performance during the 1994 Northridge earthquake. This chapter presents a methodology for assessing performance of light frame residential construction subjected to various levels of earthquake ground motions. A finite element-based platform and stochastic models are used to simulate the behavior of wood frame structures in which shear walls provide the resistance to lateral forces. Uncertainties in ground motion are identified and incorporated in the probabilistic analysis of system behavior, leading to fragilities (conditional failure probabilities) of the shear walls for various performance limits as a function of spectral acceleration. The relationship between spectral acceleration and maximum drift as a simple tool for estimating seismic demand is discussed. Seismic hazard curves that have been determined by the U.S. Geological Survey define the probabilities of a spectrum of earthquake hazards. Probabilities of failing to meet stipulated performance goals can be calculated by convolving the structural fragility with these seismic hazard curves in a fully coupled analysis. The probability that shear wall drift limits are exceeded for earthquake ground motions with 2%, 10%, and 50% probability of being exceeded in 50 years can be estimated from this analysis. Among the more important conclusion is that partial (or improperly installed) anchoring increases the expected failure rate by 13 - 26% in region of high seismicity such as Los Angeles.

5 COMPARATIVE RISK ASSESSMENT OF HURRICANE AND EARTHQUAKE HAZARDS

5.1 Introduction

Although in many parts of the United States the hazard due to either hurricane or earthquake (but not both) is significant, in certain areas both hazards may be significant. In such areas, businesses and governmental entities may wish to manage losses from these competing hazards. Integrated building design and construction practices should address these differences to optimize strategies to achieve an overall risk that is consistent with social objectives. Furthermore, in the new paradigm of performance-based engineering, stipulated structural performance objectives must be satisfied at a prescribed confidence level at various hazard levels and for different hazards. Recent developments in the United States in performance-based engineering have focused on the seismic hazard. However, the implications of the performance-based engineering paradigm are broader, and should address alternate and competing hazards (e.g. hurricane) in order to achieve an integrated design goal. To do this effectively, the relative risks associated with performance under a spectrum of natural hazards must be understood.

A comparative assessment of hurricane and earthquake risks can help address the above issues by providing tools for rank-ordering approaches for managing risks due to these natural hazards from the standpoint of regional and national public policy and disaster

planning purposes, as well as for insurance underwriting. Comparative risk assessment requires: a fragility modeling process for typical light-frame construction utilizing traditional (often non-engineered) construction practices, and probabilistic models of natural hazard occurrence and intensity.

5.2 Perspectives on hurricane and earthquake risk

Hurricane and earthquake hazards are different in terms of the nature of the hazards, frequency of occurrence and associated return period for design, hazard-resistant design philosophy, consequence, and disaster mitigation strategies. Management of risks due to natural hazards through proper design, construction practices, and occupancy and code enforcement presents a challenge to the structural engineering community as well as facility owners and policy makers.

Even though hurricane and earthquake loads both are treated as "lateral loads" in design, the way that these loads act on wood-frame residential construction is different. In hurricanes, the most vulnerable part of the building is its envelope. Damage to the building envelope leads to contents damage by wind and rain. The damage usually occurs at the weakest area of the envelope. The wind load acts as a static load because the natural frequency of most low-rise residential construction ranges between 1.2 to 18 Hz, a range that is higher than the range in frequency of wind pressure fluctuations that account for most of the wind energy (Foliente, 1997). The design to enhance wind

resistance of components that are crucial to maintain overall building integrity is based on the presumption of elastic behavior and on force control.

Unlike wind load, seismic loading causes damage to residential construction by imposing excessive inelastic deformations. The earthquake effect on the structure usually is dynamic in nature, because the frequency content of earthquake excitation typically overlaps with the natural frequency of residential construction. Accordingly, the philosophy in earthquake-resistant design is to maximize energy dissipated during response of structural and non-structural components by increasing the ductility of the structural system. Design is based on fictitious elastic forces for convenience, but the force requirements are devised in such as way as to achieve deformation control.

The return periods associated with hurricane and earthquake hazards on which design is based are different. The threat to life safety by hurricanes is mitigated by advanced warning systems operated by the National Weather Service and civil authorities. On the other hand, the economic impact of damage to building contents from wind and rain as well as building evacuation is significant. In comparison, the lack of advanced warning makes the life safety objective paramount for earthquakes. For both hazards, the disruption and downtime in the local business community, as well as the need for certain essential facilities to maintain their integrity for post-disaster recovery, must factor into any comparative risk assessment. The design wind speed in ASCE Standard 7-05 is based on a 50- or 100-year return period peak (3-second) gust wind speeds along the coast (ASCE-7, 2002). Until recently, the ground motion intensity for seismic design was

set as the intensity with a return period of 475 years; current seismic hazard maps stipulate 2%/50 spectral acceleration with a 2,475-year return period, the design spectral acceleration is 2/3 of the stipulated intensity.

In some cases, mitigating one risk may reduce building vulnerability to another. For instance, the use of more ductile design details and enhancing connections between components (e.g. roof-to-wall, wall-to-foundation) may reduce damage from both hurricane and earthquake loading. Installation of seismic shear wall anchors will be beneficial for residence to resist horizontal wind load. However, in other cases mitigating one hazard may increase vulnerability of other hazards. A lighter structure, such as a glass wall or light roof system, may reduce seismic force, but the potential for damage due to wind will increase. Standards and construction practices should aim at optimizing overall costs and risks. To do this effectively, the relative risks associated with building performance under a spectrum of natural hazards must be understood.

5.3 Selection of cities and limit states of damage

While severe earthquakes have occurred in mid-America (e.g. New Madrid, Missouri) and in eastern coastal regions (e.g. Charleston, South Carolina) hurricanes occur more frequently along the gulf and eastern coasts. In certain areas both hazards may be significant. To obtain some idea of the comparative hazards and risks, typical wood-frame structures in several cities are evaluated. On the east coast, the cities of Boston in MA and Charleston in SC are selected. On the west coast, Los Angeles, CA and Seattle,

WA are chosen. In addition, Honolulu, Hawaii and Anchorage, AK are considered to expand the scope of the comparison analysis. There are no hurricanes in Hawaii and Anchorage, but strong winds occurring in the cities are assumed to have the same damage mechanism as the other cities selected. Three damage states - minor, moderate, and severe – will be used in comparative assessment for wind and earthquake hazards.

The hurricane fragility analysis will focus on key components of the building envelope that are necessary to maintain overall integrity of the building and its contents. Based on the mapping between various component (e.g. roof panel, window, roof-to-wall connection) damage states and building damage states (e.g., minor, moderate, and severe) categorized by HAZUS (NIBS, 2000) and post-disaster surveys (NAHB, 1993, 1999), the three damage states in the current study are identified as follows: minor damage as loss of one roof panel; moderate damage as failure of two or more windows or multiple roof panels; and severe damage as failure of the roof-to-wall connection, leading to roof uplift and collapse of the wall due to the lack of lateral support. It should be recalled from Chapter 3 (Figure 3.6 – 3.7) that once a roof or glass panel fails, the internal pressure coefficients increase, causing an increase in pressures on the interior surfaces and increasing the limit state probabilities calculated.

Post-disaster surveys have shown that the structural and nonstructural damage to light-frame wood residential construction due to earthquake generally can be related to excessive lateral drift of the building system. The structural response quantity of interest in this study is the maximum drift (D) of the shear wall. In FEMA 273/356 (1997/2000),

the “light”, “moderate”, and “severe” damage for lateral force-resisting structural elements in light-frame wood construction subjected to seismic effects are related to transient lateral drifts of 0.01, 0.02 and 0.03, respectively.

The structural design limit states for residential buildings subjected to hurricane and earthquake are different. Ideally, comparative risk assessment of different hazards should be performed using an equivalent measure, such as percentage of replacement value or dollar losses. Due to the lack of sufficient data to support such comparison, the previous defined building damage states due to hurricane (i.e, minor, moderate, and severe) and “light”, “moderate”, and “severe” damage resulting from earthquake hazards are used directly for the risk comparison in this study.

The limit state for “minor damage” is one roof panel uplifted for hurricane wind and exceedance of 1% drift during earthquake. Removal of one roof panel will result in minor building contents property damage by accompanying rain (NAHB, 1993 and 1999), while 1% drift of wooden residence usually results of “light” damage to non-structural components and finishes (CUREE, 2004). A “moderate” damage limit state is defined as failure of two or more glass panels in windows or doors, combined with removal of at least one roof panel, resulting in additional interior property damage by rain (NIBS, 2000). Similarly, the 2% drift limit associated with moderate earthquake damage causes significant damage to interior finishes and moderate damage to the structural system (CUREE, 2004). Finally, severe damage limit states for both hazards relate to life-threatening damage in addition to property damage. The limit state for severe

hurricane damage is failure of the roof-to-wall connection, which may lead to instability of the wall and subsequent collapse of a portion of the building (Manning and Nicolas, 1991). A similar limit state for seismic damage is 3% lateral deformation (or drift), corresponding to a state of incipient collapse of light-frame wood residential buildings (FEMA 273/356, 1997/2000).

5.4 Probability of damage as a function of hazard intensity

5.4.1 Hurricane damage as function of wind speed

Two typical one-story residences with different levels of wind protection are selected to illustrate the comparative risk assessment. Both have the same configurations, with mean roof height of 11.5 ft (3.5 m). These residences both have gable roofs with a slope of 6:12 without overhang. One residence has roof panels attached to roof trusses with 6d nails (0.113 in or 2.9 mm in diameter), large-panel windows (40 sq ft; 4 sq m) with 1/8 in (3 mm) glass, and roof trusses attached to the upper sill plate of the wall with three 8d (0.131 in or 3.3 mm in diameter) nails per truss. These characteristics correspond to minimum standards for hurricane protection for residences in hurricane-prone coastal areas. The second residence has the same basic configuration but the roof panels are attached to the rafters with 8d nails instead of 6d nails. The windows are the same as above. However, the roof trusses are connected to the wall by hurricane clip connectors

(H2.5 connector). This type of construction conforms to a higher standard for resisting hurricane winds. This standard is termed with “intermediate standard” for simplicity in this study.

Figure 5.1 illustrates the probabilities of the three hurricane damage states for the residence constructed to minimum standards for hurricane wind resistance, while Figure 5.2 illustrates similar probabilities for the residence constructed to an intermediate standard of protection identified above. The three curves in each figure correspond to probabilities of minor, moderate and severe damage. By comparing Figure 5.1 with Figure 5.2, it is seem that the probability of various damage levels for the residence built with the intermediate standards are substantially reduced from levels for the similar building built with the minimum standards. If a hurricane with a 3-s gust wind speed of 130 mph (54 m/s) were to occur (the design-basis hurricane in Charleston, SC), the estimated probability of minor, moderate, and severe damage to the one-story residence with minimum design wind standards is 84.6%, 53.2% and 7.5%, respectively. By comparison, the minor, moderate, and severe damage to the same house with higher standards are 54.3%, 11.6%, and 0.2%, respectively.

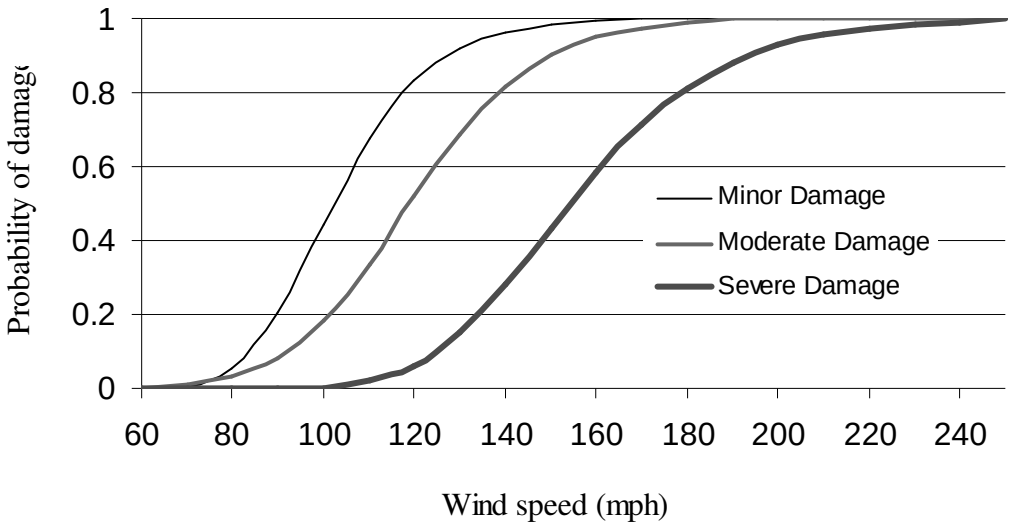

Figure 5.1 Probability of Hurricane Damage (Minimum Standard)

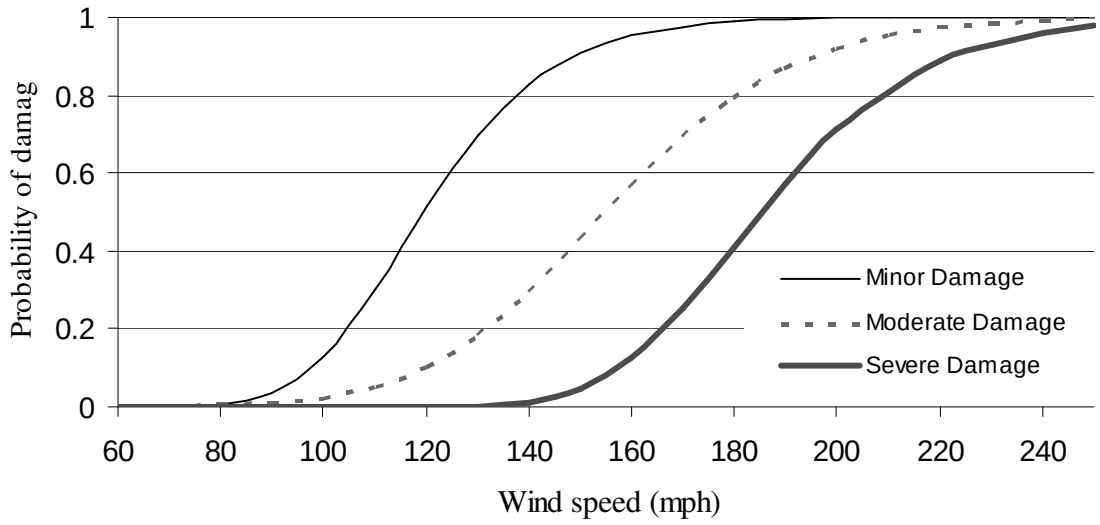

Figure 5.2 Probability of Hurricane Damage (Intermediate Standard)

5.4.2 Earthquake damage as function of spectral acceleration

The same procedure that was used to develop seismic fragility curves for Los Angeles, CA in Chapter 4 is used to predict earthquake damage for the five other cities identified above. Due to high seismicity in the western US, current building codes require residences to be designed and built with their shear walls properly anchored to the foundation. Many older houses were not built in this manner. In contrast to west-coast practice, residences in the eastern US are typically built with partially hold-down anchors. The following analysis of seismic fragilities for residences is performed for a set of one-story houses having shear walls with openings similar to that identified in Chapter 4 (Figure 4.1). To include a mixture of residences built with various shear wall constraints, shear walls that are fully (seismically) anchored and that lack positive anchorage are considered in all six selected cities.

The ground motions recorded for Los Angeles in the SAC Project Phase II [http://www.sac.org] were used in Chapter 4 to develop the seismic fragilities. Ground motions from the SAC project for Boston and Seattle can be used directly to predict structural response. In the absence of ensembles of ground motions developed specifically for the other sites considered, the ground motions identified above are scaled for use at Charleston, Anchorage and Hawaii using the hazard maps provided by the US Geological survey [http://eqhazmaps.usgs.gov] The ensembles were scaled so as to match the mean spectral accelerations at the fundamental natural period of the building (0.2 s) for events with 10% probability of being exceeded in 50 years and 2% probability of

being exceeded in 50 years from the USGS website for these building sites. The corresponding mean return periods are 475 years and 2,475 years, respectively. This process led to ensembles of 40 ground motions for Charleston, SC, Anchorage, AK and Honolulu and south Hawaii island, respectively.

For each city, two suites of seismic fragilities were developed, one for a residence that has its shear walls seismically anchored to the foundation and the second for a residence without such anchorages. Figure 5.3 to 5.12 show these seismic fragilities for all cities except Los Angeles, CA; results for Los Angeles were presented in Chapter 4. Drift limits for shear walls associated with minor, moderate, and severe damage are 1%, 2% and 3%, respectively (FEMA 273/356). These same drift limits were used to define building performance of "Immediate Occupancy", "Life Safety", and "Collapse Prevention" for the fragilities in Chapter 4.

Figure 5.3 and 5.4 are predictions of earthquake damage to the one-story residence identified above in Charleston, SC. For example, if the spectral acceleration (at a period of 0.2 sec) associated with the design earthquake is 1.0g, as might be typical in the area of Charleston (ASCE, 2002), the probabilities of minor, moderate and severe damage of the residence model with partially hold-down anchors are, respectively, 84.2%, 23.5% and 8.7%. In comparison, for the residence with its shear wall fully anchored, the probabilities of various level damages reduce to 70.3%, 15.7% and 2.8%, respectively. While the probabilities of minor damage are not significantly different, the benefits of the seismic anchorage become clearly evident in mitigating severe damage.

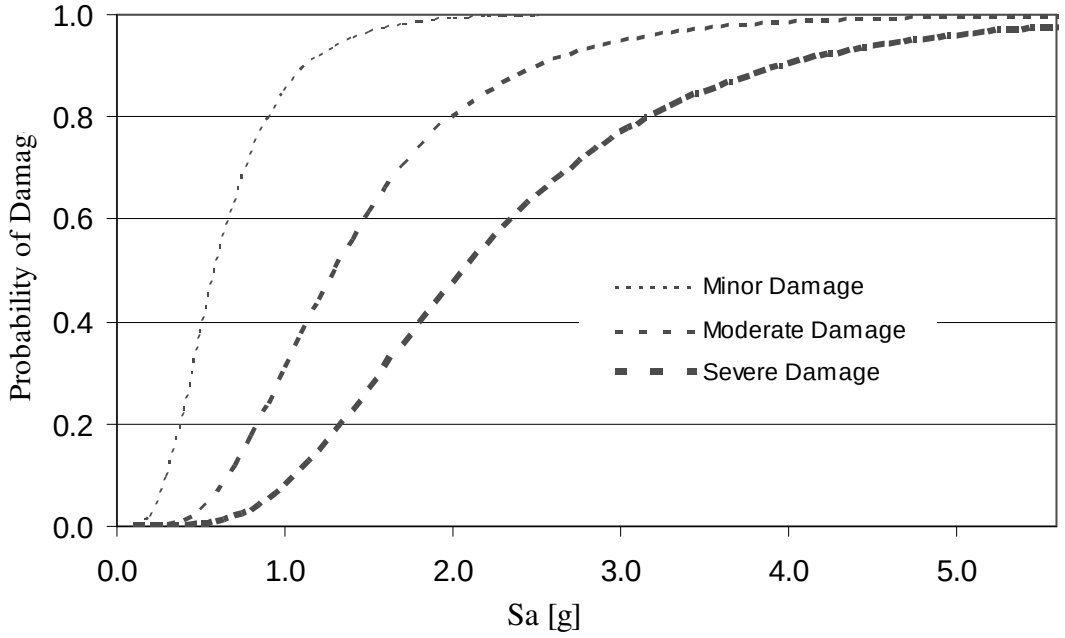

Figure 5.3 Probability of Earthquake Damage (Charleston; Partially Anchored)

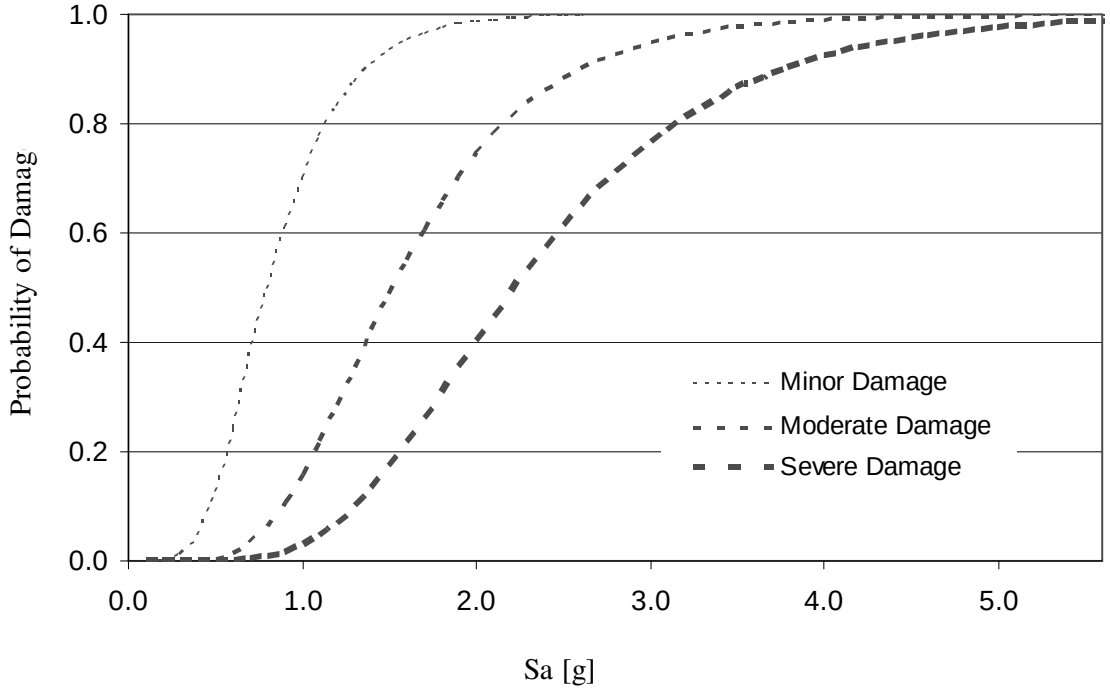

Figure 5.4 Probability of Earthquake Damage (Charleston; Fully Anchored)

Boston, MA is situated in a zone of moderate seismicity. Figures 5.5 and 5.6 show that if the spectral acceleration exceeds approximately 0.4g, minor damage to the residence is likely to occur regardless of presence of fully anchored shear wall. The probabilities of moderate damage to the residence become significant only once the spectral acceleration exceeds approximately 1.2g, a value with a return period of approximately 15,000 yr, regardless of whether or not the shear wall is fully anchored. One might conclude from this analysis that seismic anchorage for light-frame residential construction in Boston, MA would represent an unnecessary investment.

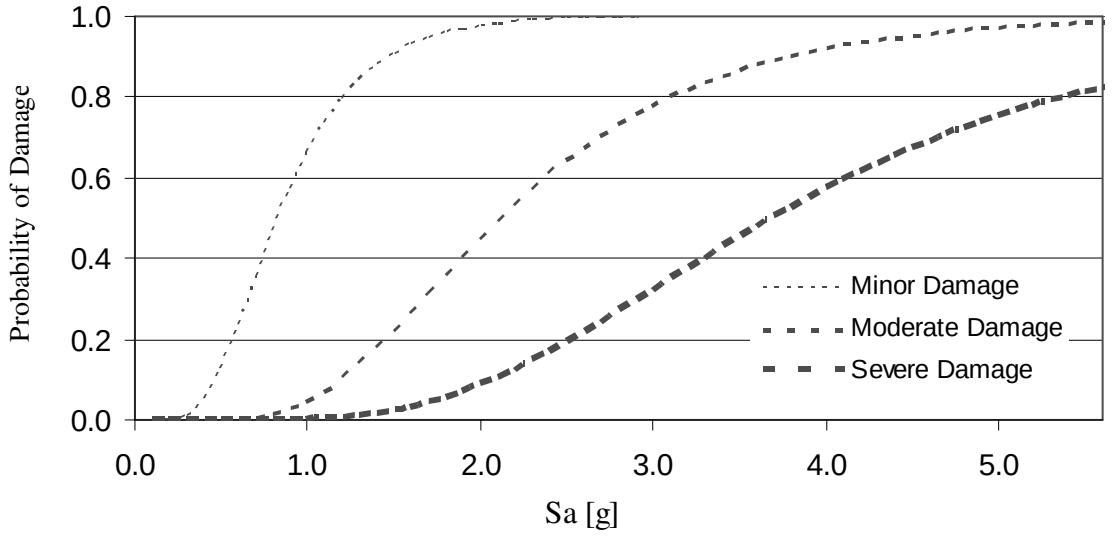

Figure 5.5 Probability of Earthquake Damage (Boston; Partially Anchored)

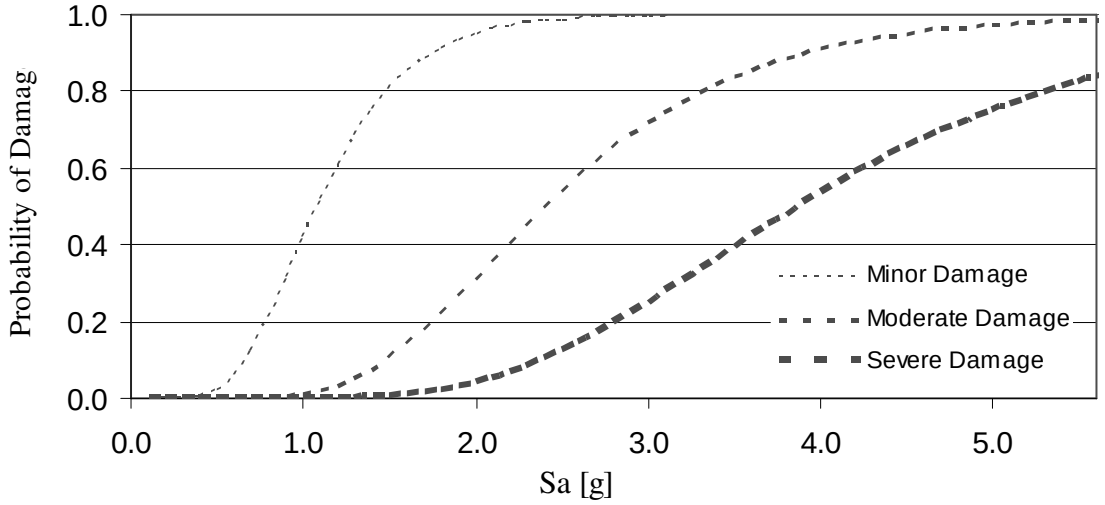

Figure 5.6 Probability of Earthquake Damage (Boston; Fully Anchored)

Seismic fragilities for the residence in Los Angeles, CA have been presented in Chapter 4. Figure 4.32 can be used to predict damage to this residence with the shear wall fully anchored to the foundation. The limit states of Immediate Occupancy, Life Safety and Collapse Prevention correspond to minor, moderate and severe damage, respectively. Likewise, Figure 4.36 represents probability of seismic damage for the residence without hold-down anchors for the shear wall.

In Seattle, WA, the effects of seismic shear wall anchorage is obvious by comparing Figure 5.7 and 5.8, where the decrease in damage probability is noticeable for the residence with the seismically anchored shear wall. If the spectral acceleration is 1.0g corresponding to a return period of 800 yr, the probability of minor, moderate and severe damage to the first house is 91.7%, 38.4% and 13.9%, respectively, while for the second house the comparable probabilities are 66.5%, 9.6% and 0.5%, respectively.

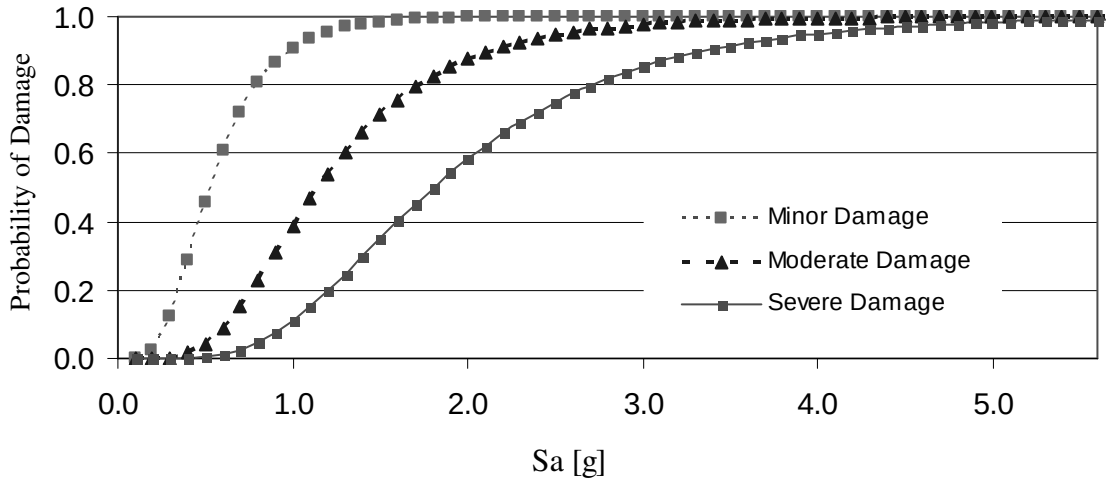

Figure 5.7 Probability of Earthquake Damage (Seattle; Partially Anchored)

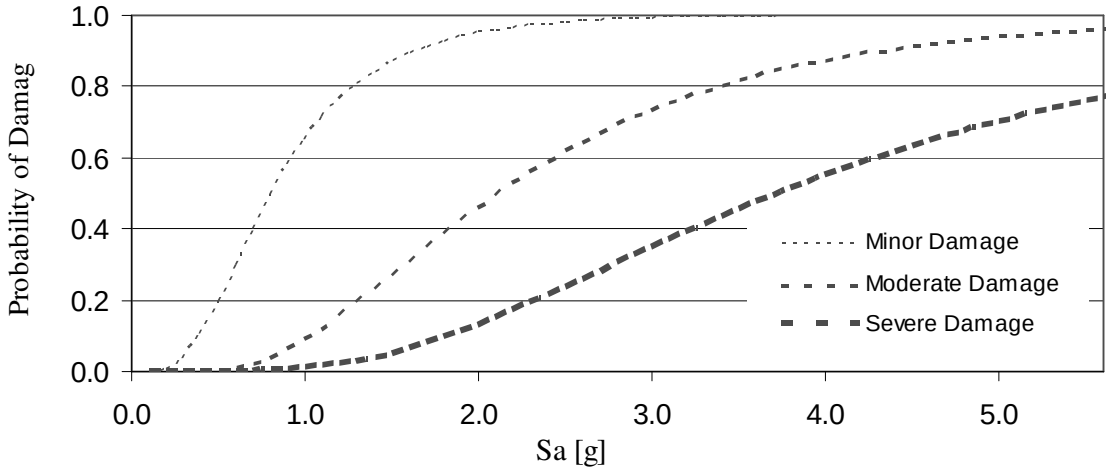

Figure 5.8 Probability of Earthquake Damage (Seattle; Fully Anchored)

Figures 5.9 and 5.10 illustrate the seismic fragilities for a residence in Anchorage, Alaska, while Figures 5.11 and 5.12 represent the comparable fragilities for the residence in Honolulu, Hawaii.

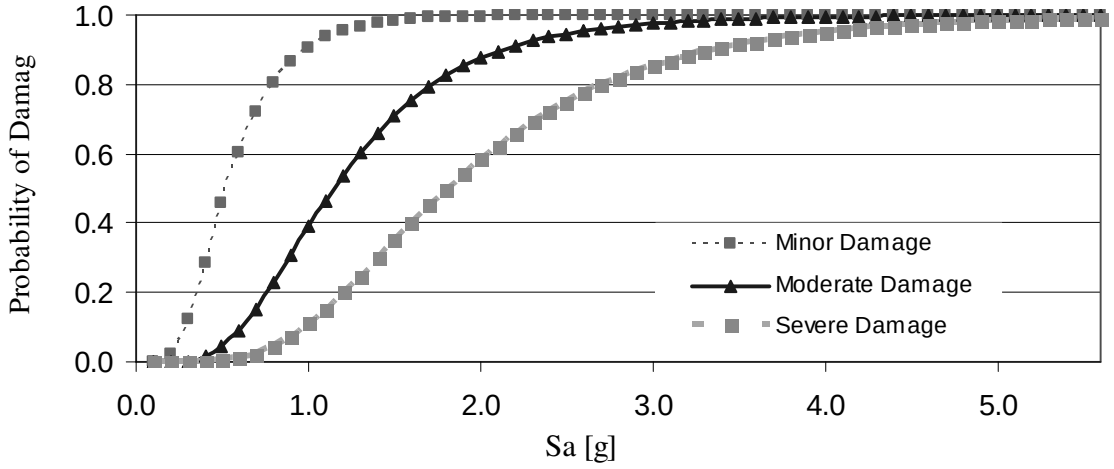

Figure 5.9 Probability of Earthquake Damage (Anchorage; Partially Anchored)

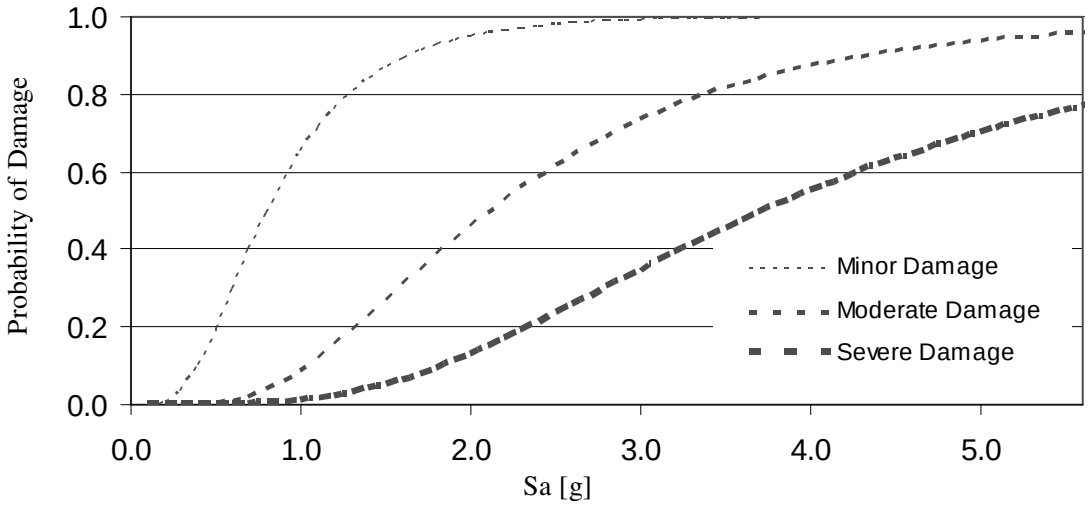

Figure 5.10 Probability of Earthquake Damage (Anchorage; Fully Anchored)

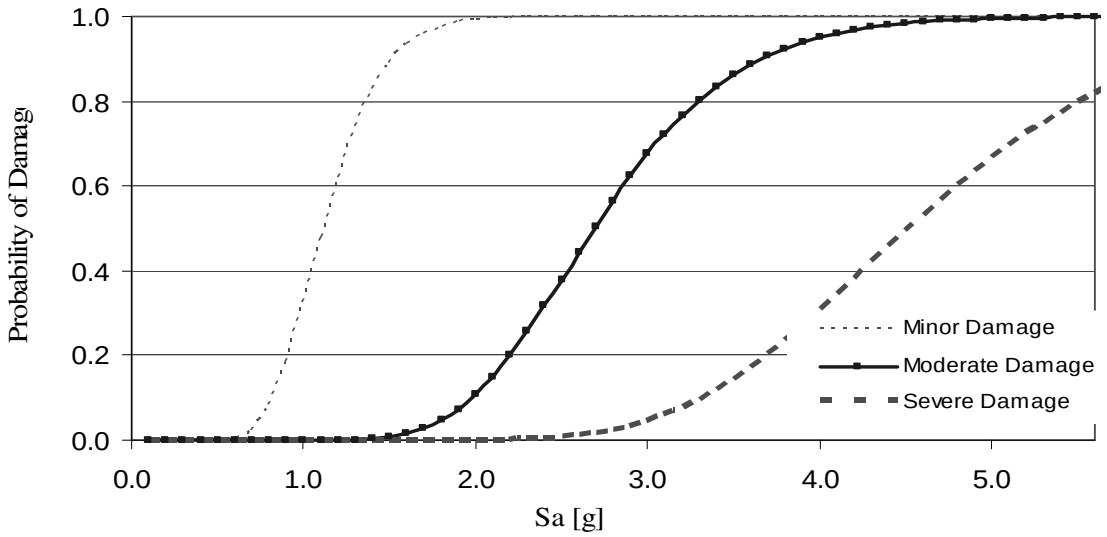

Figure 5.11 Probability of Earthquake Damage (Honolulu; Partially Anchored)

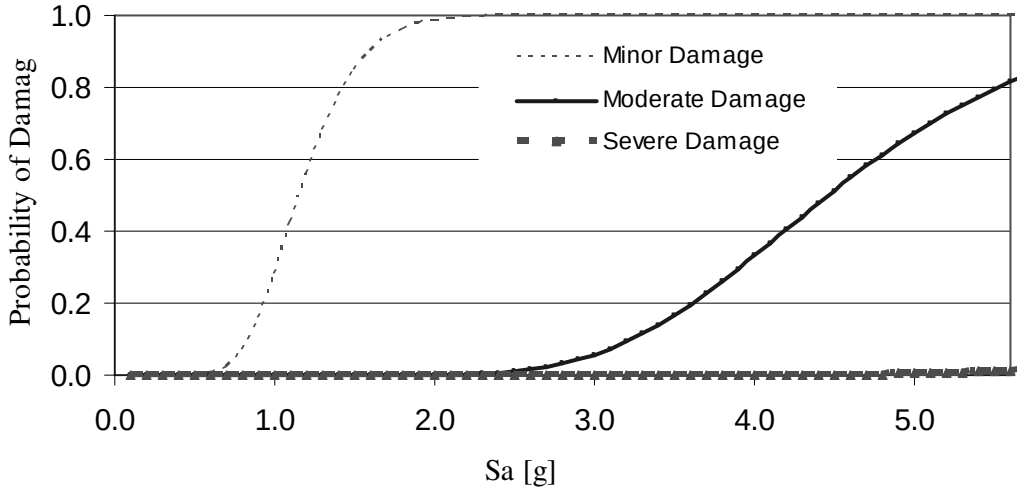

Figure 5.12 Probability of Earthquake Damage (Honolulu; Fully Anchored)

Some general observations can be made for the effects of shear wall hold-downs on probability of damage in all cities:

- The effectiveness of shear wall seismic anchorage in mitigating minor damage varies from city to city.

- The benefits of shear wall seismic anchorage are more apparent in mitigating moderate and severe damage effectively. The value of such anchorage in reducing minor damage is less apparent from Figures 5.3 through 5.12.

5.5 Probability of damage as a function of return period

5.5.1 Hurricane hazard and wind damage

Several hurricane wind field models have been developed to predict wind speed with various return periods (Chapter 3). The hurricane wind model proposed by Vickery et al. (2000) is assumed in performing the analyses in the current chapter. Figure 5.13 illustrates the 50-, 100-, 500-year return period peak (3-sec) gust wind speed along the southeast coast of the United States. For instance, the corresponding 50, 100 and 500 years return period peak gust wind speeds in open terrain in Charleston are 128, 140 and 160 mph (57, 63 and 72 m/s), respectively. In Hawaii, such winds are referred to as tropical cyclones. Design wind speeds in Los Angeles, Seattle, Anchorage and Honolulu are used subsequently for comparative risk assessment.

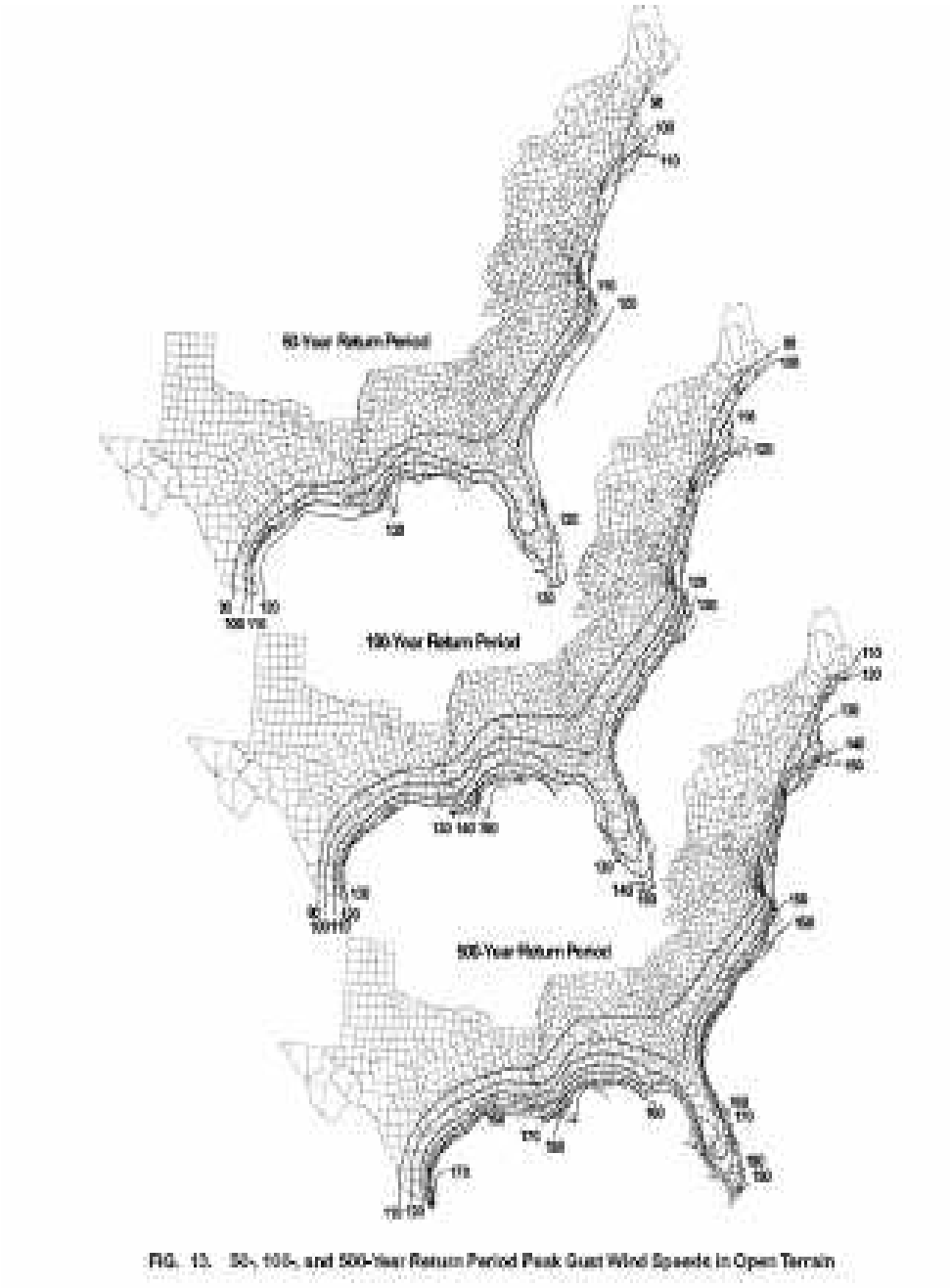

FIG. 13. 50-, 100-, and 500-Year Return Period Peak Gust Wind Speeds in Open Terrain

Figure 5.13 50, 100 and 500 Year Return Period Peak Gust on Open Terrain (Vickery et al. 2000)

Hurricane wind speeds can be modeled by the Weibull distribution (Chapter 3). The corresponding parameters can be determined from Equations 3.8 and 3.9. For instance, the Weibull distribution parameters are u = 60.02 and α = 1.86 in Charleston, SC under the assumption that the hurricane wind field model can be modeled as proposed by Vickery, et al. (2000). Table 5.1 summarizes wind speeds with various return periods and corresponding Weibull distribution parameters for Charleston, SC and Boston, MA.

Table 5.1 Wind Speeds and Weibull Distribution Parameters

	Return Period	Charleston	Boston
Wind Speed (mph)	50-yr	128	95
	100-yr	140	110
	500-yr	160	130
Weibull Distribution Parameters	μ	60.02	37.59
	α	1.86	1.468

The return period (T) of the hurricane wind at a specific location can be related to the wind speed (v), utilizing Equation 3.8 and 3.10:

$$T = 1/ \exp [-(v/u)^{\alpha}] \qquad (5.1)$$

Figure 5.14 illustrates this relationship for Charleston, SC and Boston, MA. When the return periods are less than 20 years, wind speeds basically are the same in Charleston

and Boston. For return periods exceeding 20 years, the wind speed at Charleston is higher than that for Boston.

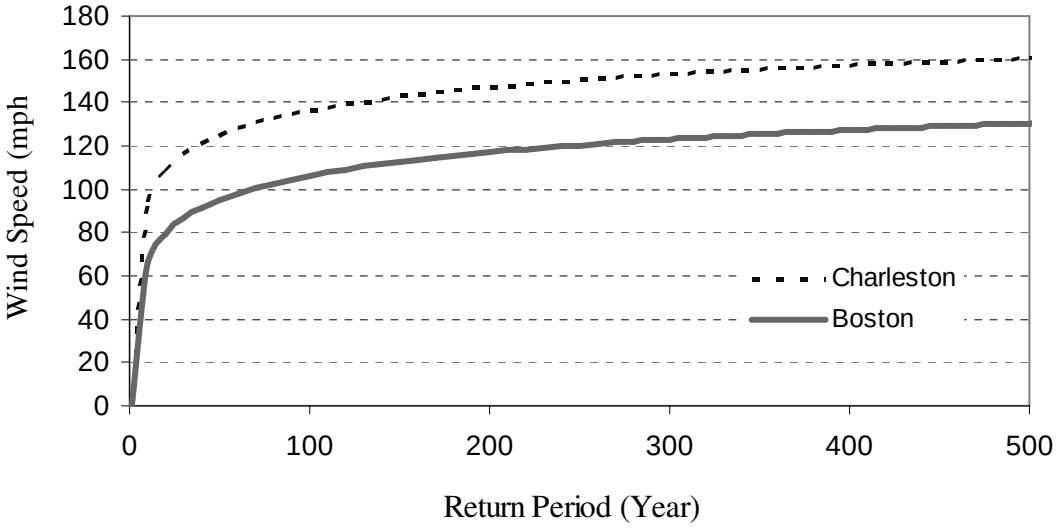

Figure 5.14 Wind Hazard Curves for Charleston and Boston

Figures 5.15 through 5.18 compare the probabilities of hurricane damage in Charleston, SC and Boston, MA as functions of wind speed return period. The wind speed control variable in Figures 5.1 and 5.2 is transformed to return period, utilizing the relationship defined in Equation 5.1 and the site-specific Weibull distribution parameters. The probability of wind damage is higher in Charleston than in Boston at all return periods. Furthermore, the adoption of higher standards for wind protection in residences as opposed to minimum standards leads to dramatic deceases in probability of wind damage in both cities. For instance, if a hurricane with a 150-year return period were to hit Charleston, SC, the estimated probability of minor, moderate and severe wind damage for

a residence with minimum hurricane protection is 97.2%, 85.6% and 31.8%, respectively. In contrast, for the residence with intermediate standards for wind protection, the probabilities of minor, moderate and severe damage reduces to 63.6%, 39.5% and 4.6%, respectively. Should a hurricane with a return period of 150 years strike Boston, MA, the likelihood of minor, moderate and severe damage to residence with minimum standards is 72.3%, 38.9% and 4.3%, respectively. These probabilities drop 20-50% for a residence utilizing intermediate wind protection standards.

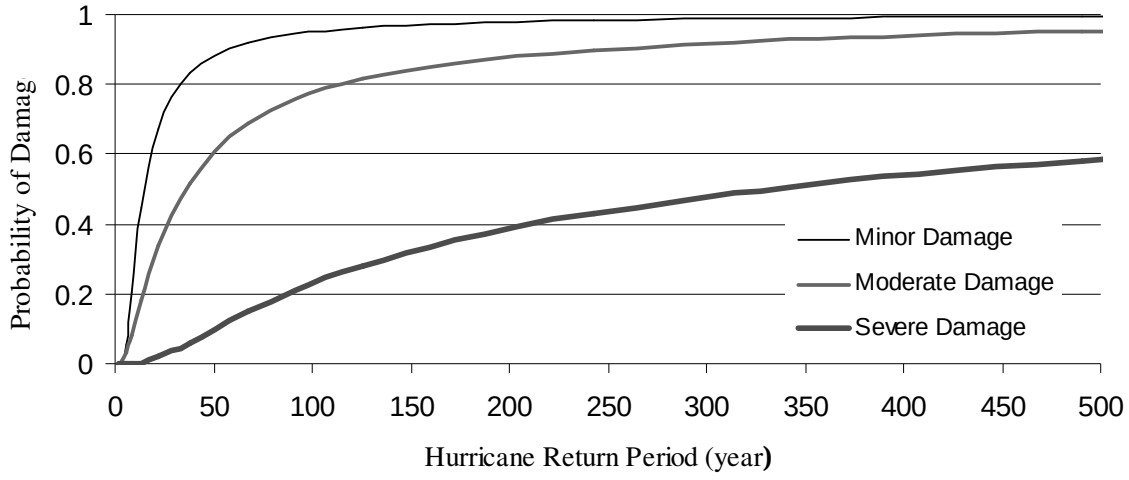

Figure 5.15 Probability of Hurricane Damage (Charleston; Minimum Standard)

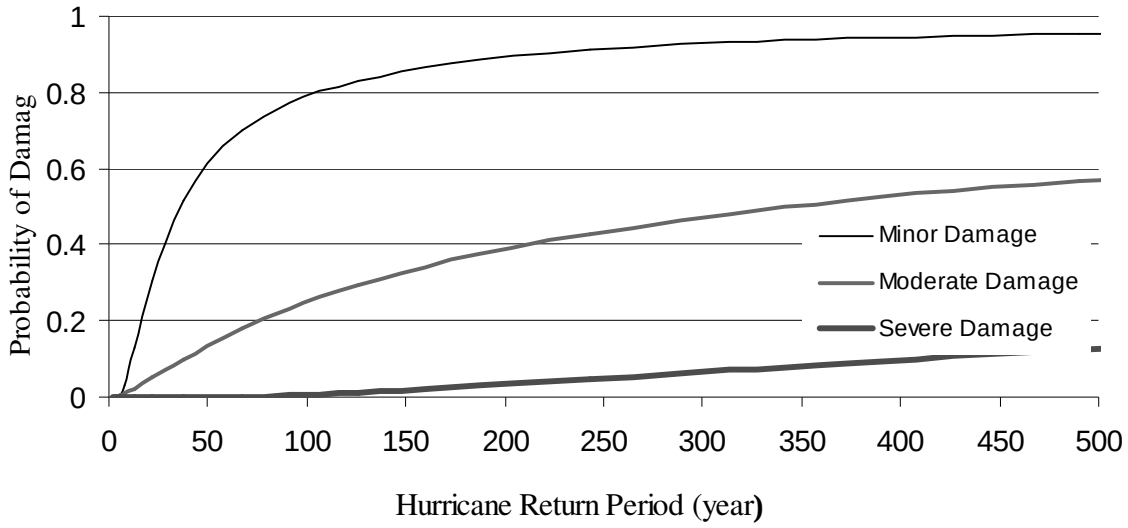

Figure 5.16 Probability of Hurricane Damage (Charleston; Intermediate Standard)

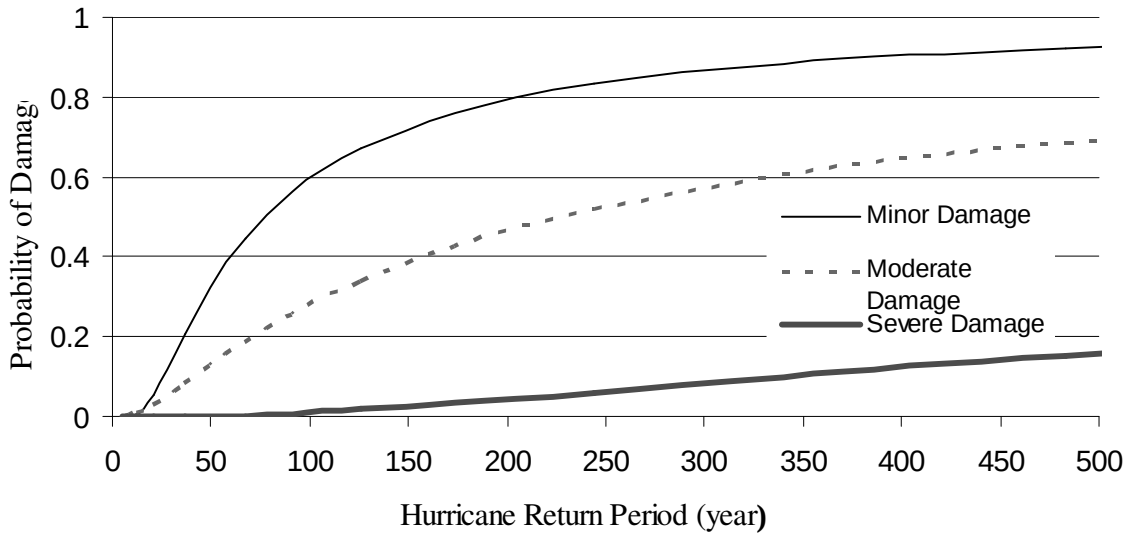

Figure 5.17 Probability of Hurricane Damage (Boston; Minimum Standard)

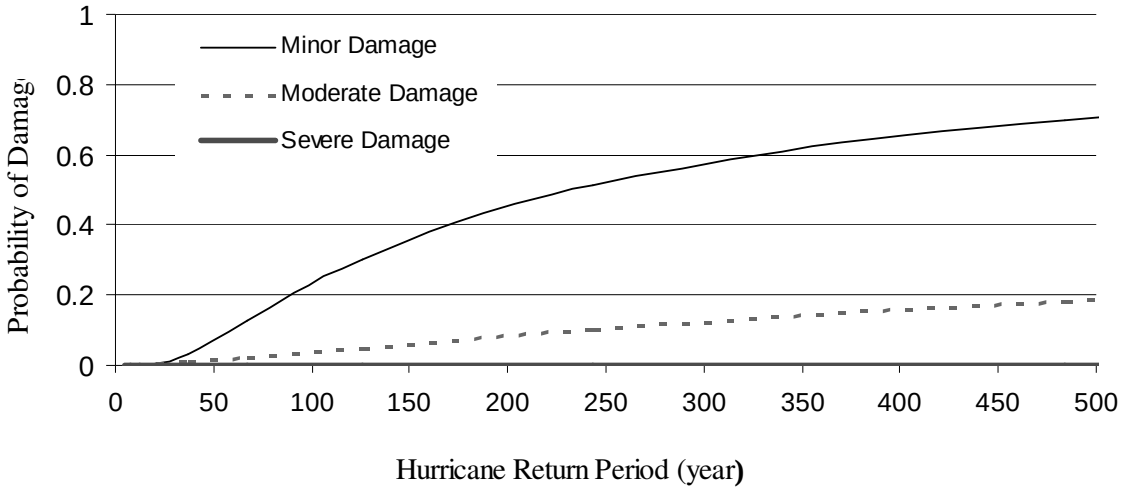

Figure 5.18 Probability of Hurricane Damage (Boston; Intermediate Standard)

5.5.2 Seismic hazard and earthquake damage

Hazard curves determined by the U.S. Geological Survey (USGS) define the probability that specific levels of ground motion (characterized by spectral accelerations) are exceeded. Table 5.2 is a summary of mean spectral accelerations at the fundamental period of 0.2 sec in the six cities and Island of Hawaii, for probabilities of exceedance of 10%, 5%, and 2% in 50 years. Spectral accelerations for 5% in 50 are not available for Anchorage and Hawaii. The purpose to include Island of Hawaii is to show the big difference in the likelihood of seismic hazard for two near locations, such as Honolulu and Island of Hawaii.

Table 5.2 Mean Spectral Acceleration [g] (T=0.2 sec) [USGS]

Probability of Exceedance		10% in 50 yrs	5% in 50 yrs	2% in 50 yrs
Annual Exceedance		0.002105	0.001026	0.000404
Return Period		475	975	2475
Location	Boston	0.11	0.18	0.34
	Charleston	0.34	0.68	1.53
	Los Angeles	1.26	1.67	2.1
	Seattle	0.75	1.14	1.61
	Anchorage	1	N/A	1.55
	Honolulu	0.3	N/A	0.7
	Hawaii Island	2.5	N/A	3.75

The mean seismic hazard is described by Equation 4.3, which represents a linear relationship on a log-log plot. Table 5.3 lists the corresponding constants defining the seismic hazard for each of the six cities considered. In selected cities on the east coast, k is between 1 and 1.5, while k ranges between 2 and 3.3 on the west coast and is highest in Anchorage (k = 3.5). k is 1.95 in Honolulu and 4.07 for south Hawaii island.

Table 5.3 Constants in Seismic Hazard Curve

Seismic Hazard Constants [$H(Sa) = ko * Sa^{-k}$]	Ko	K
Boston	0.000084	1.46
Charleston	0.000656	1.093
Los Angeles	0.004663	3.2
Seattle	0.001204	2.147
Anchorage	0.002104	3.507
Honolulu	0.000202	1.945
South Hawaii Island	0.087096	4.065

The seismic hazard curves, expressed as spectral acceleration vs. annual probability, are shown for each city in Figure 5.19. Generally, the seismic hazard curve has a steeper slope in the western US than in the eastern US; this difference in slopes k has some interesting implications of design and risk assessment. The annual probability of exceedance of various performance levels defined in Equation 4.5 is proportional to $\exp(k^2)$. That implies that the difference of annual likelihood of specific damage for a residence could be more than two orders of magnitude, considering similar residences located Los Angeles and Boston.

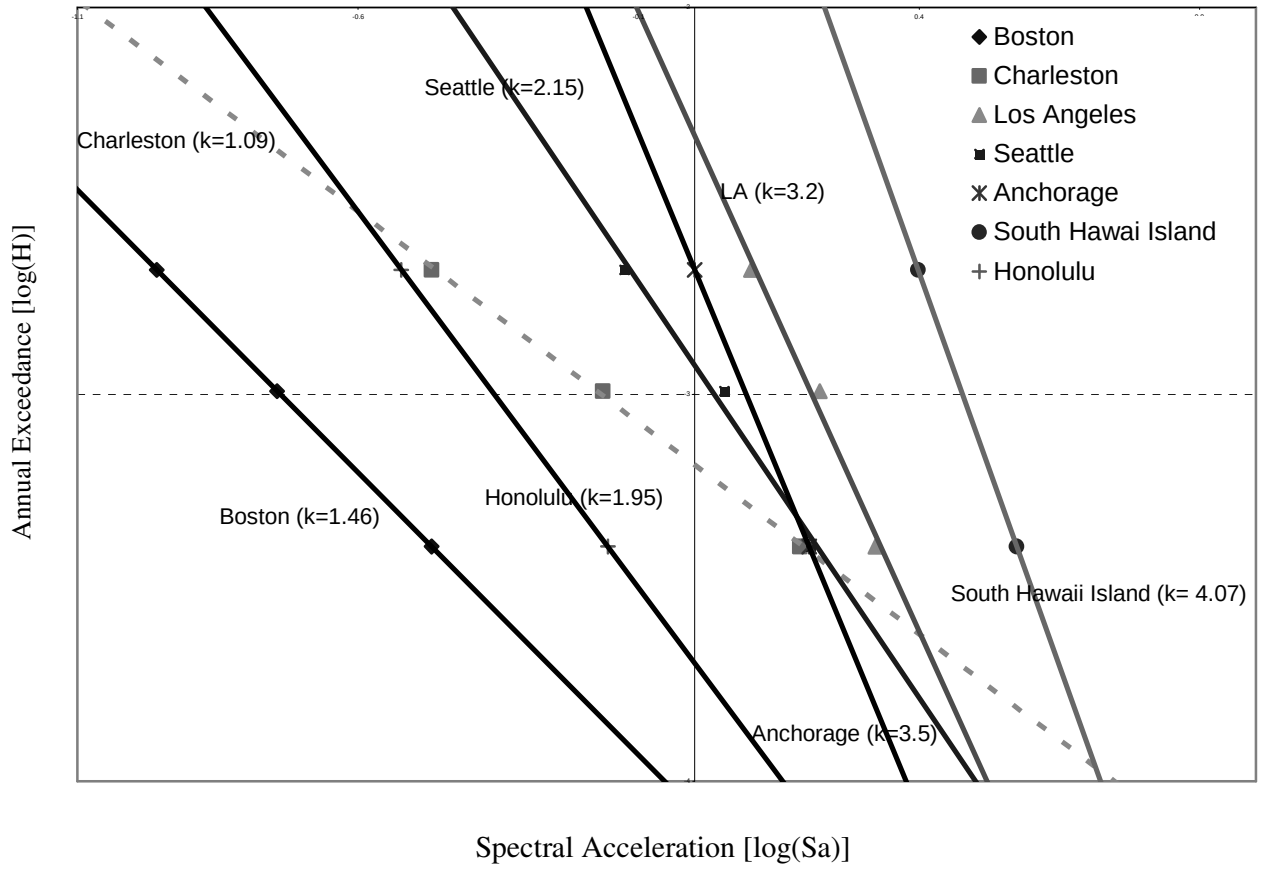

Figure 5.19 Seismic Hazard Curves

Utilizing Equation 4.3, the relationship between return period, T, and spectral acceleration, y, can be described by

$$T = 1/ H(y) = 1/ (k_o * y^{-k}) \qquad (5.2)$$

in which return period is a function of ground motion intensity. Similar to the process of changing the control variable of wind speed to return period in assessing probability of

hurricane damage, the spectral acceleration control variable can be transformed to return period (T) by Equation 5.2. The seismic damage probabilities are shown in Figure 5.20 to 5.31 as a function of return period. Residences with and without seismically anchored shear walls are considered. The probabilities of earthquake damage in Charleston and Boston (Figures 5.20-5.23) will be separately discussed in section 5.6.1, where probabilities of earthquake and hurricane damage are compared for these two cities.

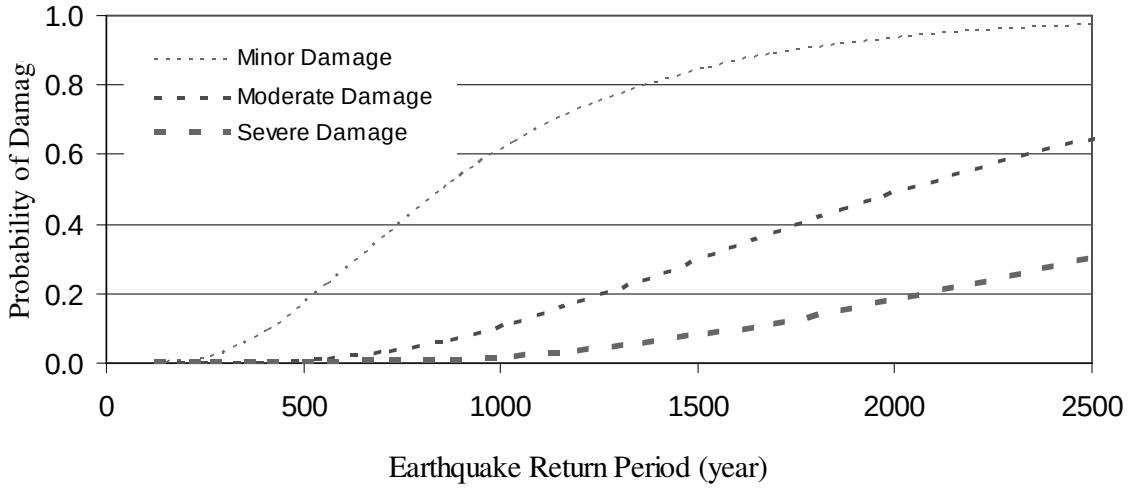

Figure 5.20 Probability of Earthquake Damage (Charleston; Partially Anchored)

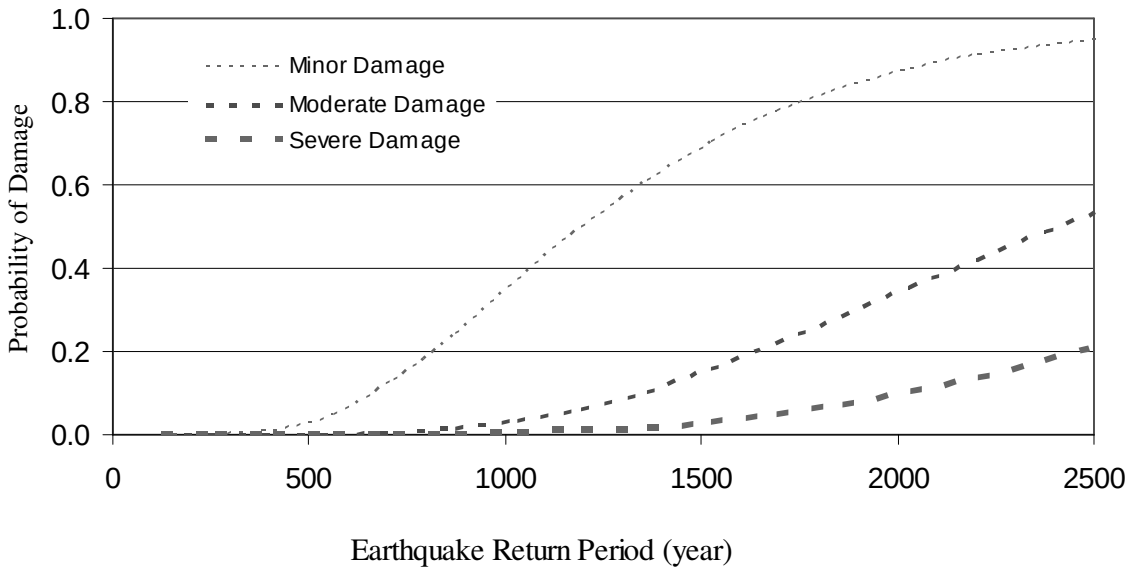

Figure 5.21 Probability of Earthquake Damage (Charleston; Fully Anchored)

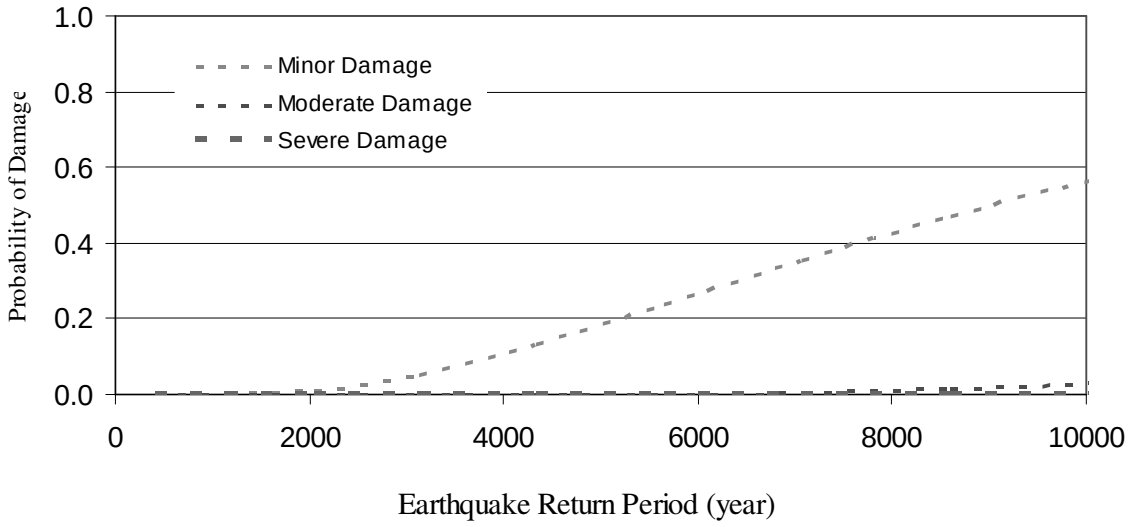

Figure 5.22 Probability of Earthquake Damage (Boston; Partially Anchored)

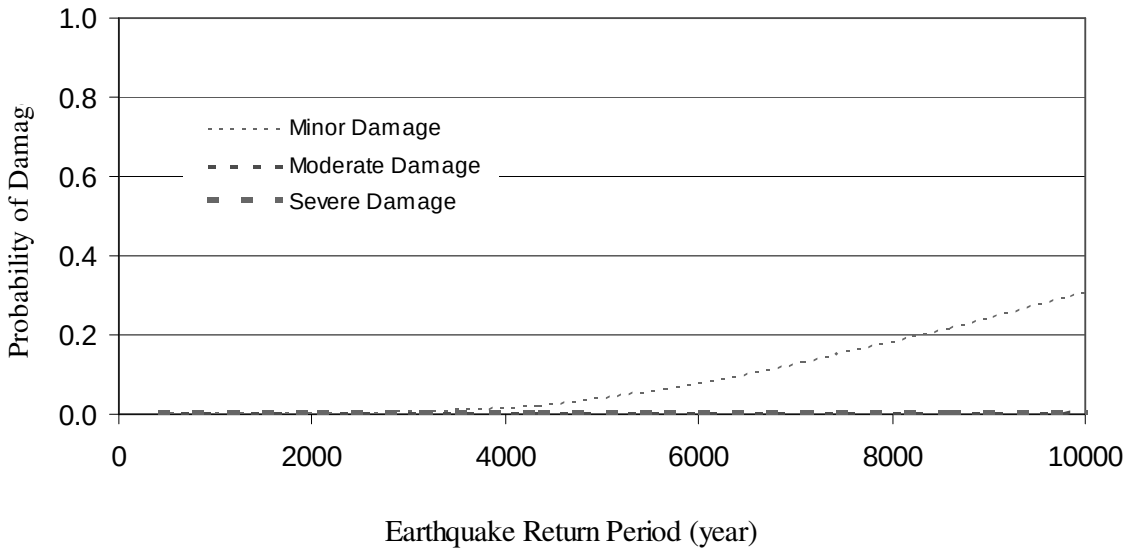

Figure 5.23 Probability of Earthquake Damage (Boston; Fully Anchored)

Figure 4.24 presented the probability of earthquake damage to a residence without shear wall hold-downs in Los Angeles, CA, while Figure 4.25 presented these probabilities for a residence in which the shear walls were fully anchored. The probability of minor earthquake damage is more than 60% when return period for Los Angeles is less than 225 years (Occasional earthquake with 20%/50 return period defined in Figure 2.1) , as shown in Figure 4.24 and 4.25. For an earthquake with a return period of less than 500 years (Rare earthquake with 10%/50 return period defined in Figure 2.1), the effect of shear wall seismic hold-downs is evident in reducing moderate and severe damage, but is less significant for minor damage. For a 10%/50 yr earthquake, the probability of severe damage to the one-story residence is virtually zero.

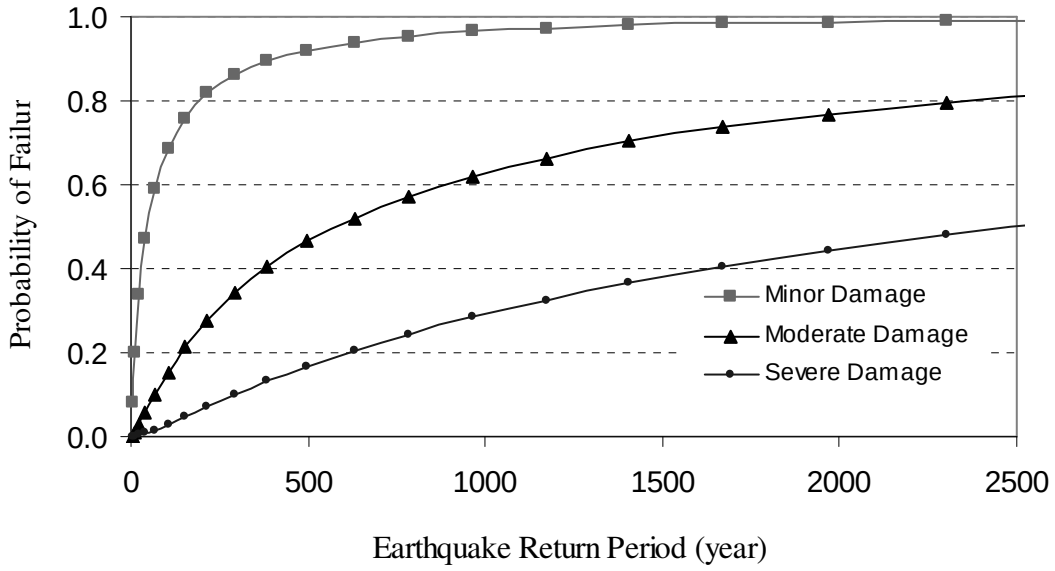

Figure 5.24 Probability of Earthquake Damage (LA; Partially Anchored)

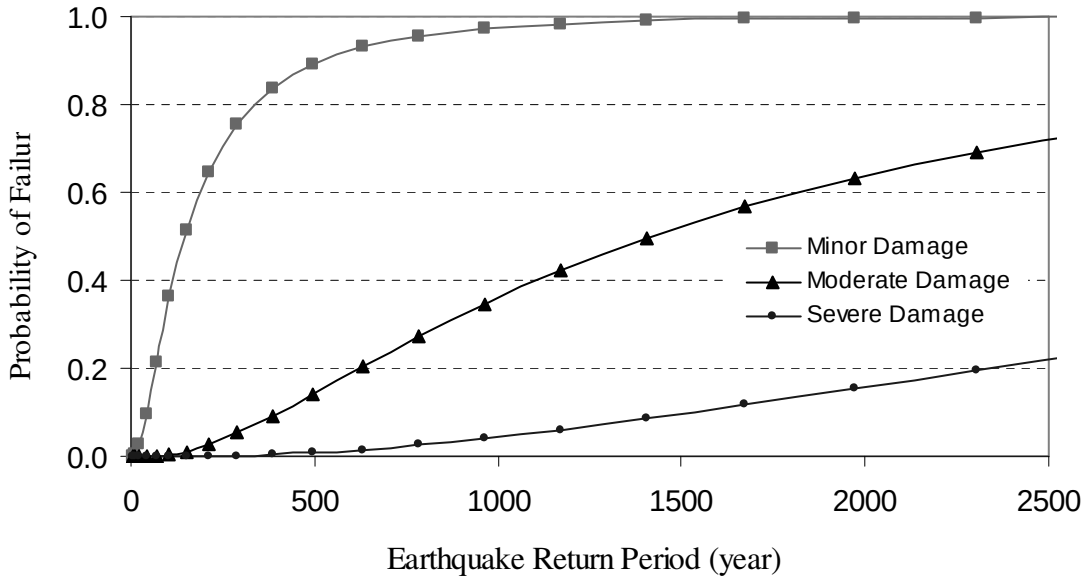

Figure 5.25 Probability of Earthquake Damage (LA; Fully Anchored)

Figures 5.26 and 5.27 show the likelihood of earthquake damage to the residence in Seattle. For return periods up to 2500 years, likelihood of moderate and severe damage can be reduced by more than 50% by utilizing fully anchored shear wall hold-downs in residential construction. .

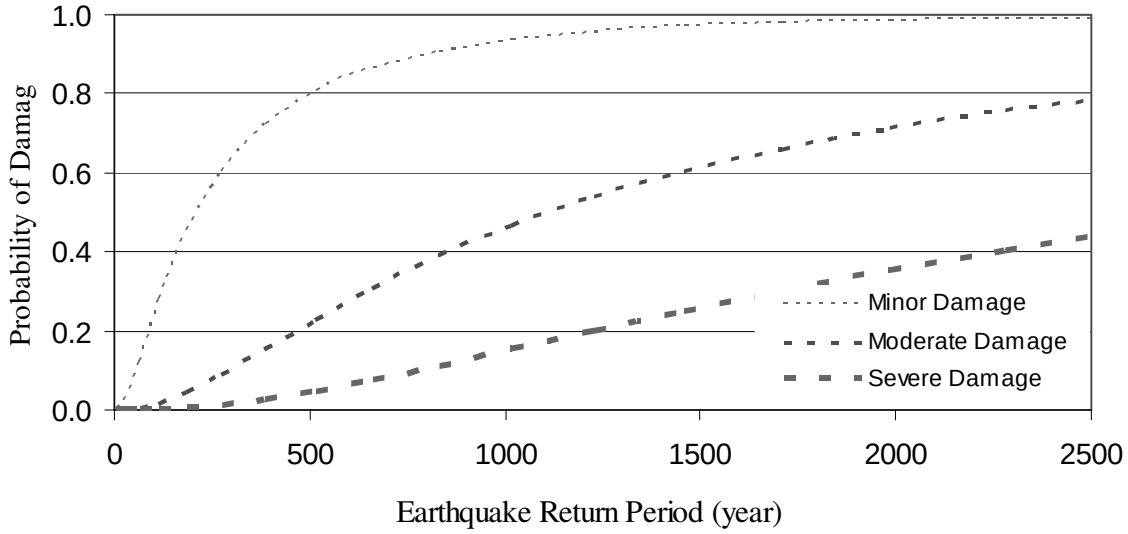

Figure 5.26 Probability of Earthquake Damage (Seattle; Partially Anchored)

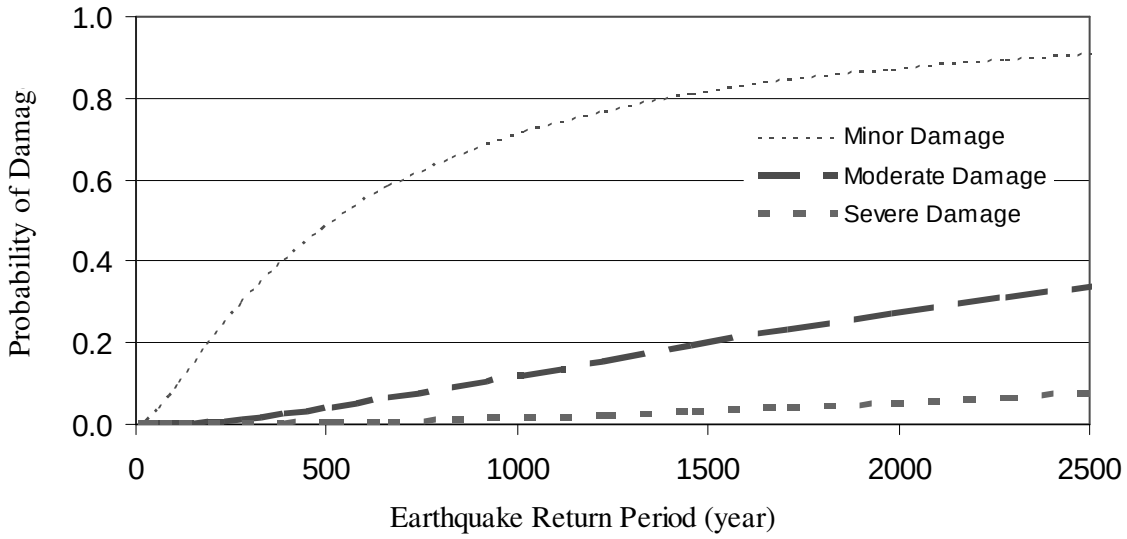

Figure 5.27 Probability of Earthquake Damage (Seattle; Fully Anchored)

Figures 5.28 and 5.29 illustrate the relationship between damage probability and earthquake return period in Anchorage, AK. The effects of seismic shear wall hold-downs on reducing moderate and severe damage are noticeable. For example, at a return period of 1500 years, house without such hold-downs is more than three times likely to suffer moderate and severe damage than that with them. Nevertheless, minor damage in the first case is only about 20 to 30% more likely than in the latter case.

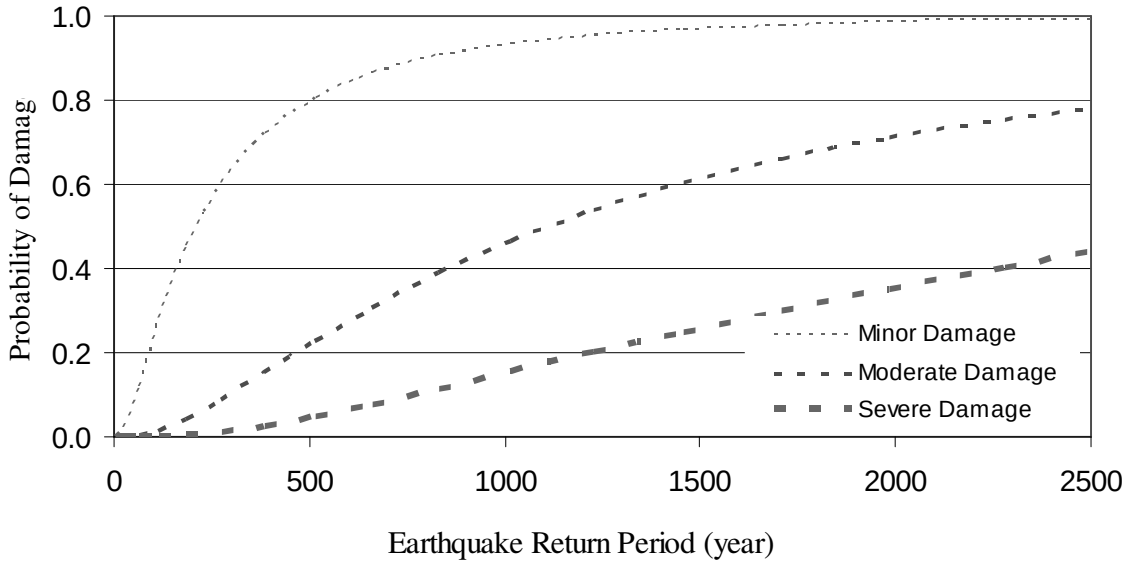

Figure 5.28 Probability of Earthquake Damage (Anchorage; Partially Anchored)

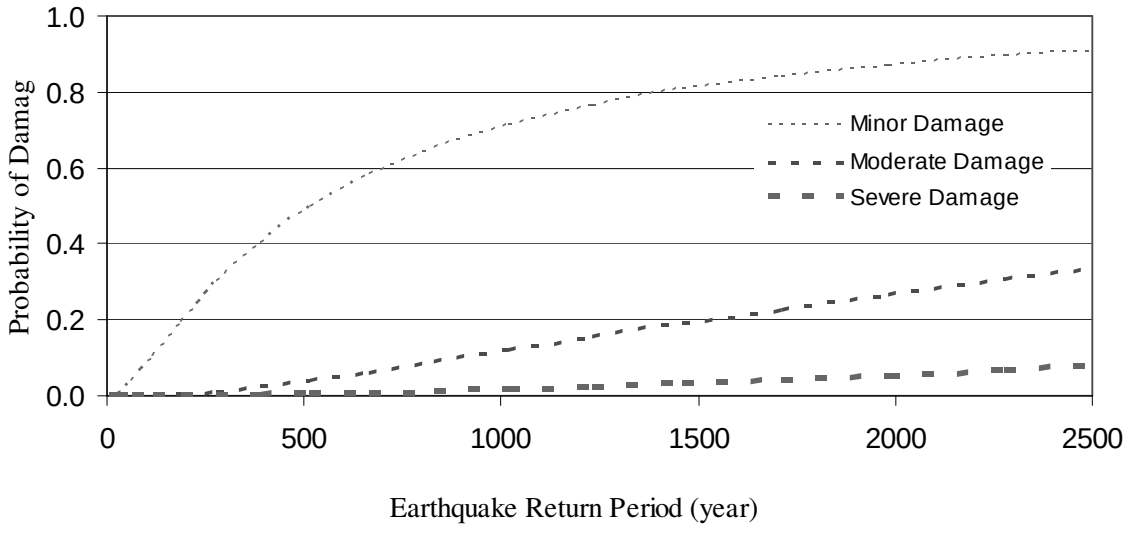

Figure 5.29 Probability of Earthquake Damage (Anchorage; Fully Anchored)

The probability of damage to residences is more significant Island of Hawaii, as shown in Figures 5.32 and 5.33, in comparison with the seismic damage in Los Angeles, Seattle and Anchorage, even Honolulu. Note that the scale used in these figures is up to 500 years, instead of 2500 years which are used in all other selected cities. Nevertheless, the likelihood of damage in Figures 5.32 and 5.33 are comparable to damage predictions in other cities, implying the high seismicity in south Hawaii island poses a great threat to this type of residence.

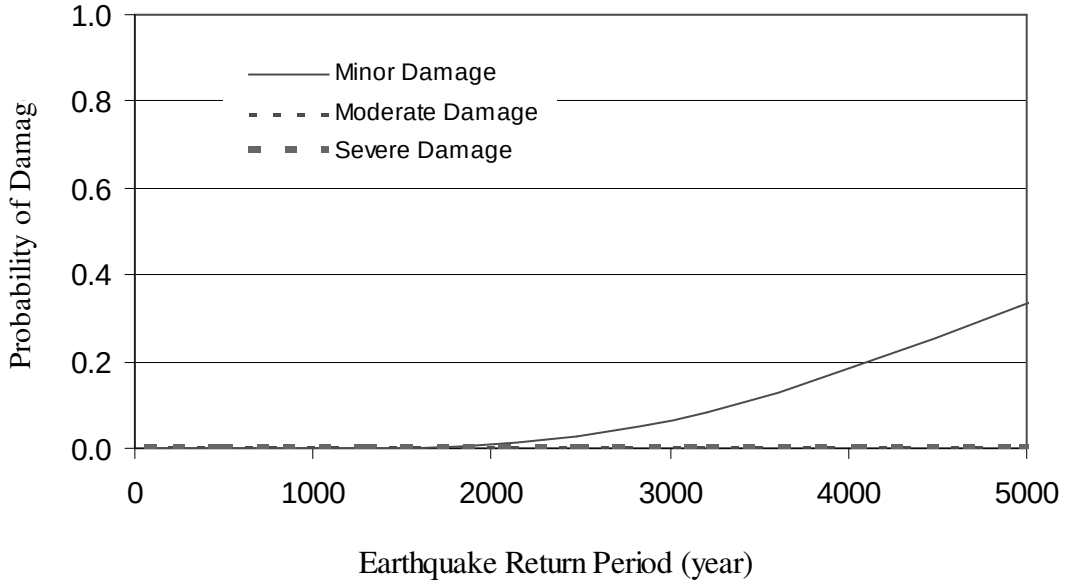

Figure 5.30 Probability of Earthquake Damage (Honolulu; Partially Anchored)

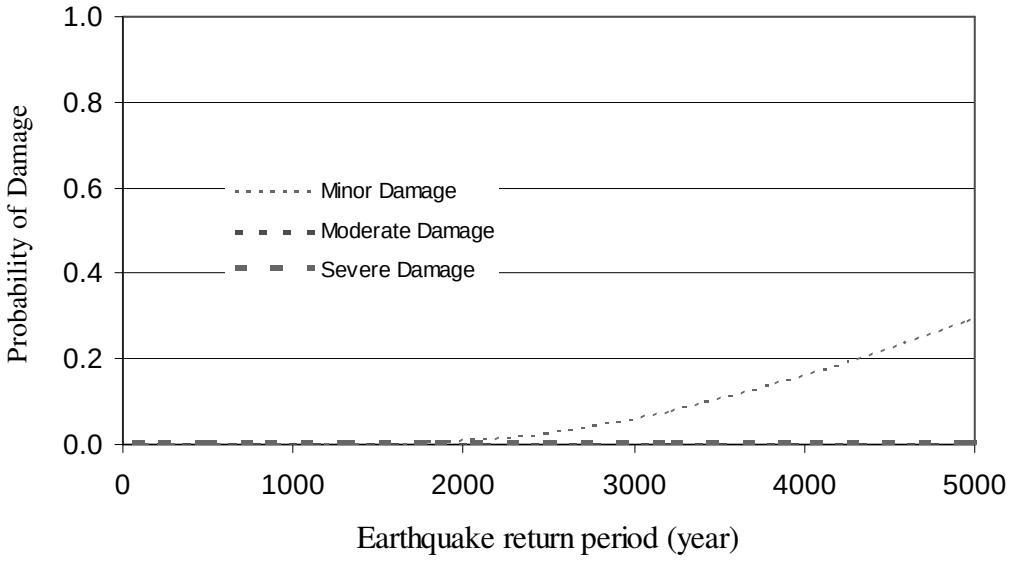

Figure 5.31 Probability of Earthquake Damage (Honolulu; Fully Anchored)

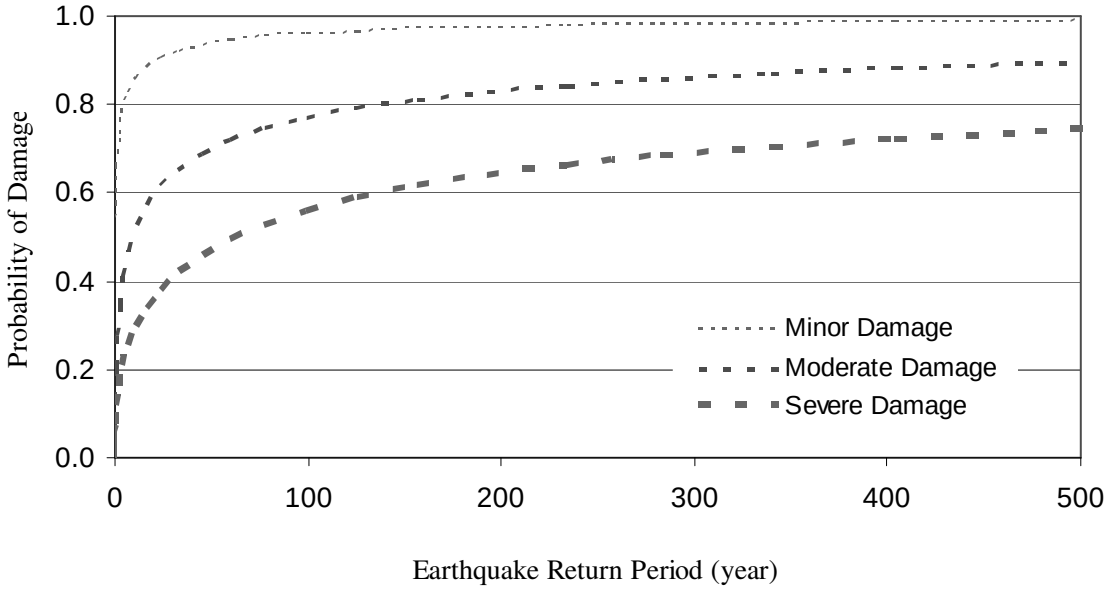

Figure 5.32 Probability of Earthquake Damage (Island of Hawaii; Partially Anchored)

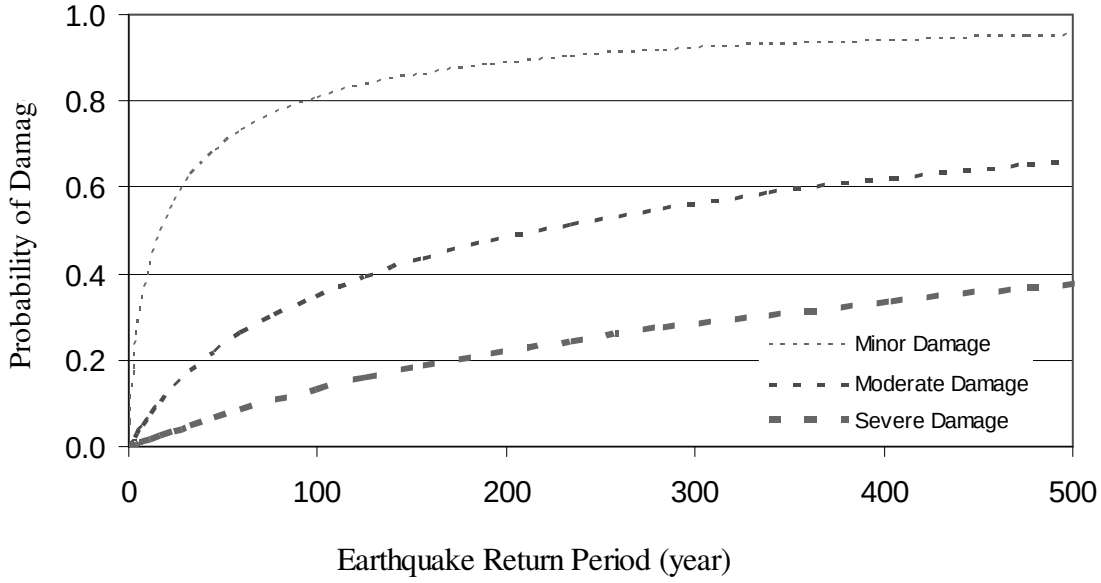

Figure 5.33 Probability of Earthquake Damage (Island of Hawaii; Fully Anchored)

5.6 Comparison of risk from hurricane and earthquake hazards

5.6.1 Risk comparison based on return period

Using the return period, T, as the common control variable in the fragility assessments to facilitate comparisons, a comparative risk assessment can be performed for hurricane and seismic hazards. Return periods are the basis for design event that are stipulated in ASCE-7 and Performance Based Engineering (e.g. Figure 2.1). Figure 5.34 shows the probability of damage to residences in Charleston, SC built with minimum wind protections and without seismic shear wall hold-downs (Lower Hazard-Resistant

Standards). Similarly, Figure 5.35 demonstrates the probability of hurricane and earthquake damage to another residence in the same city as a function of return period. The shear wall of the residence is assumed to be built with fully anchored hold-downs and intermediate wind protection standards (Higher Hazard-Resistant Standards).

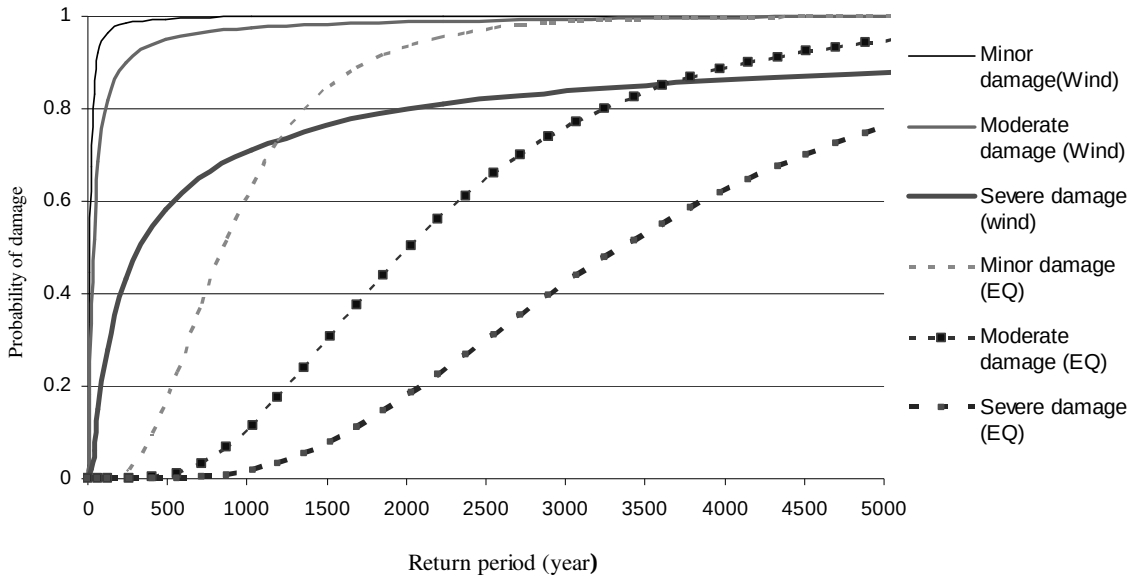

Figure 5.34 Probability of Hurricane and Earthquake Damage (Charleston; Lower Hazard-Resistant Standards)

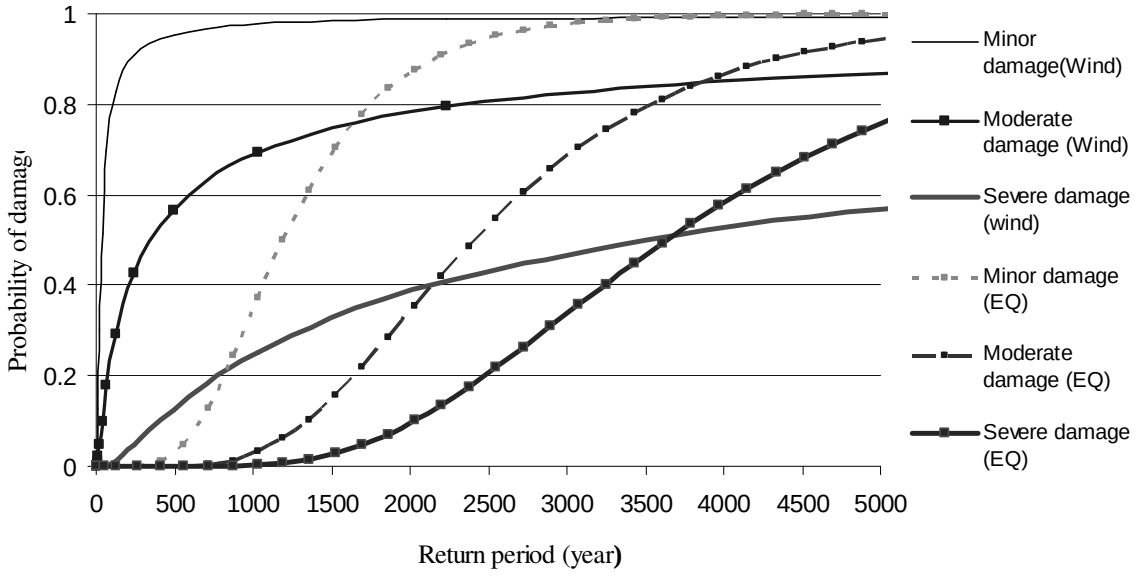

Figure 5.35 Probability of Hurricane and Earthquake Damage (Charleston; Higher Hazard-Resistant Standards)

At return periods less than 1,000 years, the dominant hazard in Charleston for a particular damage state is due to hurricanes for the residence with minimum wind protection standards and shear walls lacking hold-downs. For instance, at a return period of 250 years, the probability of hurricane wind damage for the residence with minimum protection is more than 43.2%, while the likelihood of severe earthquake damage is virtually zero. However, if an earthquake with a return period of about 2,500 years (a 2%/50yr earthquake, termed the "maximum considered earthquake" in ASCE Standards 7-02) were to occur, moderate-to-severe damage to this type of residential construction should be expected. The probability of moderate and severe seismic damage is 63.7% and 35.3%, respectively. The probability of moderate and severe damage decreases by 50% if the building's shear walls are properly anchored to withstand seismic forces.

Similarly, Figures 5.36 and 5.37 show the probability of hurricane and earthquake damage to the residence in Boston, MA as a function of return period, assuming minimum or intermediate wind and earthquake resistant standards are adopted. Severe wind damage from windstorms with return periods less than 1000 years is insignificant. With intermediate wind protection, the probability of minor and moderate damage decreases by 50% for winds with return periods between 50 to 100 years. The likelihood of seismic damage appears insignificant, even if the maximum considered earthquake were to occur.

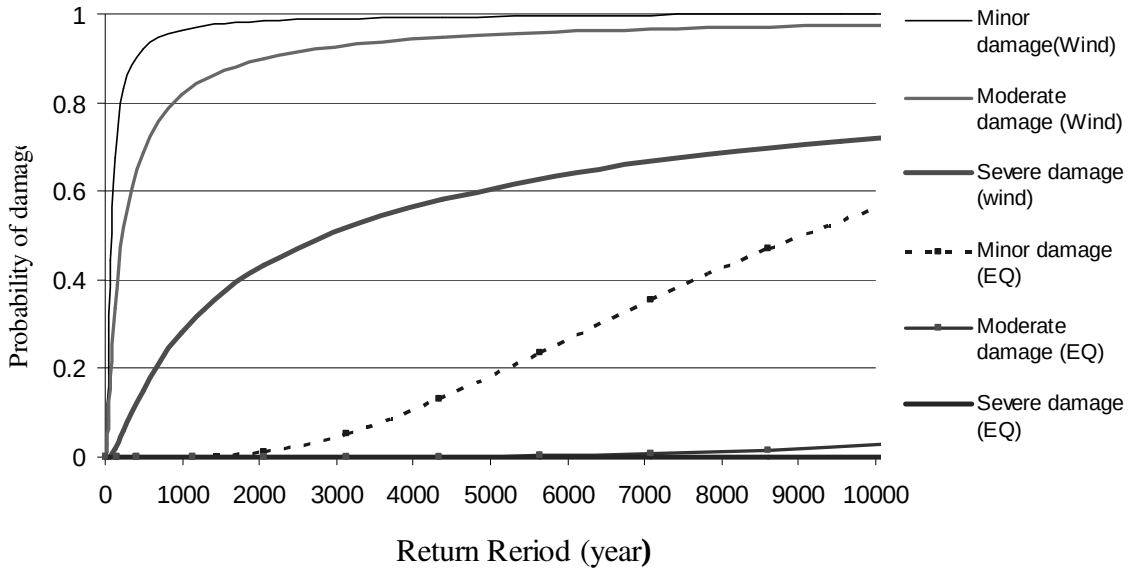

Figure 5.36 Probability of Hurricane and Earthquake Damage (Boston; Lower Hazard-Resistant Standard)

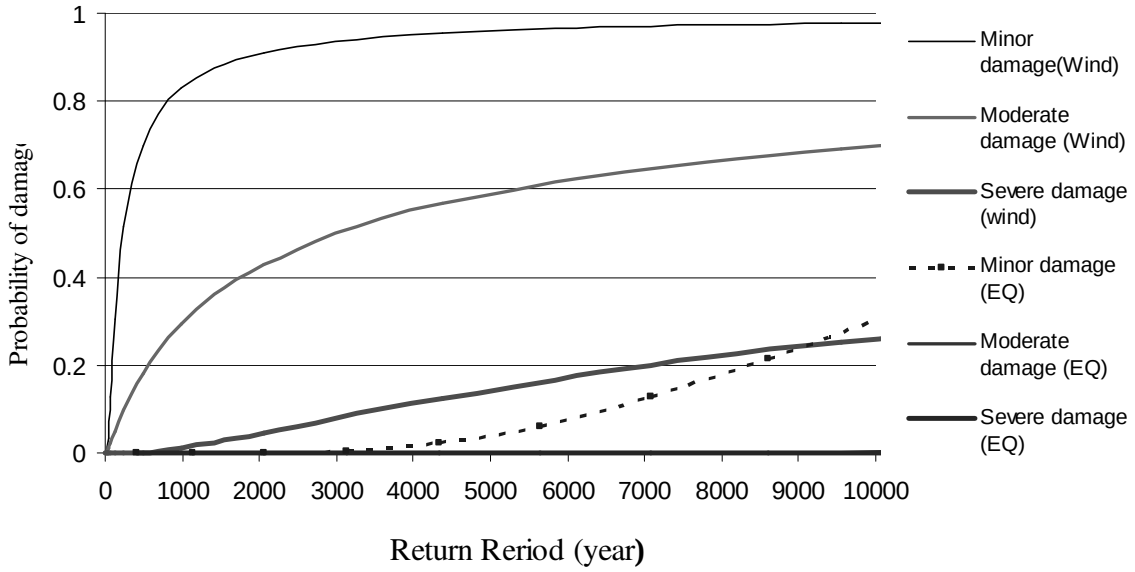

Figure 5.37 Probability of Hurricane and Earthquake Damage (Boston; Higher Hazard-Resistant Standard)

Table 5.4 summarizes the probabilities of hurricane and earthquake damage to residences in Charleston, SC and Boston, MA for events with different return periods. Some observations can be made from Table 5.4:

- Wind damage is generally more severe than earthquake damage for return periods that are less than 500 years in both Charleston and Boston.

- In Charleston, the possibility of seismic damage caused by a 500-year earthquake is not negligible, even though the dominant hazard is hurricane for return periods less than 500 years.

- In Boston, probability of earthquake damage is insignificant for earthquake with return periods less than 500 years, regardless of whether seismic anchors are used to anchor the shear walls to the foundation.

Table 5.4 Probability of Damage (%) due to Wind or Seismic Hazards Based on Return Period (Minimum Wind Protection Standards and Partially Anchored Shear Wall)

		Return period							
		50-yr		100-yr		250-yr		500-yr	
City	Damage State	Wind	Seismic	Wind	Seismic	Wind	Seismic	Wind	Seismic
Charleston	Minor	90.2	0.0003	94.5	0.001	99.5	1.5	100	17.6
	Moderate	61.5	0.0001	79.7	0.0004	92.6	0.02	96.3	0.6
	Severe	11.7	0.00004	23.4	0.0001	44.4	0.003	60.6	0.05
Boston	Minor	32.8	0	60.7	0.0001	82.1	0.0008	93.8	0.002
	Moderate	13	0	29	0	43.5	0.0003	68.2	0.001
	Severe	0.2	0	1.2	0	6.1	0.00008	17.2	0.0004

Table 5.5 summarizes the probability of hurricane and earthquake damage to a similar residence in Charleston or Boston, where the building is constructed to intermediate rather than minimum standards of construction. The impacts of utilizing intermediate standards for wind resistance vary from city to city. For example, the use of better wind protection reduces the risk more in Charleston than in Boston. For instance, if a hurricane with return period of 250-years were to hit Charleston and Boston, moderate and severe damage of will be reduced by 29.1% and 39.3%, respectively for the one-story house in Charleston adopting the higher standards. In comparison, the decrease in the probability of corresponding damage in Boston is 27.8% and 31.4%, respectively. Conversely, the effect of using hold-down anchors to reduce earthquake damage is insignificant for the one-story Boston residence. The only thing that changes in the analyses is the hazard curve (wind or seismic), since the construction details remain unchanged. The relative effectiveness of construction standard thus appears to depend on the slope of the hazard

curve, which is related to its coefficient of variation. That means if the hazard is less severe with a "flat" hazard curve, higher standards of construction are less effective in reducing damage.

Table 5.5 Probability of Damage (%) Based on Return Period (Intermediate Wind Protection Standards and Fully Anchored Shear Wall)

		Return period							
		50-yr		100-yr		250-yr		500-yr	
City	Damage State	Wind	Seismic	Wind	Seismic	Wind	Seismic	Wind	Seismic
Charleston	Minor	62.7	0.0005	80.3	0.0003	92.4	0.2	95.1	3
	Moderate	16.3	0	25.2	0.00004	43.5	0.01	58.3	0.03
	Severe	0.2	0	0.5	0	5.1	0.004	17.4	0.01
Boston	Minor	7.3	0	23.7	0	54.3	0.0003	71	0.0008
	Moderate	0.9	0	3.9	0	12.3	0.00004	19.2	0.0003
	Severe	0.008	0	0.01	0	0.2	0	0.5	0.0001

5.6.2 Risk comparison based on design wind speed and spectral acceleration

Because of the disparity in occurrence and impact of various natural hazards on building construction, the return periods associated with the design-basis natural hazard events are different in building design codes (e.g. ASCE Standard 7, 2002). To reduce the apparent difference in probability of damage for events with distinct return periods, a comparative risk assessment is performed based on design values for wind and earthquake load.

Table 5.6 is a summary of probabilities of hurricane and earthquake damage to residences in the selected cities, assuming that the events correspond to the design-basis events envisioned in ASCE-7 (2002). The one-story house with openings described in Chapter 4 (Figure 4.1) is assumed to be constructed with minimum wind protection, and its shear walls are not seismically anchored to the foundation. Design wind speed is uniformly 85 mph along the west coast of the US. In Anchorage and Hawaii, the design wind speed is 105 mph, while design wind speed may vary from city to city on East Coast. Two spectral accelerations are listed in Table 5.6. One is the 2%/50 yr spectral acceleration defining the maximum considered earthquake. The second is the spectral acceleration used in design, which is 2/3 of the 2%/50 spectral acceleration.

The comparison in Table 5.6 of probability of damage to residential building construction due to hurricane and earthquake reveals the following:

- The significance of damage due to design hurricane or earthquake hazard differs from city to city. Earthquake is the dominant natural hazard in Los Angeles and Seattle. For hurricane, it appears to be a major concern in Charleston, followed by Boston. In Anchorage and Hawaii, both hazards can cause significant damage to residence.

- A hurricane with design wind speeds leads to considerable minor damage in Charleston and Boston, followed by Anchorage and Hawaii. The probability of moderate wind damage in Charleston due to a design-basis storm is as least twice as

much as those in other cities. The probability of severe damage is less significant for all cities, except Charleston and Boston.

- Residential construction in Anchorage and south Hawaii island shows the highest likelihood of damage, followed by buildings in Los Angeles and Seattle. Earthquake damage in Boston and Honolulu is insignificant.

- If an earthquake with design spectral acceleration were to occur, the probabilities of minor damage to the buildings in Los Angeles, Seattle, Anchorage and Honolulu are close. However, the probability of moderate and severe damage in Anchorage and Hawaii is much higher than in Los Angeles and Seattle. The likelihood of severe damage associated with the design earthquake in Island of Hawaii and Anchorage is quite high: 69.3% and 52.7%, respectively.

Table 5.6 P_f and Associated Design Wind Speed and Spectral Acceleration in ASCE - 7, 2002 (Lower Hazard-Resistance Standard)

	Design wind speed [mph](50-yr return period)	Pf at Design wind speed (%)			Spectral acceleration (2% in 50-yr)	Design spectral acceleration [g] (T=0.2	Pf at Design Spectral Acceleration (%)		
Damage State		Minor	Moderate	Severe			Minor	Moderate	Severe
Charleston	**135**	94.2	74.6	20.7	**1.5**	**1**	85.4	24.2	8.5
Boston	**110**	69.7	34.5	2	**0.33**	**0.22**	0.3	0.1	0.08
Los Angeles	**85**	11.3	6.2	0.1	**2.2**	**1.47**	97.3	56.1	25.2
Seattle	**85**	11.3	6.2	0.1	**1.5**	**1**	93.1	40.3	13.4
Anchorage	**105**	48.2	25.6	0.8	**2.67**	**1.78**	99.9	85.8	52.1
Honolulu	**105**	48.2	25.6	0.8	**0.61**	**0.41**	0.76	0.24	0.12
Island of Hawaii	**105**	48.2	25.6	0.8	**2**	**1.33**	98.2	85.6	69.2

Table 5.7 is similar to Table 5.6, except the probability of damage is calculated assuming the building system is constructed with intermediate wind protection and shear wall hold-down anchors.

Table 5.7 P_f and Associated Design Wind Speed and Spectral Acceleration in ASCE - 7, 2002 (Higher Hazard-Resistance Standards)

	Design wind speed [mph](50-yr return period)	Pf at Design wind speed (%)			Spectral acceleration (2% in 50-yr)	Design spectral acceleration [g] (T=0.2 sec)	Pf at Design Spectral Acceleration (%)		
Damage State		Minor	Moderate	Severe			Minor	Moderate	Severe
Charleston	**135**	68.3	23.2	1.1	**1.5**	**1**	68.3	16.6	3.2
Boston	**110**	23.7	4.3	0.35	**0.33**	**0.22**	0.15	0.08	0.03
Los Angeles	**85**	1.1	0.3	0.08	**2.2**	**1.47**	95.2	27.3	3.5
Seattle	**85**	1.1	0.3	0.08	**1.5**	**1**	67.4	9.7	0.5
Anchorage	**105**	20.5	2.8	0.17	**2.67**	**1.78**	95.9	40.2	11.5
Honolulu	**105**	20.5	2.8	0.17	**0.61**	**0.41**	0.28	0.16	0.09
Island of Hawaii	**105**	20.5	2.8	0.17	**2**	**1.33**	87.3	46.6	20.5

The relative effectiveness of using higher standards to resist wind and earthquake hazard to residence varies from city to city. Table 5.7 shows that:

- Adopting higher wind protection standards would be most efficient in Seattle and Los Angeles, followed by Anchorage and south Hawaii island. The smallest percentage decrease in probability of damage to from better wind protection design occurred in Charleston, Boston, and Honolulu.

- For the hurricane wind hazard, utilizing higher standards of construction reduces moderate and severe damage dramatically in all cities, but the reduction is less significant for minor damage.

- Residential construction with shear walls fully fixed to the foundation should reduce severe damage in Seattle, Los Angeles, Anchorage and south Hawaii island, but is less efficient in lowering the probability of minor and moderate damage.

5.6.3 Risk comparison based on annual probability of damage

A fully coupled reliability analysis provides a framework to integrate information on uncertainties in structural system and loading and the resulting limit state or damage probability provides an overall numerical performance measure. This probability can be calculated by convolving the structural fragility and natural hazard. The probability of failure is determined for a certain period of time; in the current study, it is annualized because the hurricane and earthquake hazard curves are presented in terms of annual probability in Equation 3.7 and 4.5, respectively. The annual probability of damage can be related to economic terms, such as percentage of replacement values**.** Table 5.8 shows the annual probability for various level damage due to hurricane and earthquake hazards in Charleston, SC and Boston, MA.

Table 5.8 Comparison of Annual Probabilities of Various Damage due to Wind and Seismic Hazards

		Wind Hazard (%)		Seismic Hazard (%)	
City	Damage State	Minimum Standard	Intermediate Standard	Partially Anchored Shear Wall	Fully Anchored Shear wall
Charleston	Minor	7.6	3.6	0.125	0.076
	Moderate	4.9	1.2	0.052	0.035
	Severe	0.76	0.068	0.031	0.022
Boston	Minor	1.7	0.69	0.022	0.01
	Moderate	1	0.21	0.007	0.004
	Severe	0.12	0.019	0.003	0.002

Although the annual probability of earthquake damage is much lower than that due to hurricane in both Charleston and Boston, earthquakes should not be perceived as a low-risk hazard, since the consequences of an earthquake in an unprepared area are severe. Using intermediate wind protection as opposed to minimum standards in residential construction, the annual rate of minor, moderate, and severe wind damage rate reduces 2-3 times, 4-5 times and 6-10 times, depending on the city considered. However, the difference in annual earthquake damage probabilities for residences, with or without shear wall hold-downs, is about 50%, regardless of damage state.

5.7 Summary

A comparative risk assessment of the impact of hurricane and earthquake hazards is presented, considering the differences of these two natural hazards. The risk comparison has two major components – natural hazard probabilistic modeling and structural system fragility modeling to represent the conditional probability of damage. A typical one-story residential building configuration exposed to both hurricane and earthquake hazards in several cities is selected to demonstrate the risk assessment analysis. The common control variable for this comparative risk assessment is the return period of the natural hazard, design wind speed and spectral acceleration, and annual probability of damage.

6 SUMMARY, CONCLUSIONS AND FUTURE WORK

6.1 Summary

Damage to residential construction and social disruption caused by hurricanes and earthquakes have been severe during the past two decades. A better understanding of residential building performance and improved performance prediction tools are required if the goal of mitigating risk from natural hazards is to be achieved. A general methodology has been developed to assess fragilities (conditional failure probabilities) and reliability of light-frame wood residential construction subjected to various levels of hurricane and earthquake ground motions. Performance goals and limit states (structural and nonstructural) have been identified from a review of the performance of residential construction during recent hurricanes and earthquakes in the United States. For hurricanes, it is assumed that building contents damage and consequent structural damage result from breach of the building envelope, and the limit states are defined as the failure of roofs, windows and doors. Post-disaster surveys following earthquakes have shown that a large portion of the structural and nonstructural damage to light-frame wood residential construction can be related to excessive lateral drift of the building system. Wood frame buildings lateral drift limits defined in FEMA 273/356 are used to identify specific damage states in this study.

Uncertainties in structural system, wind load, and ground motion have been identified and incorporated in the probabilistic analysis of system behavior. First order reliability analysis was used to determine conditional probability of failure (fragility) for hurricane

winds, the effect of which on the structure is static. In contrast, a finite element-based platform and stochastic models were required to simulate the nonlinear dynamic behavior of wood frame structures in which shear walls provide the resistance to lateral force in earthquakes. Fragility of structural systems for the performance levels identified above were developed as a function of 3-s gust wind speed (hurricanes) and spectral acceleration (earthquakes), leading to a relation between limit state probabilities and the hazard stipulated in ASCE Standard 7. In addition, vulnerability curves showing levels of damage to contents and the residence, expressed as a damage ratio, was developed as a function of hurricane wind speed. Sources of epistemic (knowledge-based) uncertainties due to competing plausible hurricane wind speed models and databases on structural resistance were explicitly included in the reliability analysis, and their implications for risk-informed decision-making was examined.

The point and interval estimates of annual limit state probabilities due to hurricane were determined from a fully coupled reliability analysis using simulated hurricane windfield at coastal stations in the southeast US. The seismic hazard defined by the U.S. Geological Survey by zipcode on its website was used to define the probabilities of a spectrum of earthquake hazards.

The nature and consequence of these two hazards for wood construction are different. Building design and construction practices should address these differences to optimize strategies to achieve an overall risk that was consistent with social objectives. A comparative assessment of the impact of hurricane and earthquake hazards is conducted to provide tools for rank-ordering approaches for managing risks due to these natural

hazards. Such tools have two major components – structural system fragility models developed for assess damage states and probabilistic models of natural hazard occurrence and intensity. The comparative risk assessment was illustrated for a single-family residence in six cities, some of which are exposed to both hurricane and earthquake hazards. The implication and effects of natural hazard mitigation measure were discussed.

6.2 Conclusions

The fragility analysis and risk assessment methodology can be used for quantitative risk assessment for residential buildings under various levels of hurricane and earthquake hazards. Use of this methodology should lead to more predictable building performance and facilitate the introduction of performance-based engineering for wood-frame residential construction, improving the utilization of wood and wood-based composites leading to more reliable and economical design of wood-frame construction.

Secondly, the methodology can support improvements in building codes by identifying the most vulnerable types of light-frame construction and questionable construction practices, and to suggest cost-effective improvements to building codes.

Lastly, the risk assessment tool developed can be useful for engineering decision-making in evaluating the potential impact of a natural hazard in public planning, and mitigating the consequent economic losses and social disruption. It also provides a basis for loss

estimation and appropriate underwriting by the insurance industry to project losses for specific buildings for insurance purposes.

Some specific conclusions drawn from this study are listed as the following:

1. Performance-based engineering has focused on the seismic hazard in recent years in the United States. This study includes a performance-based evaluation for a competing hazard (i.e. hurricane) in order to appropriate design measures to achieve an integrated design goal. The relative risks associated with performance under a spectrum of natural hazards can be compared based on similar performance objectives.

2. A structural fragility includes uncertainty in structural system and loading, and displays the relationship between wind speed or spectral acceleration and probability of exceeding the limit states. The lognormal CDF is a suitable model for hurricane fragility after a series of tests. It was noted that the lognormal model for hurricane fragility appeared superior to the Weibull distribution, despite the fact that the glass resistance to wind pressure is modeled by a Weibull distribution.

3. The structural behavior of the wood shear wall ranges from the elastic at small S_a to the highly nonlinear at large S_a (the total deformation range is approximately h/600 to h/20, in which h is the height of the shear wall). The relationship between spectral

acceleration and maximum drift provides a simple tool for estimating seismic demand.

4. The parametric sensitivity analyses conducted to identify the relative importance of each variable and the main sources of uncertainty that affect the structural performance show that:

    - Breach of the building envelope from roof panel removal or damage to windows and doors increases probability of roof panel and connection failure by approximately 15-30%.

    - The presence of roof overhang on panel fragility is significant. Conversely, the height of the house has little impact on fragility.

    - Failure of 3/16 in glass of larger windows or sliding glass doors leading to internal pressurization of the building is dominated by wind pressure for wind speeds less than approximately 110 mph.

    - Roof panel nailing (6d vs. 8d), roof-to-wall connection details (toenail vs. hurricane clip), and building exposure (open vs. suburban) impact the fragility significantly.

The parametric sensitivity analysis of earthquake hazard could be summarized showed that:

- The shear modulus of the sheathing has little effect on the performance of the shear wall.

- The overall structural deformation of shear walls is dominated by the individual behavior of sheathing-to-framing connections.

- The residential building with partially anchored shear wall has larger displacements comparing with that has shear wall foundation fully fixed when it is subjected to an earthquake. The increase of drift ranges from 13-26% for different level of ground motions.

5. A fully coupled reliability analysis provides a framework to integrate information on uncertainties in structural system and loading and the resulting limit state or damage probability provides an overall numerical performance measure. For instance, the annual probabilities of exceeding immediate occupancy damage state due to earthquakes is approximately 10 times that for the life safety damage states for all shear wall models considered. In comparison, the difference in annual likelihood of exceedance of drift limit of life safety and collapse prevention is about 5 times.

6. A relatively small range of gust wind speeds (v) accounts for the major part of probability of failure. The range of return period of wind speed that comprises 90% of P_f for roof panel uplift and roof–to–wall connections is approximately 30 to 700 years, compared to the 50-yr return period in ASCE Standard 7-02. Estimates of wind speeds in that range should be further refined by meteorologists, and risk mitigation efforts should be focused on storms with that range.

7. Epistemic uncertainty plays an important role in reliability assessment and engineering decision analysis. Modeling uncertainty associated with the various wind field models has far more impact to reliability than that from different connection testing programs. The magnitude of difference in P_f due to sources of connection resistance data is about 30-50%, while the difference in P_f result from the various wind speed models can reach an order of magnitude. Developing a professional consensus on wind models is important to loss estimation and engineering decision analysis. Investigation of effects of epistemic uncertainty in earthquake ground motions on risk assessment could not be performed due to a lack of data on competing round motion models.

8. A comparative risk assessment performed for hurricane and seismic hazards reveals that:

- Wind damage is generally more severe than earthquake damage for return periods that are less than 500 years in both Charleston and Boston.

- The significance of damage of the residence due to design hurricane or earthquake hazard differs from city to city. Earthquake is the dominant natural hazard in Los Angeles and Seattle. For hurricane, it appears to be a major concern in Charleston, followed by Boston. In Anchorage and Island of Hawaii, both hazards with design intensity can cause significant damage to residence.

- Storms with design-level wind speeds would lead to considerable minor damage in Charleston and Boston, followed by Anchorage and Hawaii. The probability of moderate wind damage in Charleston due to a design-basis storm is as least twice as much as that in other cities considered.

- Residential construction in Anchorage and Island of Hawaii shows the highest likelihood of any specific level of damage given a design-basis earthquake, followed by buildings in Los Angeles and Seattle. Earthquake damage in Boston and Honolulu is insignificant.

9. The relative effectiveness (in terms of risk mitigation) of adopting higher standards to resist wind and earthquake hazard to residences varies from city to city. The higher wind protection standards reduce moderate and severe damage dramatically in all cities, but are less effective for minor damage. For earthquake, residential construction with shear walls fully fixed to the foundation is effective in reducing severe damage in Seattle, Los Angeles, Anchorage and Hawaii, but less efficient in

lower probability of minor and moderate damage. The effect of using fully hold-down anchors to reduce earthquake damage is insignificant for the one-story Boston residence. Using intermediate wind protection as opposed to minimum standards in residential construction reduces the annual rate of minor, moderate, and severe wind damage 2-3 times, 4-5 times and 6-10 times, respectively, depending on the city considered. However, the difference in annual earthquake damage for residence with or without shear wall hold-down is about 50%, regardless of damage state. The relative effectiveness of construction standard appears to depend on the slope of the hazard curve. In other words, if the hazard curve is "flat", higher standards of construction are less effective in hazard mitigation.

10. More attention should be given to hazards with low probability of occurrence but very high consequences. For instance, wind damage is generally more severe than earthquake damage for return periods that are less than 500 years in both Charleston and Boston. However, earthquakes should not be perceived as a low-risk hazard, since the consequences of an earthquake in an unprepared area are severe. In Charleston, the possibility of significant seismic damage under a 500-year earthquake is not negligible.

6.3 Future work

Further work is recommended in the following areas:

- Examine the impact of torsional effects due to mass eccentricity and irregular layout on hurricane and earthquake fragility.

- Develop a more rational mapping of damage state to structural limit state. In this study, seismic damage for light-frame wood construction was measured by the drift limit state defined in FEMA-273 (e.g. 2% drift for life safety limit state), while hurricane damage was related to damage to the building envelope, supported by post-disaster surveys. A more quantitative relationship (e.g. percentage of replacement value) between various level of damage and structural response should be sought, particularly in setting the equivalences between hurricane and earthquake damage.

- Include epistemic uncertainty in earthquake ground motions into seismic risk assessment and investigate the effects of this knowledge-based uncertainty on risk assessment. In the current study, the SAC project ground motions were used to represent inherent uncertainty in earthquake. Effects of selection for other ground motions (e.g. Wen and Wu, 2001) on risk assessment should be investigated.

- Expand regional risk assessment of wood frame buildings, considering the large variety of sizes, shapes, components and structural systems of buildings constructed over the years under diverse wind and seismic design codes.

- Relate annual probability of exceedance of performance limit states due to hurricane and earthquake to expected annual loss. The process should include uncertainties in structural system behavior, loading, damage and cost for loss estimation and decision-making.

- Compare the cost and benefit from adopting stricter standard hazard-resistant design for mitigation of different hazards measures. Such an analysis would allow building owner to compare benefits through investment to achieve a specific performance goal and the risk that otherwise the owner would face. Investigate the feasibility of life-cycle analysis for wood-frame residential construction, allowing a building to be designed for natural hazards in an optimal manner considering its entire lifespan.

BIBLIOGRAPHY:

AF&PA/American Society for Civil Engineers (ASCE) 16-95. (1996). Standard for Load and Resistance Factor Design (LRFD) for Engineered Wood Construction. AF&PA/ASCE 16-95, APA Supplement, Structural-Use Panels, New York.

ASCE (1999). Minimum Design Loads for Buildings and Other Structures (ASCE Standard 7-98), Am. Soc. of Civil. Engineers, Reston, VA.

ASCE (2003). Minimum Design Loads for Buildings and Other Structures (ASCE Standard 7-02), Am. Soc. of Civil. Engineers, Reston, VA.

ASTM, (2003). Standard Practice for Determining Load Resistance of Glass in Building. E-1300-03, American Society for Testing and Materials, West Conshohocken, PA.

ASTM. (2002). Standard Specification for Performance of Exterior Windows, Glazed Curtain Walls, Doors and Storm Shutters Impacted By Windborne Debris in Hurricanes. E-1996-02, American Society for Testing and Materials, West Conshohocken, Pa.

Ayscue, Jon K. (1996), Hurricane damage to residential structures: risk and mitigation, Natural Hazards Research and Applications Information Center, University of Colorado, Boulder, CO.

Baskaran, A., and Dutt, O. (1997). Performance of Roof Fasteners under Simulated Loading Conditions. Journal of Wind Engineering and Industrial Aerodynamic, 72(1–3), 389–400.

Batts, M. E., Cordes, M. R., Russell, L. R., Shaver, J. R., and Simiu, E. (1980). Hurricane Wind Speeds in the United States. Rep. No. BSS-124, National Bureau of Standards, U.S. Department of Commerce, Washington, D.C.

Beason, W. L., Kohutek, T. L., and Bracci, J. M. (1998). Basis for ASTM E 1300 Annealed Glass Thickness Selection Charts. Journal of Structural Engineering, 124(2), 215–221.

Beason, W. L., and Morgan, J. R. (1984). Glass Failure Prediction Model. Journal of Structural Engineering, 110(2), 197–212.

Beason, W. L., Meyers, G. E., and James, R. W. (1984). Hurricane Related Window Glass Damage in Houston. Journal of Structural Engineering, 110(12), 2843–2857.

Beers, P. E. (1993). Designing Hurricane-Resistant Glazing. Prog. Arch., 74(9), 76–78.

Behr, R. A., Karson, M. J., and Minor, J. E. (1991). Reliability Analysis of Window Glass Failure Pressure Data. Structural Safety, 11, 43–58.

Behr, R. A., and Kremer, P. A. (1996). Performance of Laminated Glass Units under Simulated Windborne Debris Impacts. Journal of Architectural Engineering, 2(3), 95–99.

Bulleit, W.M., Pang, W-C and Rosowsky, D.V. (2005). Modeling Wood Walls Subjected to Combined Transverse and Axial Loads. Journal of Structural Engineering, 131(5), 781-793.

Canfield, L.G., Niu, S.H., and Liu, H. (1991). Uplift Resistance of Various Rafter-Wall Connections, Forest Products, 41(7/8): 27-34.

Ceccotti, A. and Foschi, R.O. (1998). Reliability Assessment of Wood Shear Walls under Earthquake Excitation, Proceedings of International Conference on Computational Stochastic Mechanics, Santorini, Greece, June 1998.

Collins, M., Kasal, B., Paevere, P., and Foliente, G. C. (2005). Three-Dimensional Model of Light Frame Wood Buildings – I: Model Description and II: Experimental Investigation and Validation of the Analytical Model." Journal of Structural Engineering, 131(4), 676–692.

Cope, A., Gurley, K., Pinelli, J.-P., and Hamid, S. (2003). A Simulation Model for Wind Damage Predictions in Florida. Proc., 11th Int. Conf. on Wind Engineering, Texas Tech Univ., Lubbock, TX.

Cornell, C. A., Jalayer, F., Hamburger, R. O., and Foutch, D. A. Probabilistic Basis for the 2000 SAC Federal Emergency Management Agency Steel Moment Frame Guidelines. Journal of Structural Engineering, 2002; 128(4), 526–533.

Cunningham, T. P. (1993). Roof Sheathing Fastening Schedules for Wind Uplift. APA Rep. No. T92-28, American Plywood Association, Tacoma, WA.

CUREE (2000). CUREE-Caltech Woodframe Project. <www.curee.org/Projects/Woodframe>.

CUREE (2004). Guidelines for the Assessment and Repair of Earthquake Damage in Residential Buildings. [Http://www.curre.org/Projcts/EDA/Dosc/EDA-02_2004-1.Pdf.]

Dinehart, D.W. and Shenton, H.W. (1998). Comparison of Static and Dynamic Response of Timber Shear Walls, Journal of Structural Engineering, ASCE, 124(6), 686-695.

Dinehart, D.W. and Shenton, H.W. (2000). Model for Dynamic Analysis of Wood Frame Shear Walls, Journal of Engineering Mechanics, ASCE, 126(9), 899-908.

Dinehart, D. W., Shenton, H. W., III, and Elliott, T. E. (1999). the Dynamic Response of Wood-Frame Shear Walls With Viscoelastic Dampers,'' Earthquake Spectra, 15(1), 67–86.

Dolan, J. D. (1989) The Dynamic Response of Timber Shear Walls. PhD Dissertation, Dept. of Civil Engineering, Univ. of British Columbia, Vancouver, Canada.

Dolan, J.D. and Madsen, B. (1992). Monotonic and Cyclic Tests of Timber Shear Walls, Canadian Journal of Civil Engineering, 19(3), 115-122.

Dolan, J.D. and Heine, C.P. (1997). Sequential Phased Displacement Cyclic Tests of Wood-Frame Shear Walls With Various Openings and Base Restraint Configurations VPI&SU Report #TE-1997-002, Virginia Polytechnic Institute and State University.

Durham, J. P. (1998). Seismic Response of Wood Shear Walls with Oversized Oriented Strand Board Panels. MASc thesis, Univ. of British Columbia, Canada

Durham, J., Lam, F., and Prion, G. L. (2001). Seismic Resistance of Wood Shear Walls With Large OSB Panels.'' Journal of Structural Engineering, 127(12), 1460–1466.

Ellingwood, B. (1990). Validation studies of seismic PRAs. Nuclear Engineering and Design, 123(2): 189-196.

Ellingwood, B.R. (1994), Probability-Based Codified Design: Past Accomplishments and Future Challenges. Structural Safety, 13(3):159-176.

Ellingwood, B. (1997). Probability-based LRFD for engineered wood construction. Structural Safety, 19(1): 53-65.

Ellingwood, B., J.G. Macgregor, T.V. Galambos and C.A. Cornell (1982). Probability-Based Load Criteria – Load Factors and Load Combinations, Journal of Structural Division, ASCE 108(5): 978-997.

Ellingwood, B.R. and Rosowsky, D.V. (1991). Duration of Load Effects in LRFD for Wood Construction. Journal of Structural Engineering. ASCE, 117(2):584-599.

Ellingwood, B. R., Rosowsky, D. V, Li, Y. and Kim, J. H. (2004). Fragility Assessment of Light-Frame Construction Subjected to Wind and Earthquake Hazards, Journal of Structural Engineering, ASCE, 130(12): 1921-1930.

Ellingwood B. R., and Tekie, P.B. (1999). Wind Load Statistics for Probability-Based Structural Design, Journal of Structural Engineering, ASCE, 125(4): 453-463.

FEMA-273. (1997) NEHRP Guidelines for the Seismic Rehabilitation of Buildings. Report FEMB-273, Federal Emergency Management Agency, Washington, DC.

FEMA-356. (2000). Prestandard and Commentary for the Seismic Rehabilitation of Buildings, Federal Emergency Management Agency, Washington, DC.

FEMA-366. (2001). HAZUS 99: Estimated Annualized Earthquake Losses for the United States. ies, Inc. Washington, DC.

Foliente, G.C. (1995). Hysteresis Modeling of Wood Joints and Structural Systems, Journal of Structural Engineering, ASCE, 121(6),1013-1022.

Foliente, G.C. (1997). Timber Structures in Seismic Regions—General Overview and Research Needs. G.C. Foliente, Ed. Earthquake Performance and Safety of Timber Structures, Forest Products Society, Madison, Wisconsin, Pp. 3-23.

Foliente, G.C., Paevere, P. J., Saito, T., and Kawai, N. (1999). Seismic Reliability Analysis of Timber Buildings.'' Proceedings, Pacific Timber Engineering Conference.

Foliente, G.C., Paevere, P., Saito, T. and Kawai, N. (2000). Reliability Assessment of Timber Shear Walls under Earthquake Loads, Proceedings of 12 The World Conference on Earthquake Engineering (12th WCEE), Auckland, New Zealand.

Folz, B., and Filiatrault, A. (2000). CASHEW—Version 1.0, A Computer Program for Cyclic Analysis of Wood Shear Walls.'' Rep. No. SSRP-2000/10, Structural System Research Project, Dept. of Structural Engineering, Univ. of California San Diego, La Jolla, Calif. .

Folz, B., and Filiatrault, A. F. (2001). Cyclic Analysis of Wood Shear Walls. Journal of Structural Engineering, ASCE, 127(4), 433-441.

Foschi, R.O. (1977). Analysis of Wood Diaphragms and Trusses, Part I, Diaphragms, Canadian Journal of Civil Engineering, 4(3), 345-352.

Frangopol, D.M. (1999). Bridge Safety and Reliability. ASCE, Reston, VA.

Frangopol, D.M., Kong, J.S. and Gharaibeh, E.S. (2001). Reliability-Based Life-Cycle Management of Highway Bridges, Journal of Computing in Civil Engineering, ASCE 15(1), 27-34.

Filiatrault, A. (1990), Static and Dynamic Analysis of Timber Shear Walls, Canadian Journal of Civil Engineering, 17(4), 643-651.

Filiatrault, A. and Folz, B., (2002). Performance-Based Seismic Design of Wood Framed Builings. Journal of Structural Engineering, ASCE, 128(1), 39-47.

Filiatrault, A., Fischer, D., Folz, B., Uang, C. M., and Seible, F. (2001). Shake Table Test of A Two-Story Woodframe House.'' Proc., Element 1, Research Meeting, January 12, 2001, CUREE-Caltech Woodframe Project, San Diego.

Filiatrault, A., Fischer, D., Folz, B., and Uang, C-H (2002). Seismic Testing of Two-Story Woodframe House, Influence of Wall Finish Material. Journal of Structural Engineering, ASCE, 128(10), 1337-1345.

Filiatrault A, H. Isoda B, B. Folz C. (2003). Hysteretic Damping of Wood Framed Buildings. Engineering Structures, (25), 461–471.

Filliben, James J. (1975). The Probability Plot Correlation Coefficient Test for Normality, Technometrics, 17(1): 111-117.

Galambos T.V., Ellingwood, B., Macgregor, J.G., and Cornell, C.A. (1982). Probability-Based Load Criteria – Assessment of Current Design Practice. Journal of Structural Division, ASCE 108(5): 959-976.

Georgiou, P. N. (1985). Design Wind Speeds in Tropical Cyclone-Prone Regions. Phd Thesis, Fac. of Engineering Sci., University of Western Ontario, London, Ont., Canada.

Georgiou, P. N., Davenport, A. G., and Vickery, B. J. (1983). Design Wind Speeds in Regions Dominated By Tropical Cyclones. Journal of Wind Engineering and Industrial Aerodynamics, Amsterdam, the Netherlands, 13(1), 139–152.

GIIS (Georgia Insurance Information Service). (2004). The Insurance Industry: Globally, Across the U.S.A. and In Georgia. [http://www.giis.org/giis/giis_pc_facts.shtml]

Green, D.W. and Evans, J.W. (1987). Mechanical Properties Of Visually Graded Lumber, Vols. 1 – 5, Forest Products Laboratory, USDA, Madison, WI.

Gupta, A.K., and Kuo, G.P. (1987). Wood-Framed Shear Walls with Uplifting. Journal of Structural Engineering, 113(2), 241–259.

Gupta, A.K., and Kuo, G.P. (1985). Behavior of Wood-Framed Shear Walls. Journal of Structural Engineering, 111(8), 1722–1733.

Harris, P. L. (1978). Effects of Thickness and Temper on the Resistance of Glass to Small Projectile Impact, Masters Thesis Presented to Texas Tech University, Lubbock, Texas.

He, M., Lam, F. and Foschi, R.O. (2001). Modeling Three-Dimensional Timber Light-Frame Buildings. Journal of Structural Engineering. 127(8), 901-913.

Huang, Z., Rosowsky, D.V., and Sparks, P.R. (2001). Long-Term Hurricane Risk Assessment and Expected Damage to Residential Structures. Reliability Engineering and System Safety, 74, 239–249.

IBHS. (2001) The Ten Most Wanted: A Search for Solutions to Reduce Recurring Losses from Natural Hazards, Institute for Business & Home Safety, ASCE.

Kasal, B., Collins, M., Paevere, P., and Foliente, G. C. (2004). Design Models of Light-Frame Wood Buildings under Lateral Loads. Journal of Structural Engineering 130(8), 1263–1271.

Kasal, B., Leichti, R., and Itani, R. (1994). Nonlinear Finite-Element Model of Complete Light-Frame Wood Structures." Journal of Structural Engineering, 120(1), 100–119.

Kennedy RP and Ravindra MK. (1984). Seismic Fragilities for Nuclear Power Plant Studies. Nuclear Engineering and Design, 79(1):47–68.

Khanduri, A.C., and Morrow, G. C. (2003). Vulnerability of buildings to windstorms and insurance loss estimation. Journal of Wind Engineering and Industrial Aerodynamics, 91, 455–467.

Kyung H.L. and Rosowsky D.V. (2005). Fragility Assessment for Roof Sheathing Failure in High Wind Regions. Engineering Structures 27, 857–868.

Krawinkler, Parisi, F., Ibarra, L., Ayoub, A., and Medina, R. Development of a Testing Protocol for Wood Frame Structures. CUREE Publication No. W-02, Richmond, Calif, 2000.

Lee K. and Foutch, D.A. (2002). Seismic Performance Evaluation of Pre-Northridge Steel Frame Buildings with Brittle Connections. Journal of Structural. Engineering. 128(4), 546-555.

Li, Y. and Ellingwood, B. R. (2004) Assessment of Wood Residential Construction Subjected to Earthquakes, 13th World Conference on Earthquake Engineering, Vancouver, Canada.

Luco, N., and Cornell, C.A. (2000) Effects of Connection Fractures on SMRF Seismic Drift Demands. Journal of Structural Engineering, 126(1), 127–136.

Manning, B. R. and Nichols. G. G. (1991). Hugo Lessons Learned. in: Hurricane Hugo One Year Later, Benjamin A. Sill and Peter R. Sparks, Editors. New York: ASCE.

Mehta, K.C. and Marshall, R.D. (1997). Guide to the Use of the Wind Load Provision of ASCE 7-95, ASCE, Reston, VA.

Mehta, K.C. and Perry, D.C. (2001). Guide to the Use of the Wind Load Provision of ASCE 7-98, ASCE, Reston, VA.

Melchers, R. E. (1999). Structural Reliability Analysis and Prediction, Wiley, New York.

Minor, J. E. (1994). Windorne Debris and the Building Envelope. Journal of wind engineering and industrial Aerodynamics, 53(1-2), 207–227.

Minor, J.E. (1997). New Philosophy Guides Design of the Building Envelope. Proc., Structures Congress XV, ASCE, New York, 1–5.

Minor, J. E., Beason, W. L., and Harris, P.L. (1976). Window Glass Failures In Windstorms, Journal of Structural Division, ASCE 102 (1): 147–160.

Minor, J. E., Beason, W. L., and Harris, P.L. (1978). Design for Windborne Missiles in Urban Areas. Journal of Structural Engineering, ASCE 104 (11): 1749-1760.

Minor, J.E., Mehta, K. C., and Mcdonald, J. R. (1972). Failure of Structures Due to Extreme Winds. Journal of Structural Division, ASCE, 98(11), 2455–2471.

Minor, J.E., and Schneider, P.J. (2002). Hurricane Loss Estimation—the HAZUS Hurricane Preview Model. Proc., Americas Conference on Wind Engineering—2001, CD-ROM, American Association for Wind Engineering, Clemson Univ., Clemson, SC.

Minor, J. E. and Norville, H.S. (1998). A Simple Window Glass Design Chart. America Ceramic Society Bulletin, (77&78): 1467-1470.

Mizzell, D.P. and Schiff, S.D. (1994). Wind Resistance of Sheathing for Residential Roofs. Wind Load Test Facility Report, Department of Civil Engineering, Clemson University, Clemson, SC.

Murden, J.A. (1991). Hugo 1989: the Performance of Structures in Wind. in Hurricane Hugo One Year Later, Benjamin A. Sill and Peter R. Sparks, Editors. New York: ASCE.

NAHB (1990). Manufactured of Housing Shear Wall Tests Using ASTM Method E72 and E564. Prepared for the US Department of Housing and Urban Development By the NAHB Research Center, Upper Marlboro, MD.

NAHB (1993). Assessment of Damage to Single-Family Homes Caused By Hurricane Andrew and Iniki, NAHB Research Center Report, Upper Marlboro, MD

NAHB (1994). Assessment of Damage to Residential Buildings Caused by the Northridge Earthquake. NAHB Research Center Report, Upper Marlboro, MD

NAHB. (1996). Assessment of Damage to Homes Caused By Hurricane Opal, Prepared for the Florida State Home Builders Association By the NAHB Research Center, Upper Marlboro, MD.

NAHB. (1999a). Reliability of Conventional Residential Construction: An Assessment of Roof Component Performance in Hurricane Andrew and Typical Wind Regions of the United States. NAHB Research Center Rep., Upper Marlboro, MD.

NAHB. (1999b). An Industry Perspective on Performance Guidelines for Structural Safety and Serviceability of One and Two-Family Dwellings. Research Center Rep., National Association of Home Builders, Upper Marlboro, MD.

NAHB. (2002). Roof Framing Connections In Conventional Residential Construction. NAHB Research Center, Upper Marlboro, MD.

NIBS. (2000). HAZUS Wind Loss Estimation Methodology. Draft Technical Manual, National Institute of Buildings Sciences, Washington, D.C.

Norville, H.S. and Minor, J. E. (1985). Strength of Weathered Window Glass. Journal of Wind Engineering and Industrial Aerodynamics, (64): 197-204.

Norville, H. S., and Minor, J. E. (2000). Simplified Window Glass Design Procedure. Journal of Architectural Engineering, 6(4), 105–115.

Paevere, P., and Foliente, G. C. (2000). Hysteretic Pinching and Degradation Effects on Dynamic Response and Reliability. Proceedings, International Conference on Applications of Statistics and Probability.

Perkins, J. B., Boatwright, J. and Chaqui, B. (1998). Housing Damage and Resulting Shelters Needs, Model Testing and Refinement Using Northridge Data. Proc. NEHPR Conf. and Workshop on Research on the Northridge California Earthquake of January 17, 1994, Richmond, Calif., I, I-1.

Peterka J.A. and Shahid, S. (1998). Design Gust Wind Speed in the United States, Journal of Structural Engineering, ASCE, 124(2): 207-214.

Philpot, T.A. Rosowsky, D.V. and Kenneth J. F. (1995). Reliability of Wood Joist Floor Systems with Creep. Journal of Structural Engineering, 121(6). 946-954.

Reed, T. D. Rosowsky, D. V., and Schiff, S. D. (1997). Uplift Capacity of Light-Frame Rafter to Top Plate Connections. Journal of Architectural Engineering, ASCE, 3(4), 156–163.

Reinhold, T.A., Vickery, P.J., and Powell, M.D. (1993). Windspeeds in Hurricane Andrew: Myths and Reality, 7th US National Conference on Wind Engineering, Univ. of California, Los Angeles, Pp. 553 - 562.

Richard, N., Daudevill, L., Davenne, L., and Kawai, N. (1998) Numerical Analysis of Seismic Response of Timber Shear Walls With Nailed Joints. Proc., 11th European Conf. on Earthquake Engineering.

Richard J.C. and Russell C.M. (1989), Modeling Laterally Loaded Light-Frame Buildings. Journal of Structural Engineering, ASCE, 115(1): 201-217.

Rigato, A., Chang, P., and Simiu, E. (2001). "Database-assisted design, standardization, and wind direction effects." Journal of Structural Engineering, ASCE 127(8), 855–860.

Rosowsky, D. (2002). Reliability-Based Seismic Design of Wood Shear Walls. Journal of Structural Engineering, ASCE, 128(11), 1439-1453.

Rosowsky, D.V. and Cheng, N. (1999). Reliability of Light-Frame Roofs in High-Wind Regions, I: Wind Loads; II: Reliability Analysis, Journal of Structural Engineering, ASCE, 125(7):725-739.

Rosowsky, D.V. and Ellingwood, B. R. (2002). Performance-Based Engineering of Wood Frame Housing, Fragility Analysis Methodology. Journal of Structural Engineering, ASCE, 128(1), 32-38.

Rosowsky, D.V and Schiff, S.D. (1996). Probabilistic Modeling of Roof Sheathing Uplift Capacity, Proceedings: Probabilistic Mechanics and Structural Specialty Conference, ASCE, Worcester, MA, Pp. 334-337.

SAC (2000). SAC Steel Project. [www.sac.org].

SEAOC (1995). Vision 2000 - A Framework for Performance Based Design, Volumes I, II, III. Structural Engineers Association of California, Vision 2000 Committee. Sacramento, California.

Saxe, T. J., Behr, R. A., Minor, J. E., Kremer, P. A., and Dharani, L. R. (2002). Effects of Missile Size and Glass Type on Impact Resistance of `Sacrificial Ply' Laminated Glass. Journal of Architectural Engineering, 8(1), 24–39.

Schierle, G. G., Ed. (2001). Woodframe Project Case Studies. CUREE Publication No. W-04, CUREE-Caltech Woodframe Project, Consortium of Universities for Research in Earthquake Engineering, Richmond, Calif.

Sheets, R. C. (1994). Catastrophic Hurricanes May Become Frequent Events in Caribbean and Along the United States East and Gulf Coasts. in Hurricanes of 1992, Ronald A. Cook and Mehrdad Soltani, Editors. New York: ASCE.

Singhal A. Kiremedjian A.S. (1996). Method for Probabilistic Evaluation of Seismic Structural Damage. Journal of Structural Engineering, ASCE, 122(12): 1459-1467.

Shinozuka M., M. Q. Feng, J. Lee, and T. Naganuma (2000). Statistical Analysis of Fragility Curves. Journal of Engineering Mechanics, ASCE, 126(12): 1224-1231.

Song J. Ellingwood B.R. (1999)."Seismic reliability of special moment steel frames with welded connections II," Journal of Structural Engineering, ASCE, 125(4): 372-384.

Sparks, P. R., Schiff, S. D., and Reinhold, T. A. (1994). Wind Damage to Envelops of Houses and Consequent Insurance Losses, Journal of Wind Engineering and Industrial Aerodynamics, 53, 145–155.

Stewart, M.G. and Attard, M.M. (1999). Reliability and Model Accuracy for High-Strength Concrete Column Design. Journal of Structural Engineering, ASCE, 125(3): 290-300.

Twisdale, L.A., Vickery, P.J., and Hardy, M.B. (1992). Uncertainties in the Prediction of Hurricane Windspeeds, Proc. Hurricanes of 1992, Miami, FL, ASCE, Reston, Virginia, pp 1-3.

Unanwa, C. O., Mcdonald, J. R., Mehta, K. C., and Smith, D. A. (2000). the Development of Wind Damage Bands for Buildings, Journal Wind Engineering and Industrial Aerodynamic., 84, 119–149.

Vickery, P. J., Skerlj, P. F., Steckley, A. C., and Twisdale, L. A. (2000). Hurricane Wind Field Model for Use in Hurricane Simulations. Journal of Structural Engineering, 126(10), 1203–1222.

Vickery, P. J., Skerlj, P. F., Steckley, A. C., and Twisdale, L. A. (2000). Simulation of Hurricane Risk in the United States Using Empirical Track Modeling Technique. Journal of Structural Engineering, ASCE, 126(10), 1222–1237.

Vickery, P. J., and Twisdale, L. A. (1995a). . Prediction of Hurricane Wind Speeds in the United States. Journal of Structural Engineering, ASCE, 121(11), 1691–1699.

Vickery, P. J., and Twisdale, L. A. (1995b). Wind-Field and Filling Models for Hurricane Wind-Speed Predictions. Journal of Structural Engineering, ASCE, 121(11), 1700–1709.

Van De Lindt, J.W. and Walz, M.A. (2003). Development and Application of Wood Shear Wall Reliability Model. Journal of Structural Engineering, ASCE, 129(3), 405-413.

Van De Lindt, J.W. (2004). Evolution of Wood Shear Wall Testing, Modeling, and Reliability Analysis: Bibliography. Practice Periodical on Structural Design and Construction, 9(1), 44-53.

Veletsos, A.S. and N.M. Newmark (1960). Effect of Inelastic Behavior on the Response of Simple Systems to Earthquake Motions, Proceedings, Second World Conference on Earthquake Engineering, Tokyo, 1960, Vol. II, Pp. 895-912.

Wang, C-H and Wen, Y-K (2000), Evaluation of Pre-Northridge Low-Rise Steel Buildings – I: Modeling and II: Reliability, Journal of Structural Engineering, ASCE, 126(10): 1160-1176

Wen, Y-K. and Kang Y.J. (2001). Minimum Building Life-Cycle Cost Design Criteria. I: Methodology and II: Applications, Journal of Structural Engineering, ASCE, 127(3), 330-346.

Wen, Y-K, and Wu, C. (2001). Uniform Hazard Ground Motions for Mid-America Cities, Earthquake Spectra 17, 359–384.

Weibull, W. (1939). A Statistical Theory of the Strength of Materials. Ingeniorsvetenskapsakademiens, Handlingar NR151, Stockholm, Sweden.

Zahn, J.J. (1992). Reliability of Bolted Wood Connections. Journal of Structural Engineering, 118(12), 3362-3376

VITA

Yue Li was born in Nanning, Guangxi, China. He received the degree of Bachelor of Science in Civil Engineering in 1995 from Guangxi Institute of Technology, Liuzhou. He worked for four years as a structural engineer for Zhongfan Engineering Development Group, Inc, in Nanning. In 1999, he initiated his Ph.D. program of study in the Department of Civil Engineering at the Johns Hopkins University in Baltimore, MD. He subsequently matriculated as a graduate student and candidate for the Ph.D. degree in the School of Civil of Civil and Environmental Engineering at the Georgia Institute of Technology in 2000 in order to accompany his dissertation advisor who had accepted a position at Georgia Tech. Mr. Li received his Masters degree in Civil Engineering from Georgia Tech in 2002. In the spring 2005, he was employed as a Co-op Structural Engineer for Khafra Engineering Consultants Inc., working on the Hartsfield-Jackson Atlanta Airport International Terminal design. In the following summer, he worked as a Co-op Structural Engineer for Stanley D. Lindsey and Associates, Ltd in Atlanta, GA.